ABSTRACT

CONNOR, LAURENCE NEUMAN, JR: The One-Dimensional Unsteady Expansion of a Reacting Mixture of Gases Considering Vibrational and Chemical Nonequilibrium. (Under the direction of ROBERT WESLEY TRUITT).

An analysis was made of an unsteady one-dimensional centered expansion with vibrational excitation and finite rate chemistry included. A multi-component gas model with a number of simultaneous rate equations was used. The characteristic equations were obtained from the governing equations of the problem. The role of the frozen sound speed in a characteristic type solution was ascertained. A procedure based on the method of characteristics was established for obtaining a numerical solution in Lagrangian coordinates. Calculations were made using an electronic digital computer.

The programed method of solution was applied to three cases. First, an illustrative case was presented to show the basic structure of the nonequilibrium expansion, the general trends and the physical significance of these trends. The chemistry was found to be dominated by the recombination reactions for most of the expansion. Temperature was shown to be the flow quantity most affected by the existence of nonequilibrium in the flow. Both the expansion fan and the near-steady region following the fan were calculated and the variations of thermodynamic properties, compositions, and velocities were presented for a typical case using an air model.

A solution was obtained which illustrates the utility of the program in analyzing facilities which use an unsteady expansion to produce high velocity flow. The results showed a distinct similarity between the unsteady expansion and the quasi-one-dimensional nonequilibrium expansion in a hypersonic nozzle, particularly with regard to the freezing of the composition as the density decreases.

Finally, an experiment was proposed for the direct measurement of recombination rates. The proposed experiment was analyzed using the developed program and found to be feasible. The near steady region following the expansion fan was found to be particularly useful for rate studies due to a nearly linear variation of composition which existed over a range of slowly varying thermodynamic properties.

The utility of the developed program was assessed and recommendations were made for extensions of the present work.

THE ONE-DIMENSIONAL UNSTEADY EXPANSION OF A REACTING MIXTURE OF GASES CONSIDERING VIBRATIONAL AND CHEMICAL NONEQUILIBRIUM

by

LAURENCE NEUMAN CONNOR, JR.

A thesis submitted to the Graduate Faculty
of North Carolina State of
the University of North Carolina at Raleigh
in partial fulfillment of the
requirements for the Degree of
Doctor of Philosophy

DEPARTMENT OF MECHANICAL ENGINEERING

RALEIGH

1965

APPROVED BY:

[redacted]

[redacted]

[redacted]

[redacted]

[redacted]

Chairman of Advisory Committee

BIOGRAPHY

The author was born December 8, 1936, in Barnwell, South Carolina. He obtained his elementary and high school education in the public school system of Barnwell. In 1954 the author entered Clemson College from which he received the degree, Bachelor of Science in Mechanical Engineering, in June 1958. In June 1960, after two years as a research assistant and graduate student at North Carolina State College, he was awarded the degree, Master of Science in Mechanical Engineering. The following year was spent in full time graduate study at North Carolina State College under a National Science Foundation Fellowship. From 1962 until 1965 the author served as an officer in the United States Air Force with duty at the Langley Research Center of the National Aeronautics and Space Administration. He is presently employed as an aerospace engineer with the National Aeronautics and Space Administration.

ACKNOWLEDGEMENTS

The author would like to express his appreciation to Dr. R. W. Truitt, who provided valuable guidance and encouragement during the investigation; to Dr. H. A. Hassan, for his enlightening discussions; and to Mr. R. L. Trimpi, for his suggestion of the problem initially. Appreciation is also expressed to Miss Frances Taylor for her aid in programing the numerical solution and to Mrs. Frances Moore for typing the final manuscript.

The author is extremely grateful to the National Aeronautics and Space Administration for allowing him to carry out this investigation and for permission to present it as a dissertation.

TABLE OF CONTENTS

TABLE OF CONTENTS (continued)

TABLE OF CONTENTS (continued)

LIST OF TABLES

LIST OF ILLUSTRATIONS

LIST OF ILLUSTRATIONS (continued)

INTRODUCTION

The advent of the space age with its entry and reentry vehicles has presented many new problems in the field of gas dynamics. The study of real gas flow has assumed major importance in the analysis of reentry phenomena. The extreme temperatures experienced by bodies entering the atmosphere have rendered inadequate the use of perfect gas assumptions in solving the associated aerodynamic problems. In like manner, high enthalpy test facilities, designed for simulation of reentry flight conditions, utilize a test medium which must be evaluated using real gas concepts. Problems of this nature can no longer be analyzed neglecting the contributions of vibrational excitation, dissociation and ionization to the energy of the gas. In addition, the mechanisms controlling these contributions are rate processes and thus the flow will not necessarily remain in a state of chemical equilibrium. The solution of a gas dynamic problem in which such nonequilibrium phenomena exists becomes considerably more difficult than the perfect gas solution. The present investigation is designed to establish a method of solution for one such case, that of the nonequilibrium one-dimensional unsteady expansion of a reacting gas mixture.

The one-dimensional unsteady expansion has recently assumed new importance in the operation cycle of facilities designed to produce high enthalpy flow for reentry simulation and chemical kinetic studies. The expansion tube is designed to produce high velocity flow for reentry simulation. The operating cycle of the expansion tube

utilizes an unsteady expansion to accelerate the test gas. This expansion is a critical phase in the expansion tube cycle since any deviation from equilibrium at this point will alter the final state of the test gas. The need of a solution which can evaluate any nonequilibrium condition occurring in the expansion is apparent.

For high enthalpy gas flow, the role of chemical kinetics assumes new importance. To accurately analyze such flow, an adequate knowledge of the rates of the reactions involved is necessary. It has generally been the practice in the past to measure the forward rate of a reaction and evaluate the reverse reaction at equilibrium conditions using the equilibrium constant. The unsteady expansion process can provide a means for direct measurement of recombination rates. This investigation will establish a basis for the evaluation of an experiment which utilizes a one-dimensional unsteady expansion for recombination rate studies.

The basic objective of the present investigation is to provide an analysis of the one-dimensional unsteady expansion of a reacting mixture of gases considering vibrational and dissociative nonequilibrium. The physical model of the expansion is that of the constant velocity withdrawal of a piston from a cylinder of gas which is initially in chemical equilibrium. The chemistry and thermodynamics of the problem are formulated generally so that various gas mixtures and reactions may be considered. A method of characteristics approach is used to obtain a numerical solution. The general thermodynamic relations are used with the equations of motion for the unsteady expansion to establish characteristic lines and compatibility relations

along the lines. Particular attention is given to the role of the speed of sound in a characteristic type solution. A numerical procedure is developed for calculation of the flow field using the characteristic network. The procedure is then programed in Fortran language so that solutions may be obtained using the IBM 7094 electronic digital computer.

The solution of a typical unsteady expansion in an oxygen nitrogen mixture is presented to illustrate the general structure of such an expansion. The variations of thermodynamic properties, velocities and compositions through the expansion fan are depicted for gas particles having different residence times in the expansion, thus illustrating the effects of nonequilibrium on the expansion. For small times of residence, the flow is nearly frozen; for large residence times, the flow approaches that of an equilibrium expansion. The structure of the nearly constant property region between the tail of the expansion fan and the piston face is also calculated and evaluated.

Cases are presented which demonstrate the usefulness of the method of solution in analyzing problems of current interest. The program is used to evaluate a case typical of expansion tube operation with air as the test medium. The implications of these results are discussed. An experiment is proposed for utilizing an unsteady expansion to process a gas for recombination rate studies. A solution is presented for an argon oxygen mixture which demonstrates the feasibility of the proposed experiment.

The objective of the present investigation is not to tabulate numerical solutions of unsteady expansions over a wide range of input conditions. It is intended instead to provide the basic background and establish a method of solution in a form general enough to treat many cases involving different component species of gases and the associated reactions. The results are intended therefore to illustrate the basic structure of a nonequilibrium unsteady expansion, to evaluate the overall effects of the nonequilibrium processes, and to demonstrate the utility of the method of solution in dealing with problems of current interest.

REVIEW OF LITERATURE

The centered one-dimensional unsteady expansion of a perfect gas has been treated by a number of authors. A good physical description of such a process is found in the books of Liepmann and Roshko (1957), Patterson (1956), and Courant and Friedrichs (1948). Excellent discussions of hyperbolic systems of equations and the use of the method of characteristics in obtaining solutions for such systems are given by Courant and Friedrichs (1948). Roberts (1947) presents a number of detailed methods for applying characteristic type solutions to unsteady flow problems. The Lagrangian coordinate system is described in the work of Courant and Friedrichs (1948) and Lamb (1932).

A number of gas models have been used to represent reacting flow. These models range from the simplified "ideal dissociating gas" developed by Lighthill (1957), Freeman (1958), and Bray (1958), to the complicated multi-component, multi-reaction gas used by Hall *et al.* (1962). The model proposed by Vincenti (1961) and used by Der (1963) is very useful in that it is capable of treating a number of reacting species and reactions while retaining certain simplifying assumptions that make calculation easier.

A great deal of discussion has appeared in the literature concerning the correct speed of sound for use with a reacting gas mixture. Comments on this problem have been presented by Resler (1956), Resler (1957), and Wood and Kirkwood (1957). The work of Chu (1957) makes a major contribution to the understanding of sound speed in a reacting gas. Vincenti (1961) and Clarke and McChesney (1964) have elaborated

on the findings of Chu. The role of sound speed in a characteristic type solution can be seen in the work of Broer (1960).

The first attempt to predict the structure of an unsteady expansion for nonequilibrium flow was made by Wood and Parker (1958). Their investigation treats a centered rarefraction wave in which only vibrational nonequilibrium is present. Appleton (1960a) extended their work by introducing the "ideal dissociating gas" of Lighthill and Freeman into the problem and thereby treating dissociative nonequilibrium. Arave (1963), using a similar gas model, calculated the structure of the expansion fan. A vibrational nonequilibrium case was treated by Appleton (1963) using a more realistic rate equation than that of Wood and Parker. Wierum (1962), Napolitano (1960), and Appleton (1960b) obtained near equilibrium and near frozen solutions for a similar problem, that of a Prandtl-Meyer expansion of a reacting gas. A characteristic type solution was used by Der (1963) to analyze the two-dimensional flow of a reacting gas down a nozzle.

The use of the one-dimensional unsteady expansion for the production of hypervelocity flow in an expansion tube was proposed by Trimpi (1962). The equilibrium analysis of such a facility was detailed by Trimpi and Grose (1963). Jacobs et al. (1963) proposed a means of measuring recombination rates in a flow processed by an unsteady expansion.

The literature survey revealed that a great deal of work remains to be done in the analysis of nonequilibrium unsteady expansions. The present investigation is intended to provide a general method of solution for such an expansion and to apply the method to realistic gas models in problems of current interest.

THEORETICAL DEVELOPMENT OF THE PROBLEM

Physical Model of the Expansion

A physical picture of a centered unsteady one-dimensional expansion is necessary for a complete understanding of the problem and its related boundary conditions. A description of the physical model used is given below. The process is illustrated in Figure 1.

Consider a semi-infinite reservoir of constant cross-sectional area containing a gas mixture in a state of chemical and thermodynamic equilibrium. At time zero, the piston is suddenly withdrawn with a constant velocity. A rarefaction wave is produced which propagates into the undisturbed gas in the reservoir. The first infinitesimal pressure pulse propagates into the gas with the velocity of the speed of sound in the undisturbed gas. This is followed by an infinite number of such pulses traveling at the speed of sound of the gas into which they are progressing. These infinitesimal pulses continue until the properties at a point in question are identical with those at the piston face. Figure 1 graphically depicts the structure of the expansion in distance-time coordinates. For the perfect gas case, the centered rays of the expansion are straight lines along which the flow properties are constant. Particle paths are indicated on the x-t diagram by dashed lines.

Temperatures and pressures decrease rapidly during the passage of the rarefaction wave. If the reservoir gas existed initially in a dissociated state, the atoms must recombine as they are processed by the expansion if chemical equilibrium is to be maintained. In like

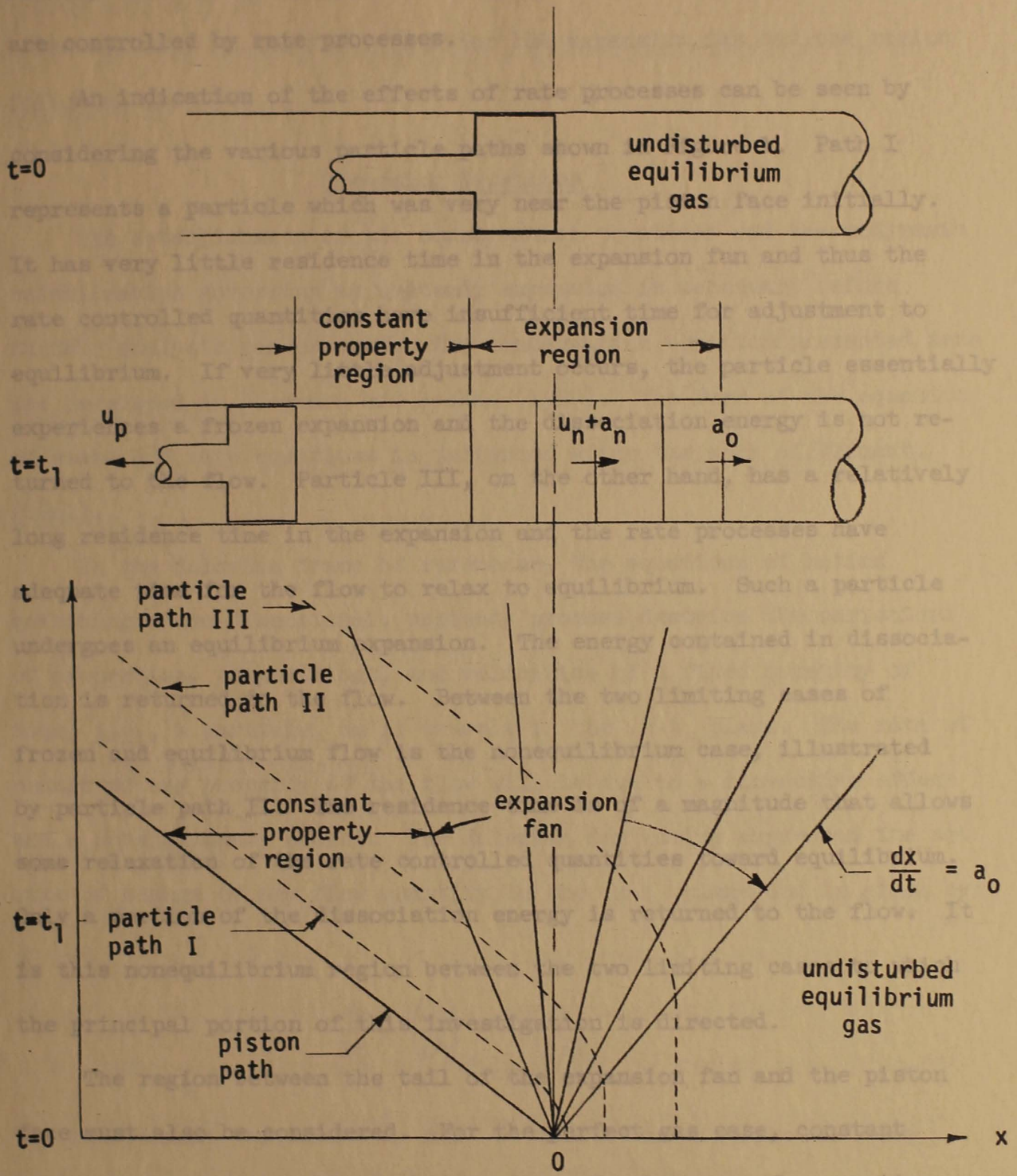

Figure 1. Distance-time diagram of an unsteady expansion

manner, the vibrational energy must decrease. Both of these phenomena are controlled by rate processes.

An indication of the effects of rate processes can be seen by considering the various particle paths shown in Figure 1. Path I represents a particle which was very near the piston face initially. It has very little residence time in the expansion fan and thus the rate controlled quantities have insufficient time for adjustment to equilibrium. If very little adjustment occurs, the particle essentially experiences a frozen expansion and the dissociation energy is not returned to the flow. Particle III, on the other hand, has a relatively long residence time in the expansion and the rate processes have adequate time for the flow to relax to equilibrium. Such a particle undergoes an equilibrium expansion. The energy contained in dissociation is returned to the flow. Between the two limiting cases of frozen and equilibrium flow is the nonequilibrium case, illustrated by particle path II. The residence time is of a magnitude that allows some relaxation of the rate controlled quantities toward equilibrium. Only a portion of the dissociation energy is returned to the flow. It is this nonequilibrium region between the two limiting cases to which the principal portion of this investigation is directed.

The region between the tail of the expansion fan and the piston face must also be considered. For the perfect gas case, constant properties exist throughout this region. In the case of a reacting gas, the properties in this region vary somewhat due to the relaxation of the rate controlled quantities.

The present investigation is designed to evaluate the existence of nonequilibrium in the flow, both for the expansion fan and the region following it.

Governing Equations

The establishment of the conservation equations and thermodynamic relationships governing an unsteady expansion is necessary before further analysis can proceed. The conservation equations presented here are developed in Liepmann and Roshko (1957). The form of the equation of state and rate equations is patterned after the work of Vincenti (1961).

In the Eulerian frame of reference, the equations of motion governing a one-dimensional, unsteady process describe the variations of properties, compositions, and velocities of a fixed quantity of mass, i.e., a particle, as it travels in the x-t plane. The rate of change of any property of the flow will be due to a convective effect and a nonstationary effect. The Eulerian derivative expresses the net rate of change of any flow quantity in the x-t plane and is given by:

$$\frac{D}{Dt} = \left(\frac{\partial}{\partial t}\right)_x + u\left(\frac{\partial}{\partial x}\right)_t$$

The independent variables x and t denote the distance and time coordinates and u represents the flow velocity in the x direction.

The following equations govern the motion of a particle moving in the x-t coordinate system.

Continuity Equation

The conservation of mass in one-dimensional unsteady flow is expressed by equation (1).

$$\frac{D\rho}{Dt} + \rho\left(\frac{\partial u}{\partial x}\right)_t = 0 \tag{1}$$

The density, in mass per unit volume, is expressed by ρ.

Momentum Equation

If body and viscous forces are neglected, the conservation of momentum is given by the expression,

$$\frac{Du}{Dt} + \frac{1}{\rho}\left(\frac{\partial P}{\partial x}\right)_t = 0, \tag{2}$$

where P denotes pressure.

Energy Equation

In this investigation, viscosity and heat conduction are neglected. The fixed quantity of mass considered is assumed to be a closed system, and while reactions may occur within the particle itself, there is no transfer of energy across the system boundaries due to heat transfer or chemical processes. Therefore, the energy equation for the fixed quantity of mass may be written as

$$\frac{Dh}{Dt} - \frac{1}{\rho}\frac{DP}{Dt} = 0, \tag{3}$$

where h represents enthalpy per unit mass.

Equation of State

The state of the reacting gas mixture can be expressed in the general form

$$h = h(P, \rho, q_1, \ldots, q_K). \tag{4}$$

The variables denoted by q_k are used to specify the vibrational and/or the chemical state of the gas. In actuality, these variables express the vibrational energy and/or the mass fraction of each component species in the gas mixture, that is,

$$q_1, \ldots, q_K = e_{v_1}, \ldots, e_{v_n}, x_1, \ldots, x_n, \tag{5}$$

where e_{v_i} is the vibrational energy per mole of the i^{th} specie, x_i is the mass fraction of the i^{th} specie and n is the total number of species. For convenience in handling the equations in the work to follow, q_k will be used to represent the vibrational and dissociative state of the gas. When more detailed operations are required, equation (5) will be introduced so that each variable can be treated in the proper manner.

For the nonequilibrium case, the value of q_k at any point in the flow will depend on the rate equations and the process which the gas has undergone. The subscripts e and f will be used to denote equilibrium and frozen conditions respectively. For equilibrium, q_k is a function of P and ρ and equation (4) may be written as

$$h_e = h\left[P, \rho, q_{k_e}(P, \rho)\right] = h_e(P, \rho) \tag{4a}$$

For frozen flow, there is insufficient time for any changes in the rate controlled quantities to occur, q_k is therefore constant and equation (4) becomes

$$h_f = h(P, \rho, q_k = \text{constant}) = h_f(P, \rho). \tag{4b}$$

The form of the equation of state given in equation (4) was chosen because of the simplicity it provides in further manipulations in the development of the characteristic equations.

Rate Equations

The rate equations can be expressed in the general form,

$$\frac{Dq_k}{Dt} = \omega_k, \tag{6}$$

where

$$\omega_k = \omega_k (P, \rho, q_1, \ldots, q_K),$$

and will later be presented in detail for each rate process considered.

Equations (1) through (6) comprise the set of basic governing equations for the unsteady one-dimensional expansion of a reacting gas mixture. Before proceding to develop the characteristics for this set of equations, it is useful to give some attention to the speed of sound in a reacting mixture.

Speed of Sound in a Reacting Gas Mixture

In any gas dynamic study, the speed of sound is a basic parameter. For nonequilibrium flow, the determination of the correct sound speed presents a new problem. No longer does an unambiguous sound speed exist as it did for the nonreacting gas. Special attention must be given to the role of sound speed in a reacting gas mixture.

The speed of sound is defined as the speed at which an infinitesimally small disturbance isentropically propagates through a gas. It is generally described by the expression

$$a^2 = \left(\frac{\partial P}{\partial \rho}\right)_s . \tag{7}$$

In the present nonequilibrium problem, the state of the gas can be established in terms of the variables P, ρ, and q_k. The entropy can therefore be expressed generally as

$$s = s(P, \rho, q_1, \ldots, q_K). \tag{8}$$

It then becomes evident that the expression given in equation (7) does not prescribe a unique value for the speed of sound, that is, more than one type of process exists in which an isentropic propagation of a disturbance can occur. The limiting cases of equilibrium and frozen sound speeds are discussed below. The speed of sound can be calculated for the constant entropy case in which q_k, representing the rate

controlled variables, always remains in a state of chemical equilibrium. For such a case, equation (7) becomes

$$a_e^2 = \left(\frac{\partial P}{\partial \rho}\right)_{s, q_k = q_{k_e}} \tag{9}$$

and a_e is referred to as the equilibrium speed of sound and the subscript e refers to equilibrium conditions. A constant entropy case may also exist in which q_k remains constant throughout the process. For this condition, equation (7) becomes the expression for the frozen speed of sound.

$$a_f^2 = \left(\frac{\partial P}{\partial \rho}\right)_{s, q_k} \tag{10}$$

A great deal of controversy exists in the literature concerning the roles played by the two limiting sound speeds, a_f and a_e, in the analysis of the flow of reacting gas mixtures. It is evident that the correct sound speed to use for a completely frozen flow is the frozen sound speed, a_f. In like manner, if the reactions are considered to be infinite, that is, the flow instantaneously adjusts to the equilibrium state, the equilibrium sound speed, a_e, appears to be the correct one to use. For nonequilibrium flow, however, the choice of a correct sound speed is not obvious.

In the present application, the derivation of the characteristic equations will establish the correct sound speed for the propagation of the characteristic lines. However, it is felt that some physical

argument should be given at this point to provide a better understanding of the mathematical results.

The works of Clarke and McChesney (1964) and Vincenti (1961) devote considerable attention to the question of sound speed in a reacting gas mixture. Their arguments are based primarily on the work of Chu (1957). Chu formulated the general equation describing the propagation of a plane acoustic wave. His analysis included the consideration of rate processes and their relaxation times. A harmonic disturbing force was assumed to exist and the propagation of the disturbance was analyzed. Chu's findings and their implications in the present problem are discussed below.

The phase velocity, a_p, of the velocity distrubance due to a harmonic wave of frequency ω, was shown to be dependent upon the product of the frequency ω, and the relaxation time, τ, of the rate process. As the product $\omega\tau$ becomes large, the phase velocity was found to approach the frozen sound speed, a_f; as $\omega\tau$ approaches zero, the phase velocity was found to approach the equilibrium sound speed, a_e.

The damping effect of the nonequilibrium process on the velocity disturbance was also evaluated as a function of wavelength. It was found that the amplitude attenuation increases as the frequency increases. It was also shown that as the relaxation time approaches zero and infinity for the respective cases of equilibrium and frozen flow, no attenuation of the amplitude of the disturbance occurs.

The propagation of an acoustic disturbance will now be examined in the light of these findings. The disturbance can be represented

by a series of harmonic waves comprised of both high and low frequency elements. The disturbance will be considered for the case of complete equilibrium, the case in which the flow is frozen, and the case in which nonequilibrium exists as the flow is processed by the disturbance.

For the case of equilibrium flow, the relaxation time, τ, is zero. Therefore, the product $\omega\tau$ is zero for each separate wave making up the disturbance no matter what the frequency of the wave is. Since $\omega\tau$ is zero, the phase velocity of each wave is that of the equilibrium sound speed and the amplitude of the disturbance is unattenuated.

If the flow remains completely frozen during the passage of the disturbance, $\tau \to \infty$, and thus $\omega\tau \to \infty$ for waves of all frequencies. The phase velocity of all waves and thus the velocity of the disturbance is then a_f and the amplitude is unattenuated.

The nonequilibrium case is more complicated. The relaxation time, τ, has a finite value greater than zero as does the product, $\omega\tau$. The high frequency waves propagate with a wave velocity approaching a_f and experience considerable attenuation (the amount is dependent upon the relaxation time and the wave frequency). The phase velocity of the lower frequency waves approach a_e and their amplitudes are attenuated less. Because their amplitudes are attenuated less, the low frequency waves carry the larger portion of the disturbance in the flow. In the case of near-equilibrium flow, the low frequency waves propagate at the velocity a_e and carry the bulk of the disturbance through the fluid. Figure 2 illustrates the propagation of a disturbance for the three cases considered.

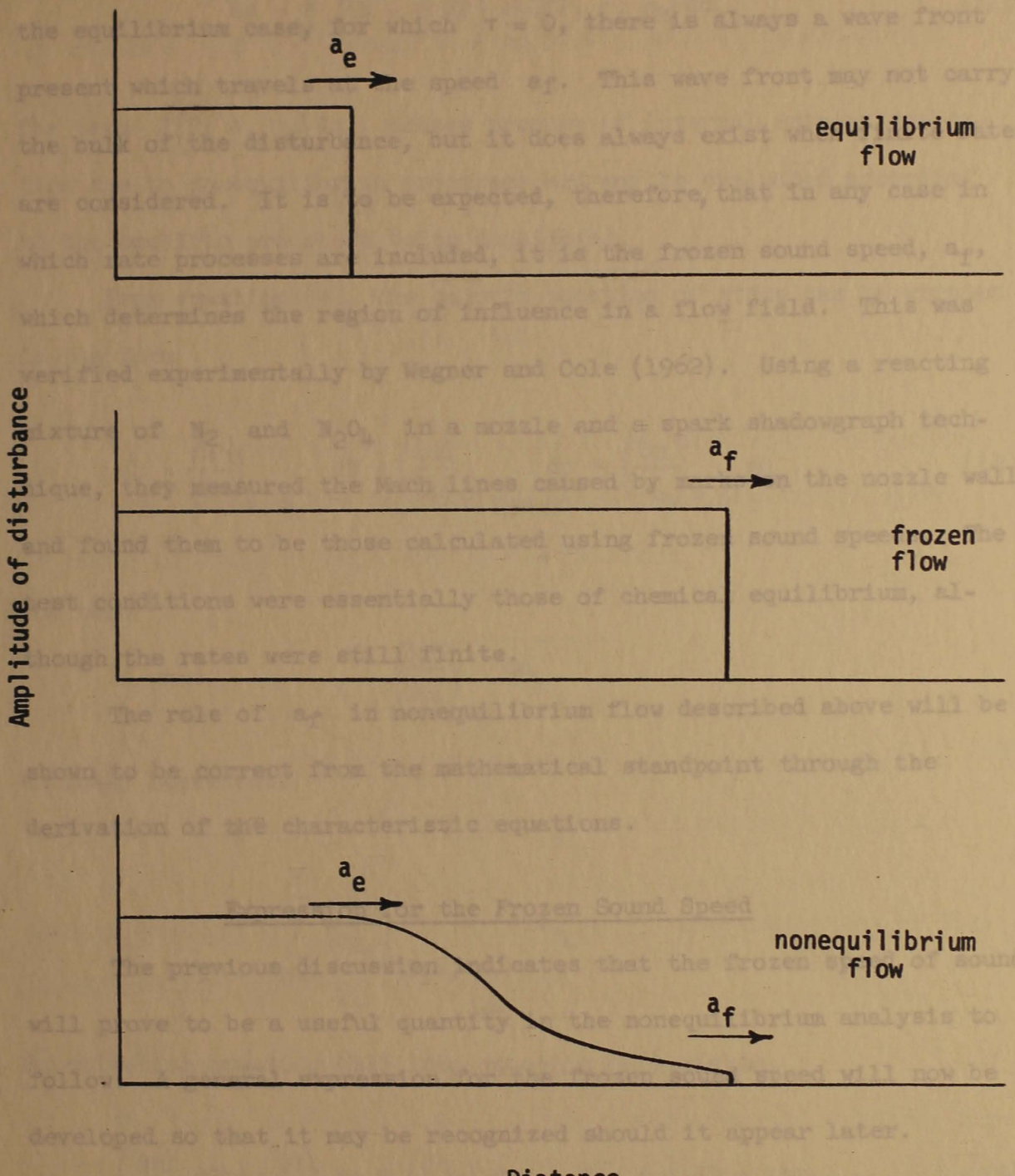

Figure 2. Disturbance propagation in reacting flows

From the above discussion, it can be concluded that except for the equilibrium case, for which $\tau = 0$, there is always a wave front present which travels at the speed a_f. This wave front may not carry the bulk of the disturbance, but it does always exist when finite rates are considered. It is to be expected, therefore, that in any case in which rate processes are included, it is the frozen sound speed, a_f, which determines the region of influence in a flow field. This was verified experimentally by Wegner and Cole (1962). Using a reacting mixture of N_2 and N_2O_4 in a nozzle and a spark shadowgraph technique, they measured the Mach lines caused by marks on the nozzle walls and found them to be those calculated using frozen sound speeds. The test conditions were essentially those of chemical equilibrium, although the rates were still finite.

The role of a_f in nonequilibrium flow described above will be shown to be correct from the mathematical standpoint through the derivation of the characteristic equations.

Expression for the Frozen Sound Speed

The previous discussion indicates that the frozen speed of sound will prove to be a useful quantity in the nonequilibrium analysis to follow. A general expression for the frozen sound speed will now be developed so that it may be recognized should it appear later.

For a reacting mixture of gases in nonequilibrium, the combined first and second laws of thermodynamics for a closed system can be written in the following form

$$ds = \frac{1}{T}\left(dh - \frac{1}{\rho}dP\right) + J\left(P,\ \rho,\ q_k\right)dq_k. \tag{11}$$

The term $J\left(P,\ \rho,\ q_k\right)dq_k$ arises because of internal entropy generation due to nonequilibrium processes and may be evaluated according to the specific processes being considered.

From equation (4), the caloric equation of state can be written in the form

$$dh = \left(\frac{\partial h}{\partial P}\right)_{\rho, q_k} dP + \left(\frac{\partial h}{\partial \rho}\right)_{P, q_k} d\rho + \left(\frac{\partial h}{\partial q_k}\right)_{P,\rho} dq_k. \tag{12}$$

The term

$$\left(\frac{\partial h}{\partial q_k}\right)_{P,\rho} dq_k$$

actually represents

$$\sum_{k=1}^{K} \left(\frac{\partial h}{\partial q_k}\right)_{P,\rho,\, q_l \atop l \neq k} dq_k .$$

Substituting equation (12) into equation (11) yields

$$\left(\frac{\partial h}{\partial P}\right) dP + \left(\frac{\partial h}{\partial \rho}\right) d\rho + \left(\frac{\partial h}{\partial q_k}\right) dq_k = Tds + \frac{1}{\rho} dP + J dq_k. \tag{13}$$

If the rate controlled quantities are considered frozen, that is, q_k is constant, and the process is isentropic, ds = 0, equation (13) becomes

$$\left(\frac{\partial P}{\partial \rho}\right)_{s,q_k} = \frac{\left(\frac{\partial h}{\partial \rho}\right)_{P,q_k}}{\frac{1}{\rho} - \left(\frac{\partial h}{\partial P}\right)_{\rho,\,q_k}} . \tag{14}$$

The left side of the above equation is immediately recognized to be the square of the frozen sound speed, a_f. The frozen speed of sound may then be expressed by the relation

$$a_f = \sqrt{\frac{\left(\frac{\partial h}{\partial \rho}\right)_{P,q_k}}{\frac{1}{\rho} - \left(\frac{\partial h}{\partial P}\right)_{\rho,q_k}}} . \tag{15}$$

This expression will prove to be of value in the development of the characteristic equations which follows.

Characteristic Equations in the x-t Plane

The basic equations governing the one-dimensional unsteady flow of an inviscid gas have been established. At this point, no restrictions have been made concerning the chemical, vibrational, or electronic state of the gas. A general method of solution of the governing

equations must now be developed. The complexity of the equations involved dictates the use of a numerical method in obtaining a practical solution. The following discussion forms the foundation for such a method.

The set of governing equations (1), (2), (3), and (6) comprise a system of quasi-linear partial differential equations which are hyperbolic in nature. For such a system, the possibility arises of constructing a solution utilizing the special properties of characteristic curves. Real valued characteristics exist for a hyperbolic system of equations. The method of characteristics then appears to be a logical tool for use in obtaining a solution. The meaning of the characteristics for a system of differential equations is discussed below.

Characteristic curves for a flow field are defined as lines across which the properties and velocities of the flow must be continuous, but across which the derivatives of the flow properties need not exist. More generally, this means that the solution of the governing equations must be continuous everywhere, but that the normal derivatives of any order can be discontinuous across the characteristic lines.

If such characteristic lines exist, the governing equations become ordinary differential equations along these lines, in other words, they may be written without containing any partial derivatives of the dependent variables. In the present problem, three characteristic directions exist with corresponding compatibility equations. The compatibility relations are ordinary first-order differential equations.

The original task of solving a complicated system of partial differential equations can therefore be reduced to the relatively easy task of simultaneously solving sets of ordinary differential equations.

Nonequilibrium Characteristics

The procedure for obtaining the characteristic curves and compatibility relationships from the set of equations, (1), (2), (3), and (6), governing nonequilibrium unsteady flow is described in detail in Appendix A. The work presented there establishes the existence of three characteristic directions. These directions will be denoted by +, -, and o.

Along the + characteristic curve given by

$$\left(\frac{dx}{dt}\right)_+ = u + a_f, \tag{16}$$

the compatibility equation,

$$\frac{dP}{dt} + \rho a_f \frac{du}{dt} - a_f^2 \left[\frac{\sum_{k=1}^{K} \left(\frac{\partial h}{\partial q_k}\right) \omega_k}{\left(\frac{\partial h}{\partial \rho}\right)} \right] = 0, \tag{17}$$

applies. In the - characteristic direction,

$$\left(\frac{dx}{dt}\right)_- = u - a_f, \tag{18}$$

the equation,

$$\frac{dP}{dt} - \rho a_f \frac{du}{dt} - a_f^2 \left[\frac{\sum_{k=1}^{K} \left(\frac{\partial h}{\partial q_k} \right) \omega_k}{\left(\frac{\partial h}{\partial \rho} \right)} \right] = 0, \tag{19}$$

must be satisfied.

It should be remembered that the frozen speed of sound, a_f, appearing in the above equations, is the local value at any point defined by equation (15) and varies throughout the flow field.

The particle path is identical to the o characteristic and is described by the equation

$$\left(\frac{dx}{dt} \right)_o = u. \tag{20}$$

Along the particle path the energy and rate equations become the ordinary differential equations

$$\frac{dh}{dt} - \frac{1}{\rho} \frac{dP}{dt} = 0 \tag{21}$$

and

$$\frac{dq_k}{dt} = \omega_k. \tag{22}$$

It is interesting to compare the characteristic equations presented above to similar equations for the perfect gas case. The perfect gas characteristics show that along

$$\left(\frac{dx}{dt}\right)_+ = u + a \tag{16a}$$

$$\frac{dP}{dt} + \rho a \frac{du}{dt} = 0 \tag{17a}$$

and along

$$\left(\frac{dx}{dt}\right)_- = u - a \tag{18a}$$

$$\frac{dP}{dt} - \rho a \frac{du}{dt} = 0. \tag{19a}$$

It can be seen that in the nonequilibrium case the frozen speed of sound, a_f, assumes the role of the perfect gas unambiguous sound speed, a, in determining the directions of the characteristic lines. The compatibility equations, however, are not analogous for the two cases due to the addition in the nonequilibrium case of the term

$$-a_f^2 \left[\frac{\sum_{k=1}^{K} \left(\frac{\partial h}{\partial q_k}\right) \omega_k}{\left(\frac{\partial h}{\partial \rho}\right)} \right].$$

which is due to the inclusion of rate processes in the formulation of the problem.

Frozen Characteristics

Consider now the limiting case of frozen flow, the case in which the rate controlled quantities have no time in which to relax. For such a case, q_k is constant and $\omega_k = \frac{Dq_k}{Dt} = 0$. The characteristic equations, (16) through (22), reduce to the following. The characteristic curves are described by

$$\left(\frac{dx}{dt}\right)_+ = u + a_f \tag{16b}$$

and

$$\left(\frac{dx}{dt}\right)_- = u - a_f \tag{18b}$$

and the associated compatibility equations are

$$\frac{dP}{dt} + \rho a_f \frac{du}{dt} = 0 \tag{17b}$$

and

$$\frac{dP}{dt} - \rho a_f \frac{du}{dt} = 0. \tag{19b}$$

Along the particle path,

$$\left(\frac{du}{dt}\right)_o = u, \tag{20}$$

only the energy equation,

$$\frac{dh}{dt} - \frac{1}{\rho}\frac{dP}{dt} = 0, \tag{21}$$

need be considered since rates are no longer involved. For the frozen case, the frozen sound speed, a_f, is constant throughout the expansion. This limiting case then reduces simply to the perfect gas case in which frozen compositions and vibrational energies are used in the evaluation of the speed of sound.

Equilibrium Characteristics

If the flow is to remain in thermodynamic equilibrium throughout the expansion, all rate processes must be assumed to occur infinitely fast. The characteristic equations for the equilibrium expansion cannot be obtained as a limiting case of the nonequilibrium process since the equation of state required is equation (4a) instead of equation (4). Thus, a continuous variation from the nonequilibrium case to the equilibrium case as the relaxation times increase does not exist. The characteristic equations can be developed separately for the mathematical model of equilibrium and are given below for such a model.

Along the characteristic lines

$$\left(\frac{dx}{dt}\right)_{\pm} = u \pm a_e \tag{16c}$$

the compatibility equations are respectively,

$$\frac{dP}{dt} \pm \rho a_e \frac{du}{dt} = 0, \tag{23}$$

and along the particle path,

$$\left(\frac{dx}{dt}\right)_o = u, \tag{20}$$

the energy equation,

$$\frac{dh}{dt} - \frac{1}{\rho}\frac{dP}{dt} = 0, \tag{21}$$

applies.

The equilibrium characteristic equations are equivalent to the perfect gas characteristics with the perfect gas sound speed replaced by the local equilibrium speed of sound, a_e, defined by equation (9).

The characteristic equations for an unsteady expansion have been developed in the x-t plane. It will prove convenient in the numerical calculations to use characteristic equations in the Lagrangian coordinate system. Thus, before a specific gas model is defined and a numerical method of solution developed, the characteristic equations will be established for the Lagrangian frame of reference.

The Lagrangian System

Description of the Lagrangian Coordinates

The unsteady, one-dimensional flow problem could be approached using the characteristic equations in the Eulerian (x-t) coordinate system previously discussed. However, because of the difficulties which appear in establishing a particle path along which the rate and energy equations can be applied in the Eulerian system, it is advantageous to set up the problem in a Lagrangian coordinate system.

In the Lagrangian frame of reference, attention is given to what happens to an individual fluid particle in the course of time. Each individual fluid particle must, therefore, be labeled. In the present work, this labeling is accomplished in the following manner. Each particle is designated by its position coordinate x, in the x-t plane at some reference time, $t = t_o$. This value is called b, the Lagrangian coordinate specifying which particle is being considered. In other words, b equals the value of x for the particular particle when $t = t_o$.

The two independent variables in the Lagrangian coordinate system defined above, are therefore b and t.

Governing Equations in the Lagrangian System

In Appendix B, a transformation is established for going from the Eulerian to the Lagrangian coordinate system. Applying this transformation to the previously developed set of governing equations, the equivalent equations in the Lagrangian frame of reference are shown to be those listed below.

Continuity Equation.

$$\left(\frac{\partial u}{\partial b}\right)_t = -\frac{\rho_o}{\rho^2}\left(\frac{\partial \rho}{\partial t}\right)_b \tag{24}$$

Momentum Equation.

$$\rho_o \left(\frac{\partial u}{\partial t}\right)_b + \left(\frac{\partial P}{\partial b}\right)_t = 0 \tag{25}$$

Energy Equation.

$$\left(\frac{\partial h}{\partial t}\right)_b - \frac{1}{\rho}\left(\frac{\partial P}{\partial t}\right)_b = 0 \tag{26}$$

Equation of State.

$$h = h\,(P,\ \rho,\ q_1,\ \ldots,\ q_K) \tag{4}$$

Rate Equation.

$$\left(\frac{\partial q_k}{\partial t}\right)_b = \omega_k \tag{27}$$

Characteristic Equations for the Lagrangian System

The development of characteristic curves in the Lagrangian system and the compatibility relationships along these curves can be accomplished using the method presented in Appendix A for the Eulerian system. Following that procedure, it can be shown that along the +

characteristics described by

$$\left(\frac{db}{dt}\right)_+ = \frac{\rho a_f}{\rho_o}, \tag{28}$$

the compatibility relation is

$$\frac{dP}{dt} + \rho a_f \frac{du}{dt} - a_f^2 \left[\frac{\sum_{k=1}^{K} \left(\frac{\partial h}{\partial q_k}\right) \omega_k}{\left(\frac{\partial h}{\partial \rho}\right)} \right] = 0, \tag{29}$$

and along the - characteristic

$$\left(\frac{db}{dt}\right)_- = - \frac{\rho a_f}{\rho_o} \tag{30}$$

the relation,

$$\frac{dP}{dt} - \rho a_f \frac{du}{dt} - a_f^2 \left[\frac{\sum_{k=1}^{K} \left(\frac{\partial h}{\partial q_k}\right) \omega_k}{\left(\frac{\partial h}{\partial \rho}\right)} \right] = 0, \tag{31}$$

holds.

The particle path in the Lagrangian system is given by

$$\left(\frac{db}{dt}\right)_o = 0 \tag{32}$$

and along this path, the energy equation,

$$\frac{dh}{dt} - \frac{1}{\rho}\frac{dP}{dt} = 0, \tag{33}$$

and the rate equations, represented by

$$\frac{dq_k}{dt} = \omega_k, \tag{34}$$

must be satisfied.

The set of equations presented above serves as the basis from which a numerical solution can be developed. Since these equations are all of the first-order variety, they may be easily converted to finite difference form for use in a numerical method of solution.

Nondimensionalization of the Characteristic Equations

Before formulating the problem in finite difference form for the numerical solution, it is convenient to restate the characteristic equations in a form in which the variables are dimensionless. Such a step facilitates the computation necessary for a numerical solution and could in some cases allow generalization of the results obtained.

With this in mind, the following dimensionless quantities are defined. The bar denotes the dimensionless quantity. The zero subscript refers to the value of the quantity in the undisturbed gas before the piston is withdrawn and V_p denotes the piston velocity required for a complete frozen expansion to $P = 0$.

$$\bar{a}_f = \frac{a_f}{a_{f_o}} \qquad \bar{P} = \frac{P}{P_o} \qquad \bar{h} = \frac{h}{h_o}$$

$$\bar{u} = \frac{u}{V_p} \qquad \bar{b} = \frac{b}{b_o} \qquad \bar{t} = \frac{t}{t'} \tag{35}$$

The reference time t' is defined as follows:

$$t' = \frac{b_o}{a_{f_o}} \tag{36}$$

The reference length, b_o, is the x position of some reference particle when t is t_o.

Substituting the above expressions into equations (28) through (34) results in the equations given below. Along the lines described by

$$\left(\frac{d\bar{b}}{d\bar{t}}\right)_{\pm} = \pm \left(\frac{a_{f_o} t'}{b_o}\right) \bar{\rho}\, \bar{a}_f, \tag{37}$$

the associated compatibility equations can be written

$$\frac{d\bar{u}}{d\bar{t}} \pm \left(\frac{P_o}{\rho_o \, a_{f_o} \, V_p}\right)\left(\frac{1}{\bar{\rho}\,\bar{a}_f}\frac{d\bar{P}}{d\bar{t}}\right) \mp \left(\frac{a_{f_o}}{V_p}\right)\left(\frac{\bar{a}_f}{\bar{\rho}\,\frac{\partial \bar{h}}{\partial \bar{\rho}}}\right)\left[t' \sum_{k=1}^{K}\left(\frac{\partial h}{\partial q_k}\right)\omega_k\right] = 0. \qquad (38)$$

Along the particle path,

$$\left(\frac{d\bar{b}}{d\bar{t}}\right)_o = 0, \qquad (39)$$

the equations

$$\frac{d\bar{h}}{d\bar{t}} - \left(\frac{P_o}{h_o \rho_o}\right)\frac{1}{\bar{\rho}}\frac{d\bar{P}}{d\bar{t}} = 0 \qquad (40)$$

and

$$\frac{dq_k}{d\bar{t}} = (t')\,\omega_k \qquad (41)$$

apply.

For simplification of the numerical work, the dimensionless groups are defined in the following manner:

$$A_1 = \left(\frac{a_{f_o}\, t'}{b_o}\right) = 1 \qquad A_2 = \left(\frac{P_o}{\rho_o \, a_{f_o} \, V_p}\right)$$

$$A_3 = \left(\frac{a_{f_o}}{V_p}\right) \qquad A_4 = \left(\frac{P_o}{h_o \rho_o}\right). \tag{42}$$

For the complicated case of nonequilibrium flow, these parameters are of no obvious value in the development of scaling laws. The existence of simultaneous rate processes precludes the establishment of such laws. It is conceivable that a flow system governed by one basic rate process could be subjected to a parametric analysis and in such a situation the dimensionless groups listed above might prove to be of value.

The dimensionless characteristic equations of an unsteady expansion in the Lagrangian coordinate system take the following form: along the + characteristic curve,

$$\left(\frac{d\bar{b}}{dt}\right)_+ = A_1 \bar{\rho}\, \bar{a}_f, \tag{43}$$

the ordinary differential equation,

$$\frac{d\bar{u}}{dt} + A_2 \left(\frac{1}{\bar{\rho}\bar{a}_f} \frac{d\bar{P}}{dt}\right) - A_3 \left[\frac{\bar{a}_f t'}{\bar{\rho}\left(\frac{\partial h}{\partial \rho}\right)} \sum_{k=1}^{K} \left(\frac{\partial h}{\partial q_k}\right) \omega_k\right] = 0 \tag{44}$$

must be satisfied; along the - characteristic,

$$\left(\frac{d\bar{b}}{dt}\right)_- = -A_1 \bar{\rho}\, \bar{a}_f, \tag{45}$$

the compatibility relation is

$$\frac{d\bar{u}}{d\bar{t}} - A_2\left(\frac{1}{\bar{\rho}\ \bar{a}_f}\frac{d\bar{P}}{d\bar{t}}\right) + A_3\left[\frac{\bar{a}_f t'}{\bar{\rho}\left(\frac{\partial \bar{h}}{\partial \bar{\rho}}\right)}\sum_{k=1}^{K}\left(\frac{\partial h}{\partial q_k}\right)\omega_k\right] = 0; \tag{46}$$

and along the particle path

$$\frac{d\bar{b}}{d\bar{t}} = 0, \tag{47}$$

the energy equation and the rate equations may be written as

$$\frac{d\bar{h}}{d\bar{t}} - \frac{A_4}{\bar{\rho}}\frac{d\bar{P}}{d\bar{t}} = 0 \tag{48}$$

and

$$\frac{dq_k}{d\bar{t}} = (t')\ \omega_k. \tag{49}$$

Equations (43) through (49) make up the set of characteristic equations which will provide the basis for the numerical analysis of the problem. One further modification can be made to simplify the analysis and will now be introduced.

Modified Lagrangian System

It will become evident in the work to follow that the application of the boundary conditions to the problem can be implemented by a

slight modification of coordinate systems. This modification is accomplished by dividing the Lagrangian particle coordinate b by the time variable t to define a new variable y, that is, y is defined by the relation

$$y = \frac{b}{t}. \tag{50}$$

The independent variables of the modified Lagrangian system are then y and t. Use of such a coordinate system eliminates the singularity which exists as $t \to 0$ and allows the boundary conditions to be applied for this condition. In addition, the network of grid points becomes more nearly rectangular in the y-t coordinates.

Replacing b by yt in equations (43) through (49), the compatibility equations remain the same and equations (43), (45), and (47), which establish the characteristic curves, become

$$\left[\frac{d(\bar{y}\bar{t})}{d\bar{t}}\right]_+ = A_1 \bar{\rho} \bar{a}_f, \tag{51}$$

$$\left[\frac{d(\bar{y}\bar{t})}{d\bar{t}}\right]_- = -A_1 \bar{\rho} \bar{a}_f \tag{52}$$

and

$$\left[\frac{d(\bar{y}\bar{t})}{d\bar{t}}\right]_o = 0 \tag{53}$$

respectively.

Equations (51), (44), (52), (46), (53), (48), and (49) make up the set of characteristic equations which, after conversion to finite difference form, will be used to obtain a numerical solution. Before proceding to obtain such a solution, the boundary conditions of the problem must be considered.

Boundary Conditions

The boundary conditions play an important part in the analysis of the present problem. In applying the method of characteristics, lines of initial data are needed to provide a starting point for the calculations. Three boundary conditions must be prescribed in the present case to permit a solution. Of these conditions, two will be used in the calculation of the expansion fan and the other in the analysis of the near-steady region between the tail of the expansion fan and the piston face. The physical reasoning supporting the selection of the prescribed boundary conditions is presented below with the listing of the conditions.

Two basic boundary conditions are prescribed for the expansion region. First, the undisturbed gas in the reservoir is assumed to be in a state of thermodynamic equilibrium. This is equivalent to saying that at $t=0$, that is, before the piston is withdrawn, the equilibrium properties of the gas mixture can be calculated. The application of this condition can be understood more completely by considering it in each of the coordinate systems which have been discussed. Referring to Figure 3, it can be seen that this boundary

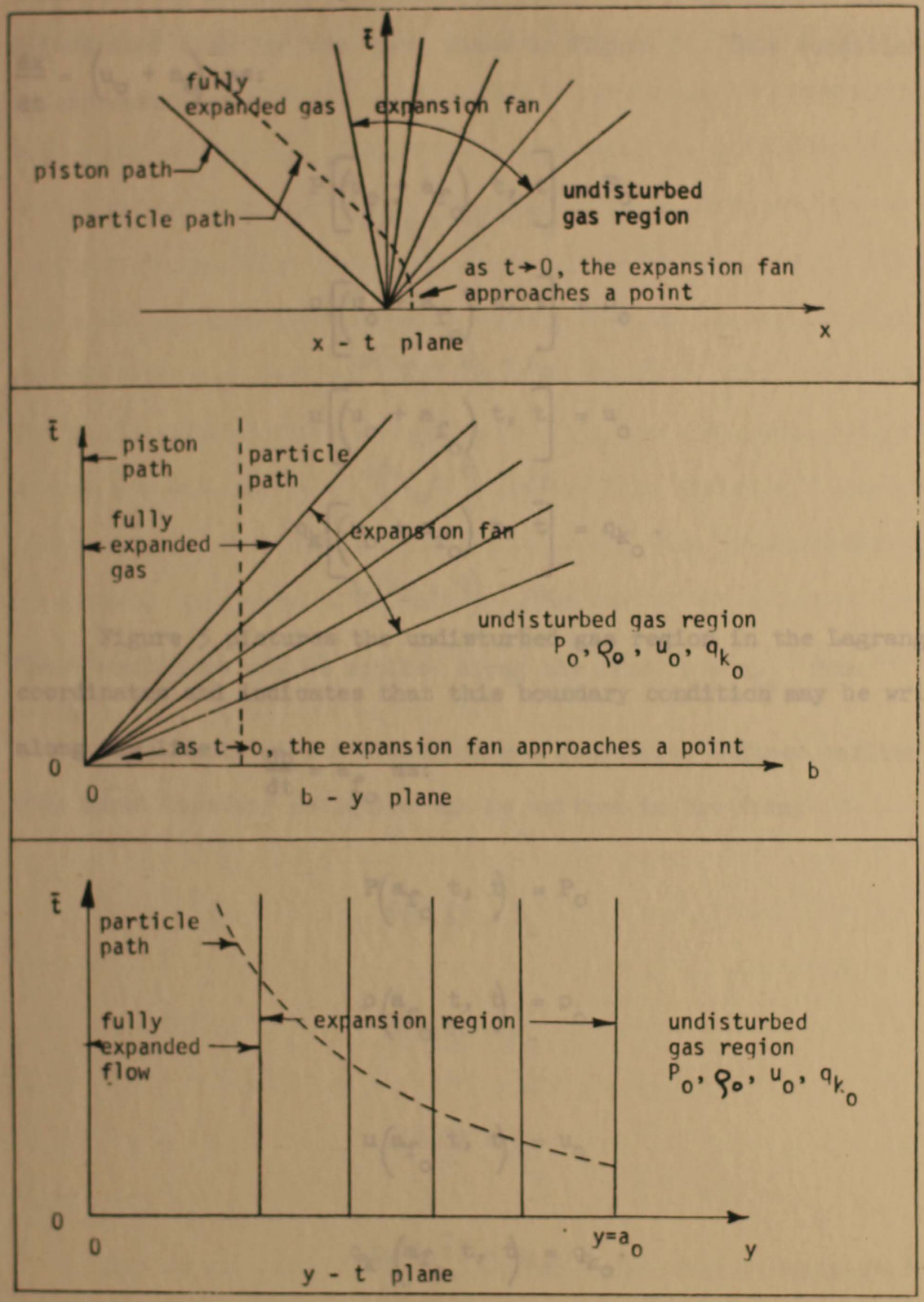

Figure 3. Boundary conditions in the three coordinate systems

condition in the x-t plane can be written along the line $\frac{dx}{dt} = \left(u_o + a_o\right)$ as:

$$
\begin{aligned}
P\left[\left(u_o + a_{f_o}\right) t,\ t\right] &= P_o \\
\rho\left[\left(u_o + a_{f_o}\right) t,\ t\right] &= \rho_o \\
u\left[\left(u_o + a_{f_o}\right) t,\ t\right] &= u_o \\
q_k\left[\left(u_o + a_{f_o}\right) t,\ t\right] &= q_{k_o} .
\end{aligned}
\tag{54}
$$

Figure 3 pictures the undisturbed gas region in the Lagrangian coordinates and indicates that this boundary condition may be written along the line $\frac{db}{dt} = a_{f_o}$ as:

$$
\begin{aligned}
P\left(a_{f_o} t,\ t\right) &= P_o \\
\rho\left(a_{f_o} t,\ t\right) &= \rho_o \\
u\left(a_{f_o} t,\ t\right) &= u_o \\
q_k\left(a_{f_o} t,\ t\right) &= q_{k_o} .
\end{aligned}
\tag{55}
$$

The equilibrium boundary condition for the undisturbed gas is illustrated also for the y-t plane in Figure 3. This condition can be expressed as:

$$P\left(a_{f_o}, t\right) = P_o$$

$$\rho\left(a_{f_o}, t\right) = \rho_o \tag{56}$$

$$u\left(a_{f_o}, t\right) = u_o$$

$$q_k\left(a_{f_o}, t\right) = q_{k_o}.$$

These conditions can be applied along the line $y = a_{f_o}$ from $t=0 \rightarrow \infty$. In terms of the dimensionless quantities defined earlier, this first boundary condition can be written in the form;

$$\bar{P}(1,\bar{t}) = \bar{P}_o$$

$$\bar{\rho}(1,\bar{t}) = \bar{\rho}_o \tag{57}$$

$$\bar{u}(1,\bar{t}) = \bar{u}_o$$

$$q_k(1,\bar{t}) = q_{k_o},$$

which will be used in the numerical analysis.

The second boundary condition is obtained by considering the unsteady expansion as $t \to 0$. A particle processed by the expansion for such a condition will have a residence time in the expansion which also approaches zero. The particles adjacent to the piston face experience such an expansion. Because of these short residence times, no relaxation of the rate controlled quantities will occur. Thus, as $t \to 0$, it seems reasonable to assume that the properties throughout the process will be those of a frozen expansion. This assumption is mathematically verified in Appendix C. In the x-t and b-t coordinate systems, as $t \to 0$, the + characteristic curves all converge to one point, thus making it difficult to apply this frozen boundary condition. As Appendix C indicates, the use of the modified coordinate system with the independent variables $\bar{y}$ and $\bar{t}$ allows the boundary condition to be written as follows:

$$\bar{P}\,(\bar{y},\, 0) = \bar{P}_f\,(\bar{y})$$

$$\bar{\rho}\,(\bar{y},\, 0) = \bar{\rho}_f\,(\bar{y}) \qquad (58)$$

$$\bar{u}\,(\bar{y},\, 0) = \bar{u}_f\,(\bar{y})$$

$$q_k\,(\bar{y},\, 0) = q_{k_f}$$

The frozen values $\bar{P}_f$, $\bar{\rho}_f$, and $\bar{u}_f$ are readily calculated for the desired values of $\bar{y}$ using the expressions developed in Appendix C.

The values of q_{k_f}, of course, remain constant at the initial undisturbed values of q_k for the frozen boundary condition.

A final boundary condition is needed to permit the calculation of the region of near-steady flow between the expansion fan and the piston face. The condition required is that the gas velocity at the piston face is that of the piston. Such a condition must exist provided no cavitation exists. Properly chosen input properties will insure that this is true.

The characteristic equations and boundary conditions for the nonequilibrium unsteady expansion have been established. An adequate thermodynamic model must now be developed to describe the reacting gas mixture and allow numerical computation.

Thermodynamic Model of the Reacting Gas Mixture

Up to this point, very few restrictions have been placed on the gas mixture. The equation of state and rate equations have been taken to be of the general forms given by equations (4) and (6). It is necessary at this stage of the investigation to develop specific relationships for the thermodynamic properties of the reacting gas and to establish detailed rate expressions for the various nonequilibrium processes. This development will begin with the equation of state of the gas.

Thermal Equation of State

The reacting gas is assumed to be made up of a mixture of perfect gases (i.e., no intermolecular forces are considered). The pressure

of the mixture is, therefore, equal to the sum of the partial pressures of the component species. The thermal equation of state can therefore be written as

$$P = \frac{\rho RT}{\mu} \tag{59}$$

where

$$\mu = \left(\sum_{i=1}^{n} \frac{x_i}{\mu_i} \right)^{-1}, \tag{60}$$

R is the universal gas constant and x_i and μ_i are the mass fraction and molecular weight of i^{th} species respectively.

Internal Energy

The internal energy of the gas contains the contributions from translational, rotational, vibrational, and electronic energy modes plus the energies of dissociation and ionization. If E is used to denote the energy per unit mass, the internal energy can be expressed as

$$E = E_{TRANS} + E_{ROT} + E_{VIB} + E_{EL} + E_{DISS} + E_{IONIZ}. \tag{61}$$

Since a mixture of perfect gases is being considered, the internal energy of the mixture is equal to the sum of the internal energies of the component species. Thus, equation (61) may be written

$$E = \sum_{i=1}^{n} \left(E_{TRAN_i} + E_{ROT_i} + E_{VIB_i} + E_{EL_i} + E_{DISS_i} + E_{IONIZ_i} \right). \tag{62}$$

A detailed evaluation of the contributions of the various energy modes to the internal energy is given in Appendix D. Several assumptions are inherent in the formulation of the expression for internal energy. Electronic excitation and ionization are neglected. Substituting the various contributions to the internal energy which are evaluated in Appendix D into equation (62), the internal energy of the reacting mixture of gases is described by the relationship

$$E = \sum_{i=1}^{n} \frac{x_i}{\mu_i} \left[\frac{3}{2} RT + f_i \left(RT + e_{v_i} \right) + N_o \Delta_i \right], \qquad (63)$$

where T is the translational temperature of the gas, N_o is Avogadro's number, and Δ_i is the heat of formation in energy per molecule for the i^{th} specie. The factor f_i is used to permit the existence of rotational and vibrational energies for molecular species and to eliminate these energy modes for atomic species. For molecular species f_i assumes the value of one; for atomic species f_i is zero. The vibrational energy per mole is written in the general form e_{v_i} in this formulation of the internal energy expression. This provides an option for treating the vibrational energy as either a rate controlled or an equilibrium process later in the analysis. With the internal energy now established, it becomes a simple matter to obtain an expression for the enthalpy of the mixture.

Enthalpy

The assumption was made earlier in this analysis that the caloric equation of state could be written in the form

$$h = h\,(P,\ \rho,\ q_1,\ \ldots,\ q_K). \tag{4}$$

The variable q_k was used to represent all of the rate-controlled variables, in this case, the mass fractions and/or the vibrational energies of each specie of gas. Using the thermal equation of state, equation (59), the expression for internal energy may be written as

$$E = \sum_{i=1}^{n} \frac{x_i}{\mu_i}\left[\frac{3}{2}\frac{P\mu}{\rho} + f_i\left(\frac{P\mu}{\rho} + e_{v_i}\right) + N_o\Delta_i\right]. \tag{64}$$

Using the definition of enthalpy,

$$h = E + \frac{P}{\rho}, \tag{65}$$

the definition of the average molecular weight of the mixture as given by equation (60), and the expression for internal energy given above, it becomes apparent that the enthalpy in units of energy per unit mass of the mixture takes the form

$$h = \sum_{i=1}^{n} \frac{x_i}{\mu_i}\left[\frac{5}{2}\frac{P\mu}{\rho} + f_i\left(\frac{P\mu}{\rho} + e_{v_i}\right) + N_o\Delta_i\right]. \tag{66}$$

A specific caloric equation of state is then established which has the form originally assumed, that is

$$h = h\,(P,\ \rho,\ q_1,\ \ldots,\ q_K)\,. \tag{4}$$

This relationship permits the evaluation of the enthalpy derivatives which appear in the compatibility equations.

Enthalpy Derivatives

Before the characteristic equations can be used, the enthalpy derivatives which appear in them must be evaluated in terms of the gas model.

The frozen speed of sound, a_f, appears in the equations specifying the characteristic curves and the compatibility relations along these lines. Since the frozen speed of sound was shown to be

$$a_f = \sqrt{\frac{\left(\frac{\partial h}{\partial \rho}\right)_{P,q_k}}{\frac{1}{\rho} - \left(\frac{\partial h}{\partial P}\right)_{\rho,q_k}}} \tag{15}$$

it becomes necessary to evaluate

$\left(\frac{\partial h}{\partial \rho}\right)_{P,q_k}$ and $\left(\frac{\partial h}{\partial P}\right)_{\rho,q_k}$ in terms of P, ρ, and q_k.

Also, in using the nonequilibrium compatibility equations, equations (29) and (31), the term $\left(\frac{\partial h}{\partial q_k}\right)_{P,\rho,q_{l\neq k}}$ must be evaluated.

The development of these partial derivatives in terms of the postulated gas model is presented below. Two nonequilibrium states of the gas are considered, one in which both the dissociation and the vibrational energy are permitted to be in nonequilibrium and the other in which the vibrational energy remains in equilibrium with the translational energy and only the dissociation is rate controlled.

Case 1. Chemical and Vibrational Nonequilibrium. Consider first the case in which the compositions and the vibrational energies are rate controlled. For such a case, q_k includes the mass fractions, x_i, and the vibrational energies per mole, e_{v_i}, for each of the component species of the gas mixture. Therefore, the partial derivative $\left(\frac{\partial h}{\partial \rho}\right)_{P,q_k}$ can be written $\left(\frac{\partial h}{\partial \rho}\right)_{P,x_i,\ldots,x_n,\,e_{v_i},\ldots,e_{v_n}}$ and the partial $\left(\frac{\partial h}{\partial P}\right)_{\rho,q_k}$ is in reality $\left(\frac{\partial h}{\partial P}\right)_{\rho,x_i,\ldots,x_n,\,e_{v_i},\ldots,e_{v_n}}$.

The expression $\sum_{k=1}^{K}\left(\frac{\partial h}{\partial q_k}\right)\omega_k$ becomes for this case

$$\sum_{k=1}^{K}\left(\frac{\partial h}{\partial q_k}\right)\omega_k = \sum_{i=1}^{n}\left(\frac{\partial h}{\partial x_i}\right)_{P,\rho,e_{v_i},\ldots,e_{v_n},x_{l\neq i}}\frac{dx_i}{dt} + \sum_{i=1}^{n}\left(\frac{\partial h}{\partial e_{v_i}}\right)_{P,\rho,x_i,\ldots,x_n,e_{v_{l\neq i}}}\frac{de_{v_i}}{dt}. \tag{67}$$

The expression for enthalpy was given in equation (66) as

$$h = \sum_{i=1}^{n} \frac{x_i}{\mu_i} \left[\left(\frac{5}{2} + f_i \right) \frac{P\mu}{\rho} + N_o \Delta_i + f_i e_{v_i} \right] \tag{66}$$

where

$$\mu = \left(\sum_{i=1}^{n} \frac{x_i}{\mu_i} \right)^{-1}. \tag{60}$$

Using equation (66), $\left(\frac{\partial h}{\partial \rho}\right)_{P, q_k}$ and $\left(\frac{\partial h}{\partial P}\right)_{\rho, q_k}$ become

$$\left(\frac{\partial h}{\partial \rho}\right)_{P, q_k} = - \sum_{i=1}^{n} \frac{x_i}{\mu_i} \left(\frac{5}{2} + f_i \right) \frac{P\mu}{\rho^2} \tag{68}$$

and

$$\left(\frac{\partial h}{\partial P}\right)_{\rho, q_k} = \sum_{i=1}^{n} \frac{x_i}{\mu_i} \left(\frac{5}{2} + f_i \right) \frac{\mu}{\rho}. \tag{69}$$

Substituting these two expressions into equation (15), the sound speed for a gas mixture with frozen compositions and frozen vibrational energies may be written as:

$$a_f = \left[\frac{- \sum_{i=1}^{n} \frac{x_i}{\mu_i} \left(\frac{5}{2} + f_i \right) \frac{P\mu}{\rho^2}}{\frac{1}{\rho} - \frac{1}{\rho} \sum_{i=1}^{n} \frac{x_i}{\mu_i} \left(\frac{5}{2} + f_i \right) \mu} \right]^{\frac{1}{2}}. \tag{70}$$

Recalling the definition of μ, equation (60), reveals that $\mu \sum_{i=1}^{n} \frac{x_i}{\mu_i} = 1$. Thus a_f assumes the more convenient form

$$a_f = \left\{ \frac{P}{\rho} \left[\frac{\sum_{i=1}^{n} \frac{x_i}{\mu_i} \left(\frac{5}{2} + f_i \right)}{\sum_{i=1}^{n} \frac{x_i}{\mu_i} \left(\frac{3}{2} + f_i \right)} \right] \right\}^{\frac{1}{2}} . \tag{71}$$

It can readily be shown that the quantity in the square brackets is γ_f, the ratio of the frozen specific heats defined in the conventional way.

In order to evaluate $\sum_{k=1}^{K} \left(\frac{\partial h}{\partial q_k} \right) \omega_k$, the derivatives

$$\left(\frac{\partial h}{\partial x_i} \right)_{P,\rho,e_{v_i},\ \ldots,\ e_{v_n},x_l,\ l \neq i} \quad \text{and} \quad \left(\frac{\partial h}{\partial e_{v_i}} \right)_{P,\rho,x_i,\ \ldots,\ x_n,\ e_{v_l}\ l \neq i}$$

must first be evaluated. Differentiating equation (66) with respect to the mass fraction, x_i, of one specie with all other variables held constant yields

$$\frac{\partial h}{\partial x_i} = \left[\left(\frac{5}{2} + f_i \right) \frac{P\mu}{\rho\mu_i} + \frac{f_i\, e_{v_i}}{\mu_i} + \frac{N_o \Delta_i}{\mu_i} \right] + \left[\sum_{i=1}^{n} \frac{x_i}{\mu_i} \left(\frac{5}{2} + f_i \right) \frac{P}{\rho} \right] \frac{\partial \mu}{\partial x_i}$$

$$= \left[\left(\frac{5}{2} + f_i \right) \frac{P\mu}{\rho\mu_i} + \frac{f_i\, e_{v_i}}{\mu_i} + \frac{N_o \Delta_i}{\mu_i} \right] - \frac{\mu^2}{\mu_i} \left[\sum_{i=1}^{n} \frac{x_i}{\mu_i} \left(\frac{5}{2} + f_i \right) \frac{P}{\rho} \right] . \tag{72}$$

Following a similar procedure, it is readily seen that

$$\frac{\partial h}{\partial e_{v_i}} = \frac{x_i \, f_i}{\mu_i} .$$

The term, $\sum_{k=1}^{K} \left(\frac{\partial h}{\partial q_k} \right) \omega_k$, present in the compatibility equations (29) and (31) because of the rate processes in the flow, may then be expressed in the following manner for the case with dissociative and vibrational nonequilibrium.

$$\sum_{k=1}^{K} \left(\frac{\partial h}{\partial q_k} \right) \omega_k = \sum_{i=1}^{n} \left(\frac{\partial h}{\partial e_{v_i}} \right) \frac{de_{v_i}}{dt} + \sum_{i=1}^{n} \left(\frac{\partial h}{\partial x_i} \right) \frac{dx_i}{dt} = \sum_{i=1}^{n} \left\{ \left[\left(\frac{5}{2} + f_i \right) \frac{P\mu}{\rho \mu_i} + \frac{f_i \, e_{v_i}}{\mu_i} + \frac{N \Delta_{o\,i}}{\mu_i} \right] - \frac{\mu^2}{\mu_i} \frac{P}{\rho} \left[\sum_{i=1}^{n} \frac{x_i}{\mu_i} \left(\frac{5}{2} + f_i \right) \right] \right\} \frac{dx_i}{dt} + \sum_{i=1}^{n} \left(\frac{x_i \, f_i}{\mu_i} \right) \frac{de_{v_i}}{dt} \tag{73}$$

The rate equations, discussed subsequently, will provide expressions for $\frac{dx_i}{dt}$ and $\frac{de_{v_i}}{dt}$ in terms of thermodynamic properties, compositions, and vibrational energies. The above equation may then be used to evaluate the nonequilibrium term in the compatibility equations and thus make possible a solution by the method of characteristics.

Case 2. Chemical Nonequilibrium with Vibrational Equilibrium.

It is quite realistic for many problems to assume that the vibrational energy remains in equilibrium with the translational and rotational energy modes while the compositions of the various species are in a state of nonequilibrium. Such a case is admittedly only a mathematical model. However, if the vibrational relaxation is much more rapid than the chemical recombination process, this model is quite adequate for describing the flow.

If only the compositions are assumed to be rate controlled, q_k simply represents the mass fractions, x_i. The vibrational energy is assumed to be represented by a system of harmonic oscillators. In Appendix D, the expression for vibrational energy is developed using the partition function for such a model. An approximate expression is then postulated and shown to be quite accurate for expressing the vibrational energy. Substituting this approximate expression,

$$e_{v_i} = \beta_i \, RT + \beta_i', \tag{74}$$

into the enthalpy expression, equation (66), yields

$$h = \sum_{i=1}^{n} \frac{x_i}{\mu_i} \left[\left(\frac{5}{2} + f_i + \beta_i \right) \frac{P\mu}{\rho} + \beta_i' + N_o \Delta_i \right]. \tag{75}$$

For vibrational equilibrium and chemical nonequilibrium, the partial derivatives $\left(\frac{\partial h}{\partial \rho}\right)_{P, q_k}$ and $\left(\frac{\partial h}{\partial P}\right)_{\rho, q_k}$ may be written as

$$\left(\frac{\partial h}{\partial \rho}\right)_{P,q_k} = \left(\frac{\partial h}{\partial \rho}\right)_{P,x_1,\ \ldots,\ x_n} = -\frac{P\mu}{\rho^2}\sum_{i=1}^{n}\frac{x_i}{\mu_i}\left(\frac{5}{2} + f_i + \beta_i\right) \qquad (76)$$

and

$$\left(\frac{\partial h}{\partial P}\right)_{\rho,q} = \left(\frac{\partial h}{\partial P}\right)_{\rho,x_1,\ \ldots,x_n} = \frac{\mu}{\rho}\sum_{i=1}^{n}\frac{x_i}{\mu_i}\left(\frac{5}{2} + f_i + \beta_i\right). \qquad (77)$$

Using the two above equations and equation (15), the speed of sound considering the vibration in equilibrium and the composition frozen may be written as:

$$a'_f = \left\{\frac{P}{\rho}\left[\frac{\sum_{i=1}^{n}\frac{x_i}{\mu_i}\left(\frac{5}{2} + f_i + \beta_i\right)}{\sum_{i=1}^{n}\frac{x_i}{\mu_i}\left(\frac{3}{2} + f_i + \beta_i\right)}\right]\right\}^{\frac{1}{2}}. \qquad (78)$$

This expression will subsequently be used in equations (28) and (30) which establish the characteristic curves and in the compatibility relations, equations (29) and (31).

For the present case, the nonequilibrium term in the compatibility equations, $\sum_{k=1}^{K}\left(\frac{\partial h}{\partial q_k}\right)_{P,\rho}\omega_k$, becomes simply

$$\sum_{k=1}^{K}\left(\frac{\partial h}{\partial q_k}\right)_{P,\rho}\omega_k = \sum_{i=1}^{n}\left(\frac{\partial h}{\partial x_i}\right)_{P,\rho,x_l\ l\neq i}\frac{dx_i}{dt}$$

$$= \sum_{i=1}^{n}\left\{\left[\left(\frac{5}{2}+f_i+\beta_i\right)\frac{P\mu}{\rho\mu_i}+\frac{\beta_i'}{\mu_i}+\frac{N_o\Delta_i}{\mu_i}\right]\right.$$

$$\left.-\frac{P}{\rho}\frac{\mu^2}{\mu_i}\left[\sum_{i=1}^{n}\frac{x_i}{\mu_i}\left(\frac{5}{2}+f_i+\beta_i\right)\right]\right\}\frac{dx_i}{dt}. \qquad (79)$$

This expression is then used in the compatibility relations, equations (29) and (31), thus permitting the use of these equations in obtaining a numerical solution for the case of vibrational equilibrium and chemical nonequilibrium.

Rate Equations

It is necessary to establish general forms of the rate equations controlling vibrational relaxation and the dissociation-recombination chemical reactions. The rate equations were previously postulated to take the form

$$\frac{dq_k}{dt} = \omega_k\left(P,\ \rho,\ q_1,\ \cdots\ q_K\right). \qquad (6)$$

This expression must now be expanded to more specific terms for use in the solution of the problem.

Chemical Equations. A rate equation will first be established to describe the dissociation and recombination rates of the reacting gas species. Such an equation must be capable of handling a number of species, the associated reactions, and the catalytic species involved in the reaction.

The formulation of the chemical rate equations for a reacting system of this nature is discussed in detail by Penner (1957, p. 217). He states,

> "According to the law of mass action, the rate of production of a chemical species is proportional to the products of the concentrations of the reacting chemical species, each concentration being raised to a power equal to the corresponding stoichiometric coefficient."

If the rate expression proposed by Penner is written in terms of mass fractions instead of concentrations, and the contributions of each reaction are included, the rate of change of the mass fraction of species i may be expressed as

$$\frac{dx_i}{dt} = \sum_{j=1}^{m} \left(\frac{dx_i}{dt}\right)_j = \sum_{j=1}^{m} k_j \left(\frac{\mu_i}{\rho}\right) \left(\nu'_{ij} - \nu_{ij}\right) \prod_{i=1}^{n} \left(\frac{x_i \rho}{\mu_i}\right)^{\nu_{ij}} \tag{80}$$

where x_i = mass fraction of the i^{th} species,

j denotes the reaction,

ν_{ij} = stoichiometric coefficient of i^{th} species of reactant in j^{th} reaction,

ν_{ij} = stoichiometric coefficient of i^{th} species of product in the j^{th} reaction,

and k_j = specific reaction rate coefficient for the j^{th} reaction.

The specific reaction rate coefficient is assumed to be a function of temperature only. Following the manner of Penner (1957),

it is assumed to be an empirically determined coefficient which can be written in the following form for the forward (dissociation) reaction.

$$k_{f_j} = A_j \, T^{Bj} \exp\left(\frac{-E_j}{kT}\right) \tag{81}$$

The parameters A_j and B_j and the activation energy E_j are constants which were previously evaluated by experimental work. The best available values of these constants will be used for the reactions considered in this investigation. The values of the constants and their sources will be presented as specific reactions are considered.

The reverse (recombination) rate coefficient, k_{r_j}, is obtained by applying the law of mass action at equilibrium. The forward and reverse rates are equal for this condition and the reverse rate coefficient is given by

$$k_{r_{j+1}} = \frac{k_{f_j}}{K_{c_j}} \tag{82}$$

where K_{c_j} is the equilibrium constant based on concentrations for the j^{th} reaction.

The form of the chemical rate equation given by equation (80) is adequate for both forward and reverse reactions provided each is treated as a separate reaction.

Vibrational Rate Equation. For cases in which residence time is not adequate for the vibrational energy of a molecule to relax to the

equilibrium value, a rate equation must be used to describe the relaxation process. Vincenti (1961) presents a thorough discussion of the formulation of the vibrational rate equation. He develops an equation of the form

$$\frac{de_{v_i}}{dt} = \frac{e_{v_{e_i}} - e_{v_i}}{\tau} \tag{83}$$

where τ, which is a function of temperature and pressure, has the dimensions of time and is called the vibrational relaxation time. Landau and Teller (1936) derived a theory which predicts the relaxation time to be of the form

$$\tau_i = \frac{F_i \, T^{\frac{1}{6}} \exp\left(K_i / T^{\frac{1}{3}}\right)}{P\left[1 - \exp\left(-\theta_{v_i}/T\right)\right]}. \tag{84}$$

Since that time, a number of experimental measurements of τ have been made. Most of the available data can be represented using an expression similar to equation (84), namely

$$\tau_i = \frac{F_i \, T^{S_i} \exp\left(K_i / T^{\frac{1}{3}}\right)}{P\left[1 - \exp\left(-\theta_{v_i}/T\right)\right]}. \tag{85}$$

The characteristic vibrational temperature, θ_{v_i}, and the equilibrium vibrational energy, $e_{v_{ei}}$, are defined in Appendix D.

The vibrational rate equation and the relaxation time expression adopted for use in the present work are given by equations (83) and (85).

SOLUTION PROCEDURE

The objective now becomes that of developing a procedure by which the characteristic equations of the system may be utilized to obtain a numerical solution. Up to this point, the characteristic equations in the modified Lagrangian system have been developed from the conservation equations and the generalized equations of state for a one-dimensional unsteady expansion of a reacting gas mixture. The characteristic equations, in their dimensionless form, must now be converted to a finite difference form suitable for numerical calculations and a procedure established for obtaining a solution over the desired flow region. The procedure must then be programed in Fortran language for computation on the IBM 7094 electronic digital computer. The transition of the characteristic equations from their exact form to the form used in machine computation is developed in the discussion which follows.

Finite Difference Form of the Characteristic Equations

The equations prescribing the characteristic directions and the compatibility relationships in the modified Lagrangian coordinates must first be converted to finite difference form. Since these equations are all first order, this conversion is a fairly simple one.

Consider the function $f(t)$ with the derivative $\left(\frac{df}{dt}\right)_o$ at point O, midway between t_{-1} and t_{+1}. The finite difference form of the derivative may be written:

$$\left(\frac{df}{dt}\right)_o = \frac{1}{2\Delta t}\left(f_1 - f_{-1}\right) , \tag{86}$$

where Δt is the distance between t_{-1} and 0 or t_{+1} and 0, and f_1 and f_{-1} are the values of the function at t_1 and t_{-1}.

The general grid pictured in Figure 4 establishes the nomenclature which will be used. The utilization of this grid in the calculation of the entire flow region will be discussed later. In using this grid, the finite difference expression is used to represent the derivatives at points midway between two grid points. Other quantities appearing in the differential equations are assumed to be the average of the values at the two grid points.

Using the nomenclature of Figure 4 and the finite difference approximations, the characteristic equations may be written in the form below.

The characteristic direction of line AP prescribed by

$$\frac{d(\bar{y}\bar{t})}{d\bar{t}} = A_1\,\bar{\rho}\,\bar{a}_f \tag{51}$$

is expressed in finite difference form as:

$$\bar{y}_P\,\bar{t}_P - \bar{y}_A\,\bar{t}_A = A_1\left[\bar{\rho}\,\bar{a}_f\right]_{AP}\left(\bar{t}_P - \bar{t}_A\right). \tag{87}$$

The finite difference form of the compatibility relation, equation (44), along the characteristic line AP becomes

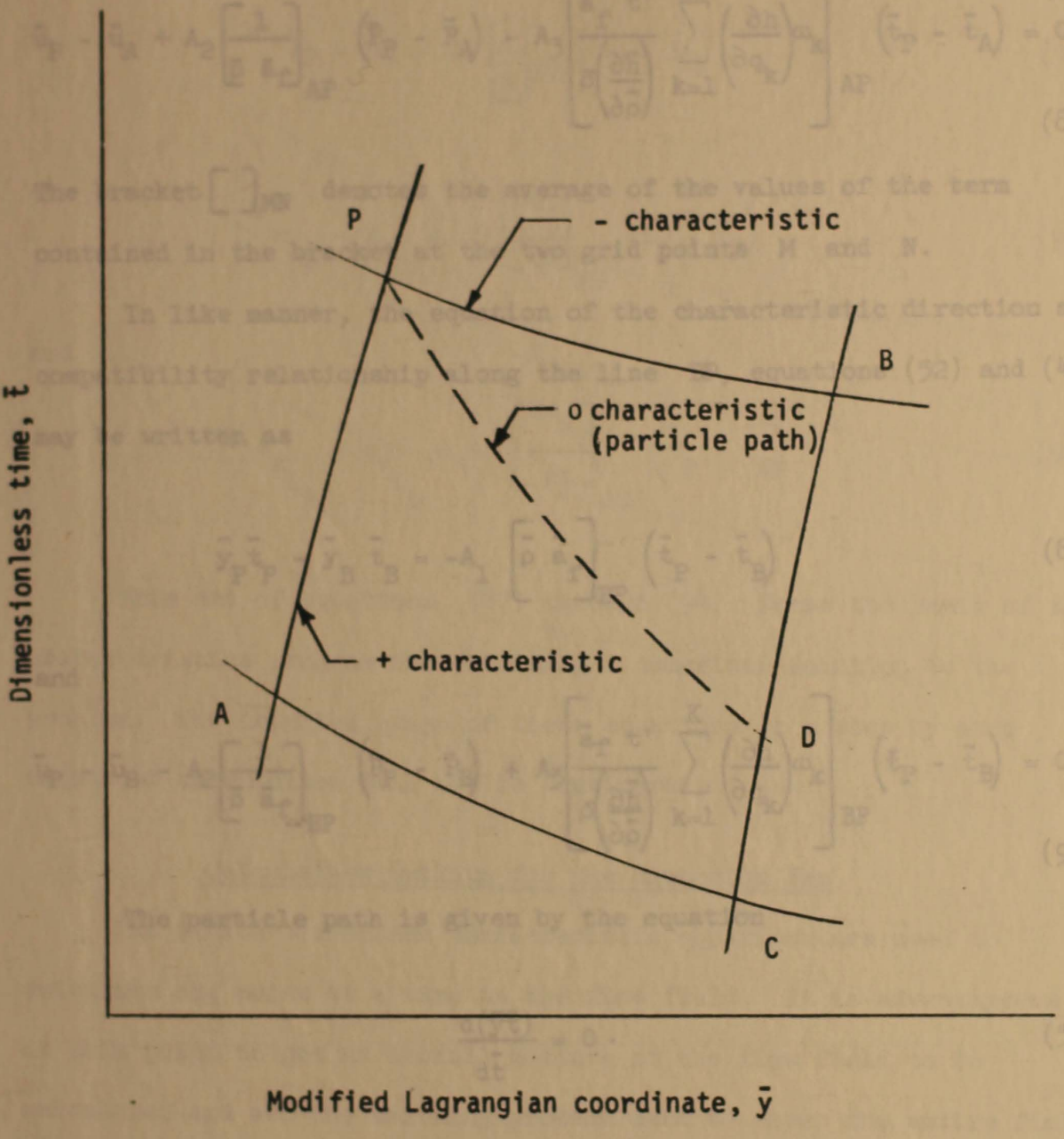

Figure 4. General grid nomenclature

$$\bar{u}_P - \bar{u}_A + A_2\left[\frac{1}{\bar{\rho}\ \bar{a}_f}\right]_{AP}\left(\bar{P}_P - \bar{P}_A\right) - A_3\left[\frac{\bar{a}_f\ t'}{\bar{\rho}\left(\frac{\partial \bar{h}}{\partial \bar{\rho}}\right)}\sum_{k=1}^{K}\left(\frac{\partial h}{\partial q_k}\right)\omega_k\right]_{AP}\left(\bar{t}_P - \bar{t}_A\right) = 0 . \tag{88}$$

The bracket $[\ ]_{MN}$ denotes the average of the values of the term contained in the bracket at the two grid points M and N.

In like manner, the equation of the characteristic direction and compatibility relationship along the line BP, equations (52) and (46), may be written as

$$\bar{y}_P\,\bar{t}_P - \bar{y}_B\,\bar{t}_B = -A_1\left[\bar{\rho}\ \bar{a}_f\right]_{BP}\left(\bar{t}_P - \bar{t}_B\right) \tag{89}$$

and

$$\bar{u}_P - \bar{u}_B - A_2\left[\frac{1}{\bar{\rho}\ \bar{a}_f}\right]_{BP}\left(\bar{P}_P - \bar{P}_B\right) + A_3\left[\frac{\bar{a}_f\ t'}{\bar{\rho}\left(\frac{\partial \bar{h}}{\partial \bar{\rho}}\right)}\sum_{k=1}^{K}\left(\frac{\partial h}{\partial q_k}\right)\omega_k\right]_{BP}\left(\bar{t}_P - \bar{t}_B\right) = 0 . \tag{90}$$

The particle path is given by the equation

$$\frac{d(\bar{y}\bar{t})}{d\bar{t}} = 0 . \tag{53}$$

In finite difference form along line PD this simply becomes

$$\bar{y}_P\,\bar{t}_P = \bar{y}_D\,\bar{t}_D . \tag{91}$$

Along the particle path, the energy and rate equations may be written

$$\bar{h}_P - \bar{h}_D = A_4 \left[\frac{1}{\bar{\rho}}\right]_{PD} \left(\bar{P}_P - \bar{P}_D\right), \tag{92}$$

$$x_{i_P} - x_{i_D} = t' \left[\frac{dx_i}{dt}\right]_{PD} \left(\bar{t}_P - \bar{t}_D\right) \tag{93}$$

and

$$e_{v_{i_P}} - e_{v_{i_D}} = t' \left[\frac{de_{v_i}}{dt}\right]_{PD} \left(\bar{t}_P - \bar{t}_D\right). \tag{94}$$

This set of equations (87) through (94) forms the basis of the characteristics program for obtaining a numerical solution to the problem. The detailed usage of these equations in a step by step method of calculation will now be considered.

Calculation Outline for the Expansion Fan

The finite difference characteristic equations are used to calculate one point at a time in the flow field. It is advantageous at this point to get an overall picture of the flow field to be calculated and see the marching process used to cover the entire field. The nature of the grid used in the calculation is shown in Figure 5. It should be remembered that for the expansion fan, the calculations are carried out in the modified Lagrangian ($\bar{y}$-$\bar{t}$) coordinate system.

The boundary conditions were discussed previously. It was shown that along the line $\bar{t}$=0, all conditions are those of a frozen

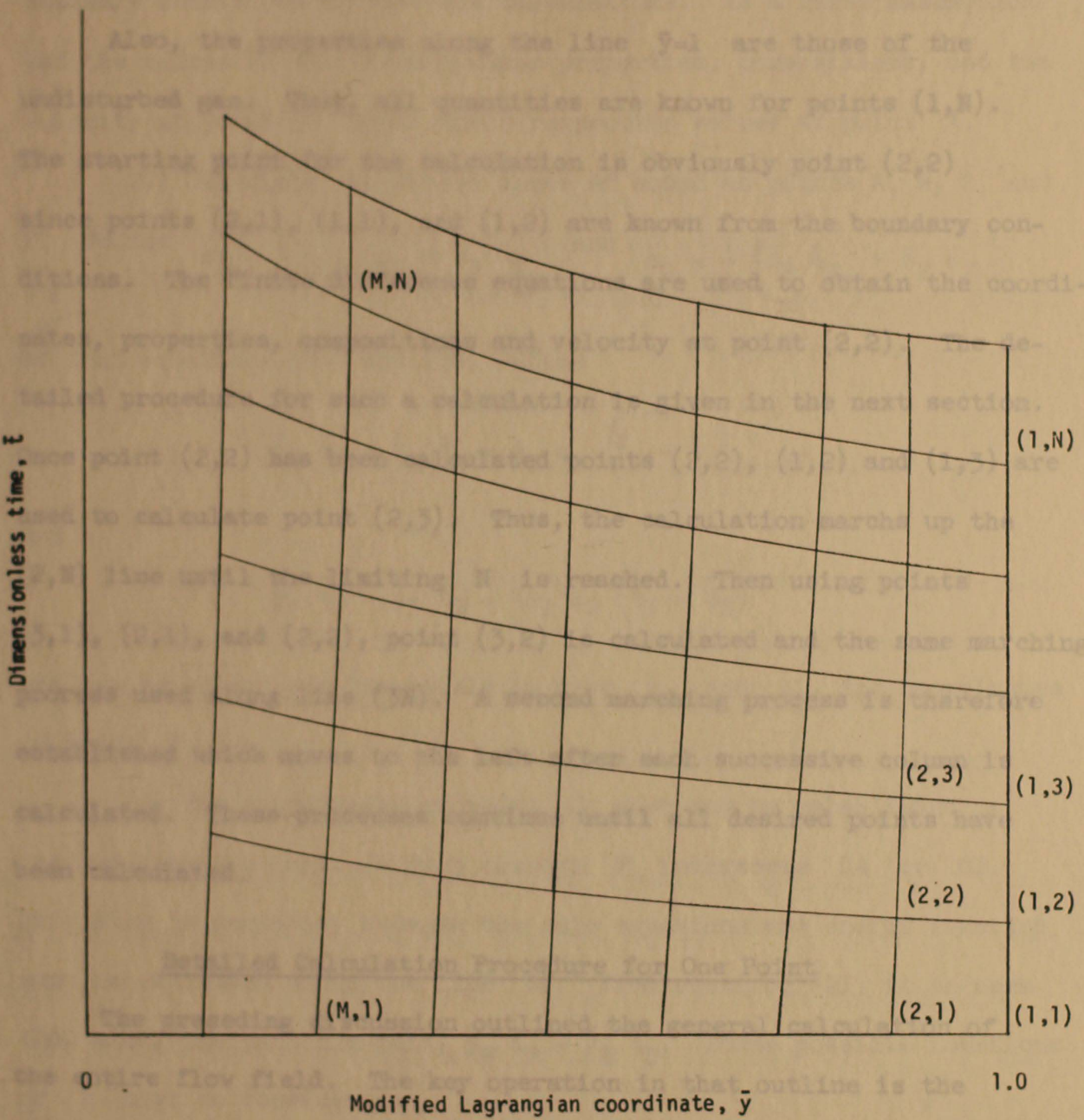

Figure 5. Complete grid network

expansion. Thus, the values of all quantities at points (M,1) are known from this boundary condition.

Also, the properties along the line $\bar{y}=1$ are those of the undisturbed gas. Thus, all quantities are known for points (1,N). The starting point for the calculation is obviously point (2,2) since points (2,1), (1,1), and (1,2) are known from the boundary conditions. The finite difference equations are used to obtain the coordinates, properties, compositions and velocity at point (2,2). The detailed procedure for such a calculation is given in the next section. Once point (2,2) has been calculated points (2,2), (1,2) and (1,3) are used to calculate point (2,3). Thus, the calculation marchs up the (2,N) line until the limiting N is reached. Then using points (3,1), (2,1), and (2,2), point (3,2) is calculated and the same marching process used along line (3N). A second marching process is therefore established which moves to the left after each successive column is calculated. These processes continue until all desired points have been calculated.

Detailed Calculation Procedure for One Point

The preceding discussion outlined the general calculation of the entire flow field. The key operation in that outline is the calculation of any unknown point using the known values at three adjacent points and the finite difference characteristic equations. This operation is an iterative process and requires a fairly elaborate calculation procedure. The steps used in this calculation are presented below. The nomenclature used in that of Figure 4.

(1.) All quantities are known at points A, B, and C from the boundary conditions or previous calculations. As a first assumption let the values of the thermodynamic properties, compositions, and the velocity at point P equal their respective values at point A.

(2.) Calculate the frozen speed of sound at points A, B, C, and P. Define $\alpha_1 = \frac{1}{2}\left(\bar{\rho}_A \bar{a}_{f_A} + \bar{\rho}_P \bar{a}_{f_P}\right)$ and $\alpha_2 = \frac{1}{2}\left(\bar{\rho}_B \bar{a}_{f_B} + \bar{\rho}_P \bar{a}_{f_P}\right)$ so that equations (87) and (89) become

$$\bar{y}_P \bar{t}_P - \bar{y}_A \bar{t}_A = A_1 \alpha_1 \left(\bar{t}_P - \bar{t}_A\right)$$

and

$$\bar{y}_P \bar{t}_P - \bar{y}_B \bar{t}_B = -A_1 \alpha_2 \left(\bar{t}_P - \bar{t}_B\right)$$

and can be solved simultaneously to give $\bar{y}_P$ and $\bar{t}_P$, the coordinates of point P.

(3.) The coordinates of point D must now be established to indicate where a particle path through P intersects CA or CB. This step is necessary because the rate equations and energy equation must be evaluated along the line DP. From equation (91) it is seen that along the particle path, $\bar{y}_P \bar{t}_P = \bar{y}_D \bar{t}_D$. Three possible locations of D must be considered.

If $\bar{y}_P \bar{t}_P > \bar{y}_c \bar{t}_c$, D is on CB. Since for the frozen case CB is a straight line, it seems reasonable to treat it as a straight line over the small interval considered here. Writing the equation of the line CB and solving this equation simultaneously with the condition, $\bar{y}_P \bar{t}_P = \bar{y}_D \bar{t}_D$, yields the values of the desired coordinates,

$\bar{y}_D$ and $\bar{t}_D$. A linear interpolation between points C and B is used to obtain values of the properties, compositions, and velocity at point D.

If $\bar{y}_P\,\bar{t}_P < \bar{y}_C\,\bar{t}_C$, D is on CA. The line CA is of the form, $\bar{y}\bar{t}$ = constant, in the frozen case, so this form appears reasonable to use here. Thus, assuming $\bar{y}_D\,\bar{t}_D^2 = \frac{1}{2}\left(\bar{y}_C\,\bar{t}_C^2 + \bar{y}_A\,\bar{t}_A^2\right)$, and using the condition $\bar{y}_P\,\bar{t}_P = \bar{y}_D\,\bar{t}_D$, the coordinates $\bar{t}_D$ and $\bar{y}_D$ are readily found. A linear interpolation of properties between A and C is used to evaluate the flow quantities at D.

If $\bar{y}_P\,\bar{t}_P = \bar{y}_D\,\bar{t}_D$, points D and C are identical and thus D is defined.

(4.) The rate expressions for the rate processes considered must now be evaluated at points A, B, P, and D for use in the compatibility and rate equations. Thus depending upon the rate processes considered, $\frac{dx_i}{dt}$ and/or $\frac{de_{v_i}}{dt}$ must be calculated using equations (80) and/or (83) for all species.

(5.) The compatibility equations, equations (88) and (90), are solved simultaneously to obtain improved values of $\bar{P}_P$ and $\bar{u}_P$. The value of $\bar{t}_P$ used is that found in step (1.). In writing equation (88) the average of the values at A and P is used for $\left[\frac{1}{\bar{\rho}\,\bar{a}_f}\right]$ and $\left[\frac{\bar{a}_f\,t'}{\bar{\rho}\left(\frac{\partial\bar{h}}{\partial\bar{\rho}}\right)}\sum_{k=1}^{K}\left(\frac{\partial h}{\partial q_k}\right)\omega_k\right]$ and for equation (90) the average of these quantities at B and P is used.

(6.) Rate equations (93) and/or (94) are applied along the particle path from D to P to obtain improved values of x_i and/or e_{v_i} at point P.

(7.) The finite difference form of the energy equation, equation (92), is applied along particle path DP to yield a new value of $\bar{h}_P$, i.e.,

$$\bar{h}_P = \bar{h}_D + \frac{2A_4 \left(\bar{P}_P - \bar{P}_D\right)}{\left(\bar{\rho}_D + \bar{\rho}_P\right)}.$$

(8.) A new temperature at point P is found using the definition of enthalpy, i.e.,

$$T_P = \frac{\bar{h}_o \bar{h}_P - \sum_{i=1}^{n} \frac{x_{i_P}}{\mu_i} \left(f_i \, e_{v_{i_P}} + N_o \Delta_i\right)}{R \sum_{i=1}^{n} \left[\frac{x_{i_P}}{\mu_i} \left(\frac{5}{2} + f_i\right)\right]}.$$

(9.) The thermal equation of state is utilized to calculate an improved density at point P.

$$\bar{\rho}_P = \frac{P_o}{R\rho_o} \frac{\bar{P}_P \, \mu_P}{T_P}$$

(10.) Improved values are thus available for the thermodynamic properties, compositions, and velocity at point P. Using these new values, the calculation returns to step (2.) and the calculation cycle is repeated. This iteration procedure continues until successive calculated values are within a prescribed degree of agreement. In the present work, since temperature is more sensitive to nonequilibrium

effects than other properties, successive temperature values are compared to establish the convergence of the iteration. When successive values are within a prescribed range of each other, the calculation proceeds to the next grid point.

The ten steps described above form the basis of the calculation of the flow field in the expansion fan. Before proceeding to discuss the computer program, attention should be given to the modifications required in the calculation procedure for treating the near-steady region.

Calculation of the Near-steady Region

A calculation procedure has been established for computing the flow in the expansion fan. The near-steady region, the region between the tail of the expansion fan and the piston face, may also be calculated using the same procedure with slight modifications. Two significant changes are necessary.

First, it is convenient to use the $\bar{b} - \bar{t}$ coordinate system instead of the $\bar{y} - \bar{t}$ coordinate system. This change affects only the equations specifying the characteristic directions. Equations (87), (89), and (91) become

$$\bar{b}_P - \bar{b}_A = A_1 \left[\bar{\rho}\ \bar{a}_f\right]_{AP} \left(\bar{t}_P - \bar{t}_A\right),$$

$$\bar{b}_P - \bar{b}_B = -A_1 \left[\bar{\rho}\ \bar{a}_f\right]_{BP} \left(\bar{t}_P - \bar{t}_B\right)$$

and

$$\bar{b}_P = \bar{b}_D.$$

The compatibility equations (88), (90), (92), (93), and (94), remain the same.

Secondly, the boundary condition of constant velocity flow is imposed at grid points adjacent to the piston face. Thus, at these points, u_P is fixed and equation (90) is adequate for obtaining an improved value of $\bar{P}_P$ (replaces step (5.) of calculation procedure). Interior points are calculated using essentially the same procedure as that used for the expansion fan.

The extension of the computing program to calculate the near-steady region is quite simple and presents no new problems. A typical characteristic network obtained in the calculation of the near-steady region will be presented later for a specific example. Attention will now be given to the computer program.

Discussion of the Computer Program

Fortran Program

Consideration of the calculation procedure reveals that a prohibitive amount of hand calculation is required to obtain a solution for even one point in the flow field. It was therefore necessary to set up the problem for solution by an electronic digital computer. The IBM 7094 computer was used to perform the computations. The problem was programed for the computer using Fortran, the language compatible with the IBM 7094. Details of this language are given by McCracken (1961).

The input for the computer program consists of the equilibrium properties of the undisturbed gas, the constants needed in the evaluation of rate coefficients, and physical constants needed in the calculation. In addition, input data is provided which specifies the number of species, the number of reactions, the grid size and grid size variation, the limits of the expansion, the tests for iteration convergence, the types of rate processes considered, and the number of grid points to be calculated. The program calculates its own boundary condition along the $\bar{t} \to 0$ line. It then marches continuously through the entire flow field, as previously described, until the desired region has been computed. The pertinent data is printed out for a sufficient number of grid points to describe the flow field. A particle path may be easily followed through this flow field since in the $\bar{y}$-$\bar{t}$ coordinate system used for the expansion region a particle path is described by $\bar{y}\bar{t}$ = constant, and in the $\bar{b}$-$\bar{t}$ coordinates used for the near-steady region, $\bar{b}$ = constant.

A copy of the Fortran program used for cases in which vibrational equilibrium and chemical nonequilibrium are considered is given in Appendix F.

Due to the complicated nature of the present problem, certain problems arose in the development of the computer program. Discussion of a few of these problems seems appropriate at this point.

The step size between grid points was found to influence the rate of convergence of the iteration at each point. This was expected since the step size directly influences the amount of change of rate controlled quantities between the two points and thus determines how much the

assumed properties must change before the iteration converges. The procedure was adopted of trying several grid sizes for the initial portion of the expansion and using the one for which the iteration converged in from two to five steps. It was observed that if the iteration converged rapidly in the initial part of the expansion in which the rate processes were rapid, no convergence problems existed later in the expansion when rates were slower.

As the computation progresses, the change in property values becomes more rapid for a given change in the grid variable, $\bar{y}$. It was necessary to decrease the increment of $\bar{y}$ as the calculation proceeded from $\bar{y} = 1$ to $\bar{y} = 0$ to allow for this phenomenon.

The size of the grid network which must be generated to follow a specific particle through an expansion also presented a problem. Consider Figure 6. The characteristic which determines the domain of influence for a given boundary input is roughly of the form, $\bar{\bar{y}}\bar{\bar{t}}^2 = \text{constant}$, while the particle path is given by $\bar{\bar{y}}\bar{\bar{t}} = \text{constant}$. In order to follow the particle shown in Figure 6, which initially has the value $\bar{t}=1$ at $\bar{y}=1$, the entire flow field shown must be calculated. This requires that input data be prescribed along the line $\bar{y}=1$ from $\bar{t}=0$ to $\bar{t} = 2.236$. From this illustration it becomes apparent that for an extreme expansion to very low densities and high velocities, the number of grid points which must be calculated in order to follow one particle through the expansion can become very large and presents a limitation because of the excessive computing time required.

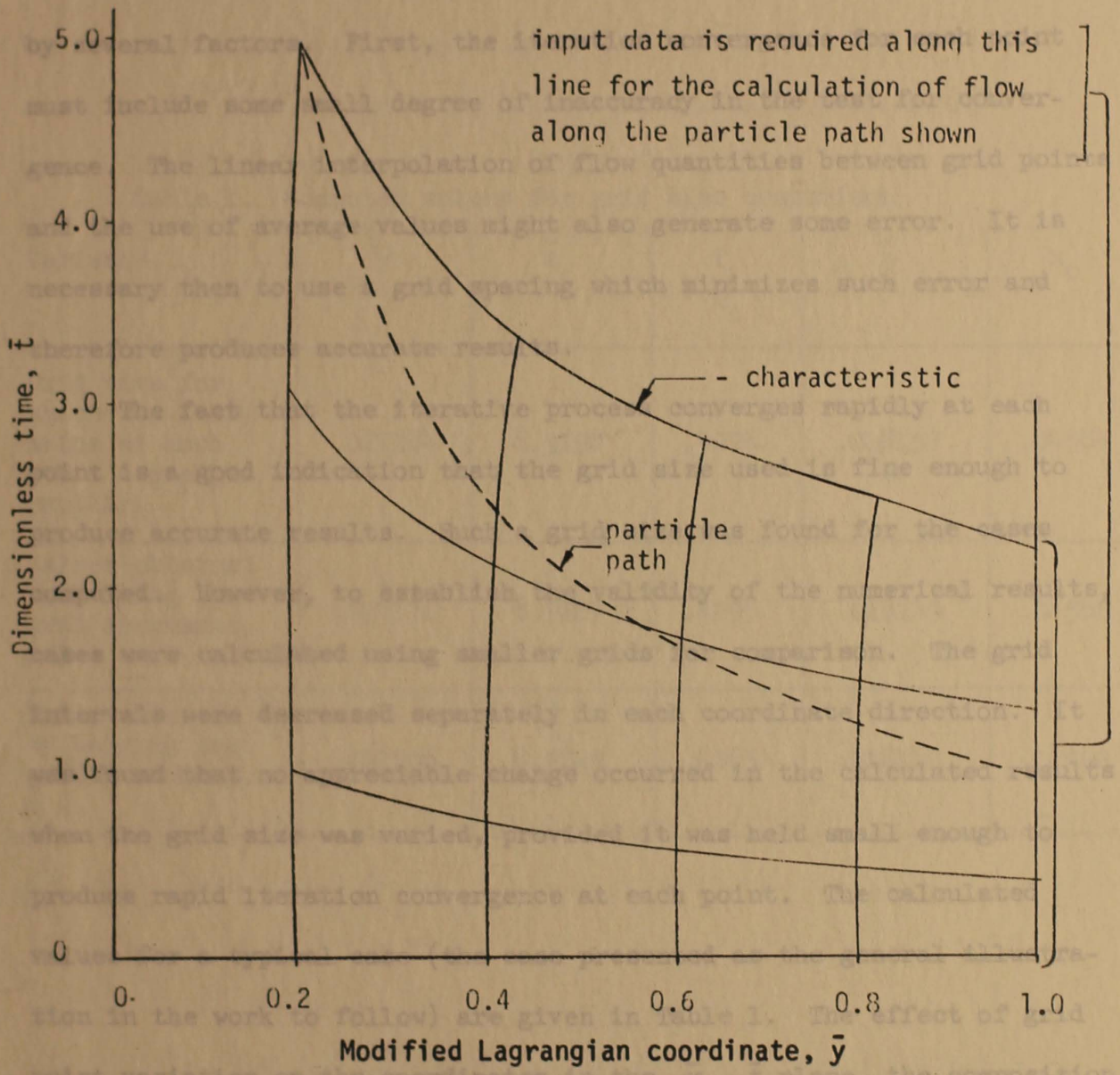

Figure 6. Calculation region illustration

Solution Accuracy

In any problem of this nature which involves a large amount of numerical calculation and finite difference equations, questions arise concerning the accuracy of the solution. Inaccuracies could be caused by several factors. First, the iteration convergence for each point must include some small degree of inaccuracy in the test for convergence. The linear interpolation of flow quantities between grid points and the use of average values might also generate some error. It is necessary then to use a grid spacing which minimizes such error and therefore produces accurate results.

The fact that the iterative process converges rapidly at each point is a good indication that the grid size used is fine enough to produce accurate results. Such a grid size was found for the cases computed. However, to establish the validity of the numerical results, cases were calculated using smaller grids for comparison. The grid intervals were decreased separately in each coordinate direction. It was found that no appreciable change occurred in the calculated results when the grid size was varied, provided it was held small enough to produce rapid iteration convergence at each point. The calculated values for a typical case (the case presented as the general illustration in the work to follow) are given in Table 1. The effect of grid point variation on the coordinates in the $\bar{y}$ - $\bar{t}$ plane, the composition, and the dimensionless temperature and pressure are presented for a point at the tail of the expansion fan. The calculation of the values

Table 1. Computed values for grid size comparison

Variable	$\bar{y}$	$\bar{t}$	$\frac{T}{T_o}$	$\bar{p}$	x_o
Grid size for which the iteration at each point converges rapidly.	.027184	8.9198	.4296	.018157	.04584
Values obtained by halving the grid increment, $\Delta \bar{y}$.	.027172	8.9227	.4295	.018149	.04586
Value obtained by halving the grid increment, $\Delta \bar{t}$.	.027206	8.9120	.4263	.018110	.04592

appearing in the first column of Table 1 required the computation of 1710 grid points. It can be seen that very little modification of the computed values occurred when the grid size was decreased.

As a result of the above comparison it is felt that the numerical error inherent in the present work is very small and negligible compared to the possible error introduced because of the uncertain accuracies of the reaction rate coefficients.

With the numerical method of solution and the computer program now established, the program will be applied to typical problems of current interest.

APPLICATIONS

The centered rarefaction wave has been the subject of many gas dynamic studies. The present investigation is intended to illustrate the use of one such centered rarefaction wave, the one-dimensional unsteady expansion, in applications of current interest. These applications involve the operation of facilities for producing high enthalpy flow and conducting chemical kinetic studies. Flow must, therefore, be considered in which vibrational excitation and dissociation may occur and in which chemical nonequilibrium may be present. The applications illustrate the utility of the programed method of solution which has been developed in the preceding pages. It should be noted that while the applications presented here deal with specific cases, the program possesses the capability of treating many reacting gas mixtures.

As a first illustration, the general structure of an unsteady one-dimensional expansion of a reacting gas mixture is presented for a representative case. A multi-component gas mixture subject to a number of simultaneous chemical reactions is considered. The relative importance of the various reactions is shown. An analysis of the effects of rate chemistry on the flow properties during the expansion is made. The overall effects of chemical nonequilibrium on the expansion are pointed out. This first application of the program is designed to illustrate the capabilities of the general method of solution and to give a more understandable physical picture of the nonequilibrium expansion being considered.

For the second application, attention is given to the unsteady expansion by which the test gas is processed in the operating cycle of the expansion tube. The expansion tube, described in detail in the work of Trimpi (1962), is a device for producing high velocity flow for reentry radiation studies. The one-dimensional unsteady expansion is an important process for accelerating the test gas of this facility to the high velocities required. Only if the chemical state of the test gas in the expansion tube is known can meaningful experimental results be obtained. The present method of solution is applied to this process to obtain the effects of chemical nonequilibrium on the state of the test gas as well as on the overall operating capabilities of the expansion tube. A typical case is presented to illustrate the evaluation of the expansion as it occurs in the expansion tube cycle.

Another problem in the forefront of chemical kinetic studies in gas dynamics today is that of the direct measurement of recombination rates. The use of an unsteady expansion provides an interesting experiment for obtaining such a measurement. The third application of the present program is in this area. The recombination rate experiment is outlined and the computer program is used to determine the feasibility of such an experiment.

The applications which are presented in the pages to follow are not designed to produce numerical values describing a wide range of conditions for a nonequilibrium unsteady expansion. They are intended, instead, to demonstrate the capability of the computer program to handle complicated mixtures of gases and associated reactions, and to

illustrate the salient features of such an expansion. Furthermore, these solutions reveal the need for the present program in current problems of interest and demonstrate its usefulness in providing solutions to such problems.

General Structure of the Expansion

The first application of the program is designed to provide a physical picture of the nonequilibrium unsteady expansion of a reacting gas mixture. A gas mixture was used which reasonably represents air for the conditions considered. Three component gases, N_2, O and O_2, were included in the mixture. The atomic nitrogen species, N, was omitted since nitrogen dissociation is negligible for the conditions investigated. The vibrational energies of the nitrogen and oxygen molecules were assumed to remain in equilibrium with the translational and rotational energies throughout the expansion. This assumption is certainly valid for the oxygen molecules. Nitrogen vibrational relaxation is somewhat slower and some vibrational nonequilibrium may actually be present. A preliminary check of nitrogen relaxation times indicates that for the larger part of the flow field, vibrational equilibrium should exist. Thus, the assumption of vibrational equilibrium appears justified for the present application. A more refined gas model for representing air should include both vibrational rates for O_2 and N_2 and the additional species N and NO. However, it is felt that the simplified air model proposed here is quite adequate for demonstrating the salient features of a nonequilibrium unsteady expansion.

The chemical reactions which control the dissociation and recombination of the various species in the gas mixture are listed below:

(a) $O_2 + O \rightarrow 3O$

(b) $3O \rightarrow O_2 + O$

(c) $2O_2 \rightarrow 2O + O_2$

(d) $O_2 + 2O \rightarrow 2O_2$

(e) $O_2 + N_2 \rightarrow 2O + N_2$

(f) $2O + N_2 \rightarrow O_2 + N_2$.

The reaction rate coefficients used are believed to be the most accurate values available at present. The values of the rate coefficients are listed in Appendix E as are the other constants which were used in the calculations.

The physical model of the expansion was taken to be that of the sudden constant velocity withdrawal of a piston from a cylinder containing a gas mixture in chemical equilibrium. The equilibrium temperature and density of the undisturbed gas were taken to be $4300^{\circ}K$ and $4.55 \times 10^{-3} \frac{gm}{cm^3}$ respectively. The piston velocity prescribed was 3.296×10^5 cm/sec.

The initial compositions were calculated with the aid of the equilibrium constant, K_p. The flow field was then calculated using the digital computer program developed earlier. The results of these calculations will now be presented and evaluated.

The characteristic calculation of the unsteady expansion fan was made using the $\bar{y} - \bar{t}$ coordinate system. A graphical

representation of the characteristic network appears in Figure 7. A comparison can be seen between the nonequilibrium – characteristics and the – characteristics for frozen flow for the same imput conditions. Particle paths are depicted by the dashed lines. Property and composition variations along these particle paths will be presented subsequently.

Calculation was also made of the region between the tail of the expansion fan and the face of the piston. This region will be known as the near-steady region since the property variations in it are due essentially to chemical changes resulting from the recombination process. Convenience dictated the use of the $\bar{b}$-$\bar{t}$ coordinate system for the calculation of this near-steady region. The input used for this calculation was obtained from the last characteristic line in the expansion fan along with the condition that the gas velocity is that of the piston at the piston face. The characteristic network which developed for the near-steady region is pictured in Figure 8.

The structure of the expansion in the x-t plane is presented in Figure 9. Since the property variations will be presented along particle paths, it is advantageous to establish the particle paths of interest in the x-t plane. Path A is representative of a particle which is initially very near the piston face. Such a particle is processed very rapidly by the expansion and has a very short residence time in the fan. The properties along particle path A would thus be expected to approach the values of a frozen expansion. The particle paths B and C are used to indicate the changes as more residence time becomes available in the expansion fan for the rate controlled

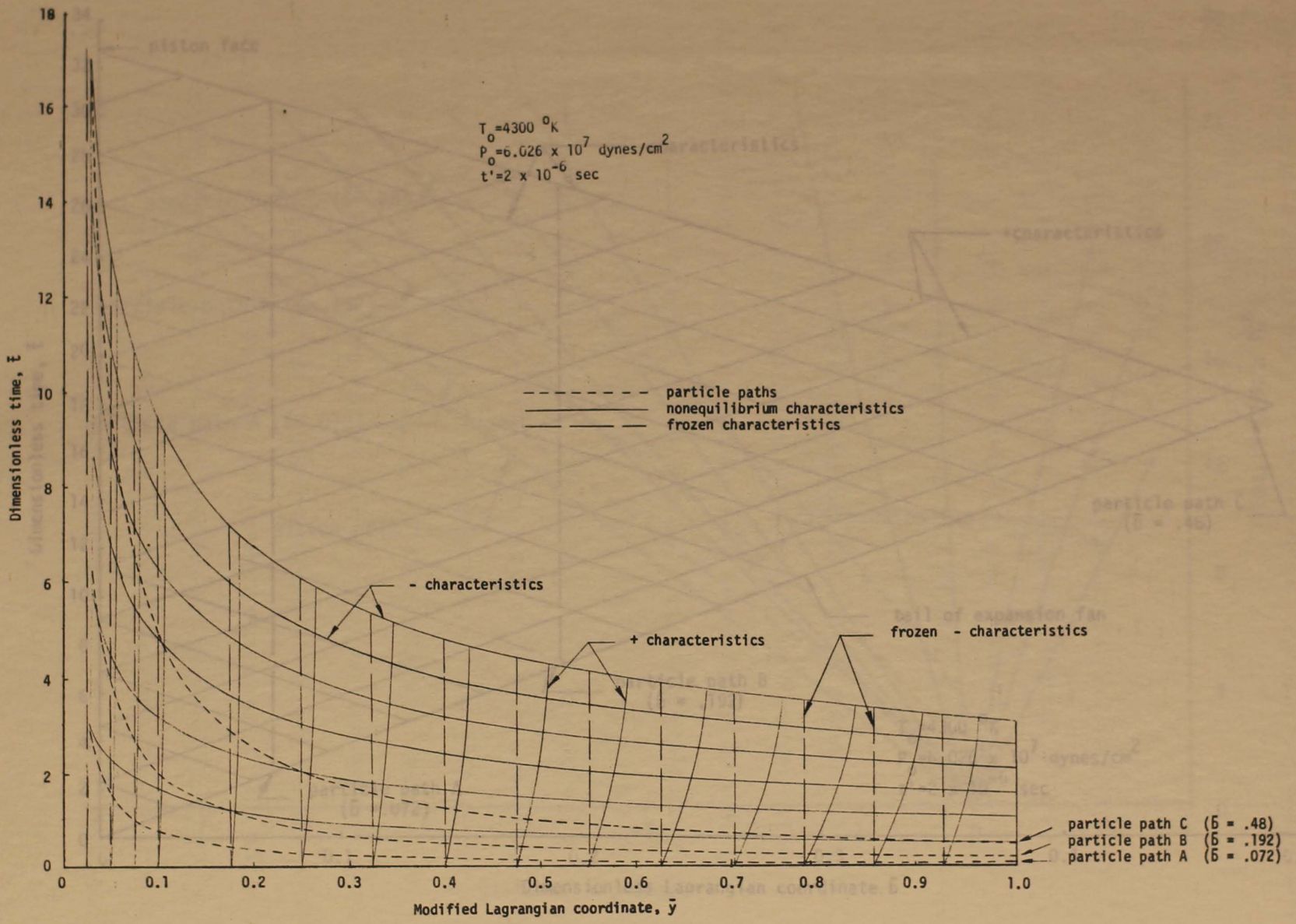

Figure 7. Characteristic network of the expansion region

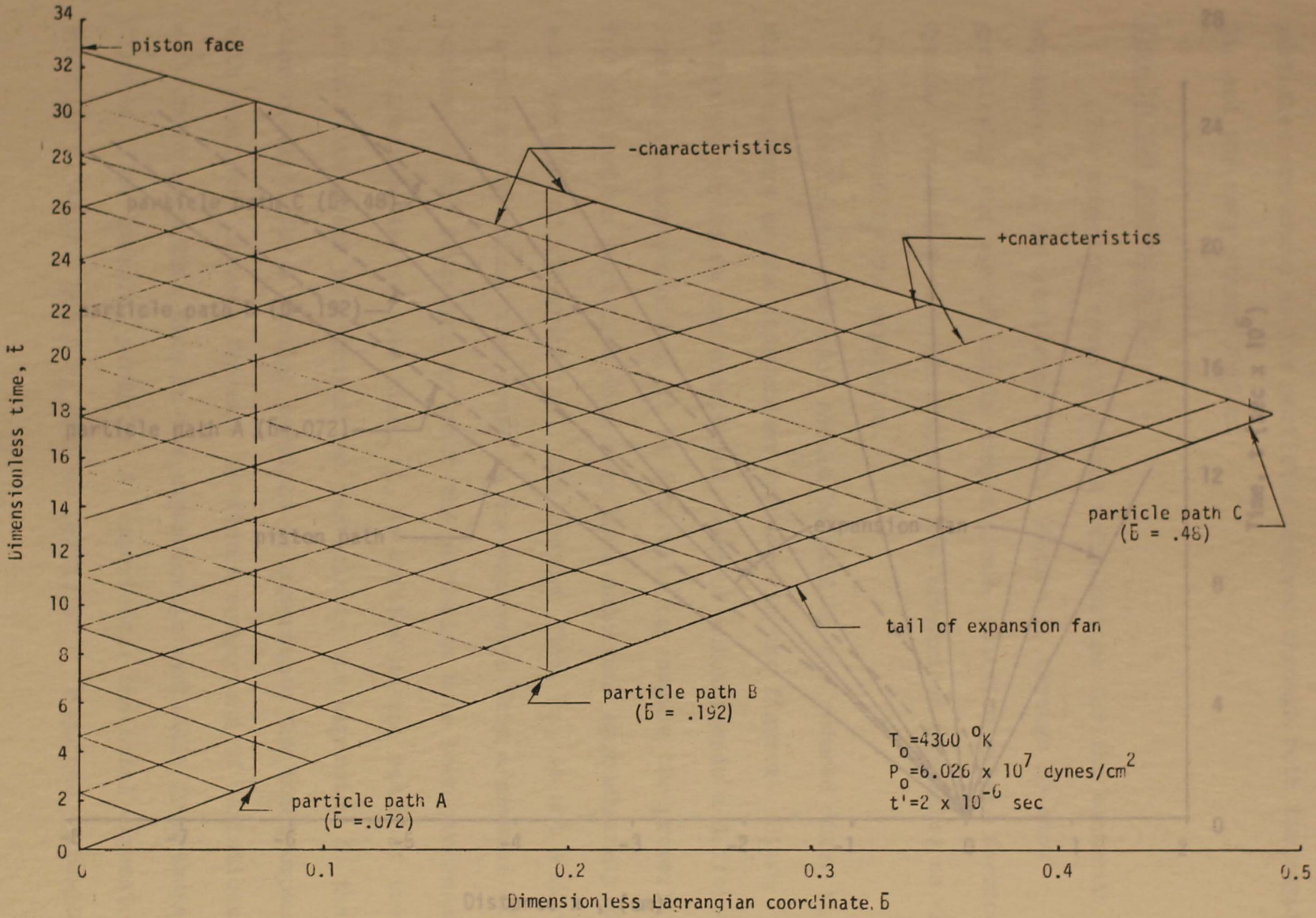

Figure 8. Characteristic network of the near-steady region

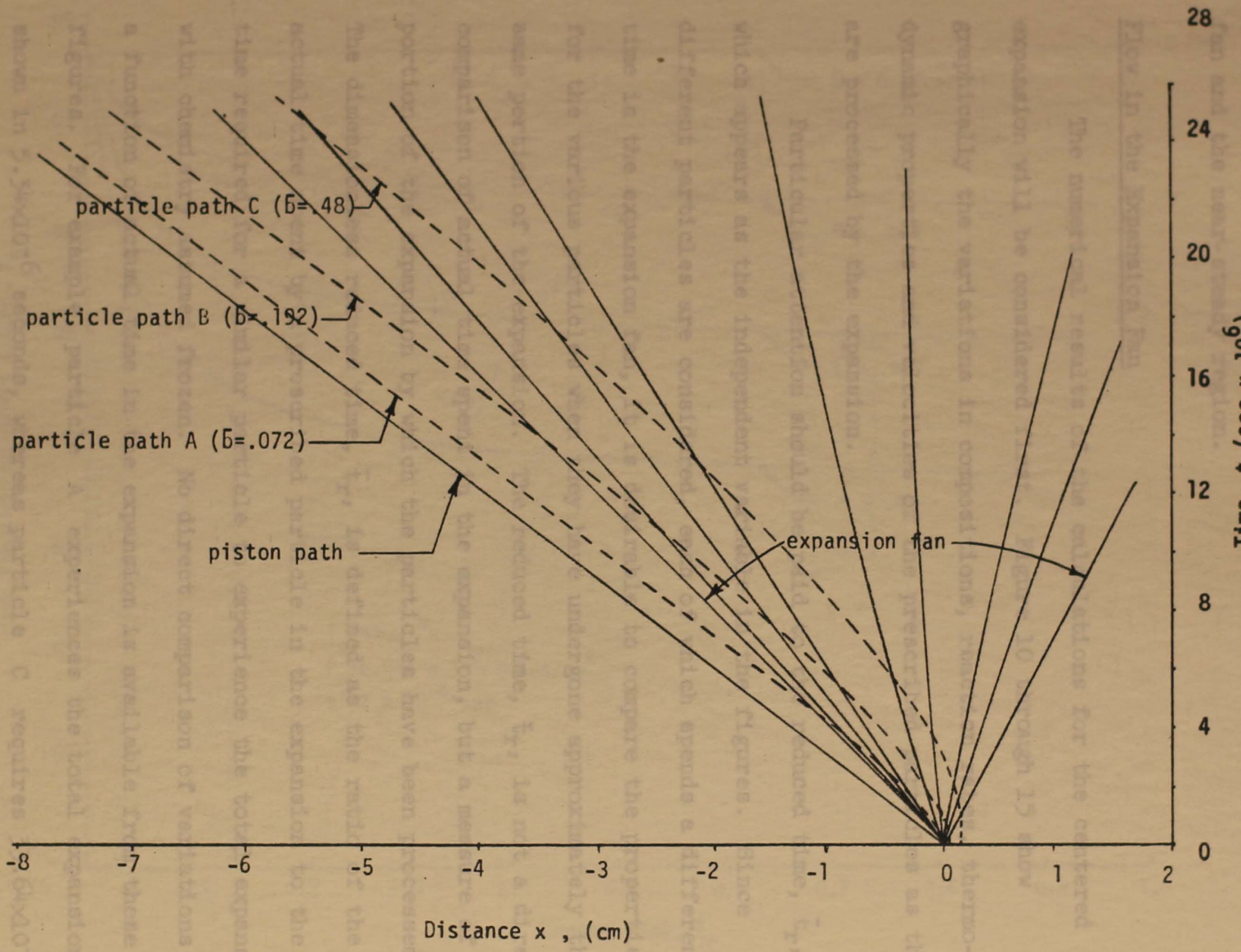

Figure 9. The expansion in the x-t plane

processes to relax toward equilibrium. The paths of the various particles are shown as the particles proceed through both the expansion fan and the near-steady region.

Flow in the Expansion Fan

The numerical results of the calculations for the centered expansion will be considered first. Figure 10 through 15 show graphically the variations in compositions, reaction rates, thermodynamic properties and velocities of the prescribed particles as they are processed by the expansion.

Particular attention should be paid to the reduced time, $\bar{t}_r$, which appears as the independent variable in the figures. Since different particles are considered, each of which spends a different time in the expansion fan, it is desirable to compare the properties for the various particles when they have undergone approximately the same portion of the expansion. The reduced time, $\bar{t}_r$, is not a direct comparison of actual time spent in the expansion, but a measure of the portion of the expansion by which the particles have been processed. The dimensionless reduced time, $\bar{t}_r$, is defined as the ratio of the actual time spent by a prescribed particle in the expansion to the time required for a similar particle to experience the total expansion with chemistry assumed frozen. No direct comparison of variations as a function of actual time in the expansion is available from these figures. For example, particle A experiences the total expansion shown in 5.34×10^{-6} seconds, whereas particle C requires 33.64×10^{-6}

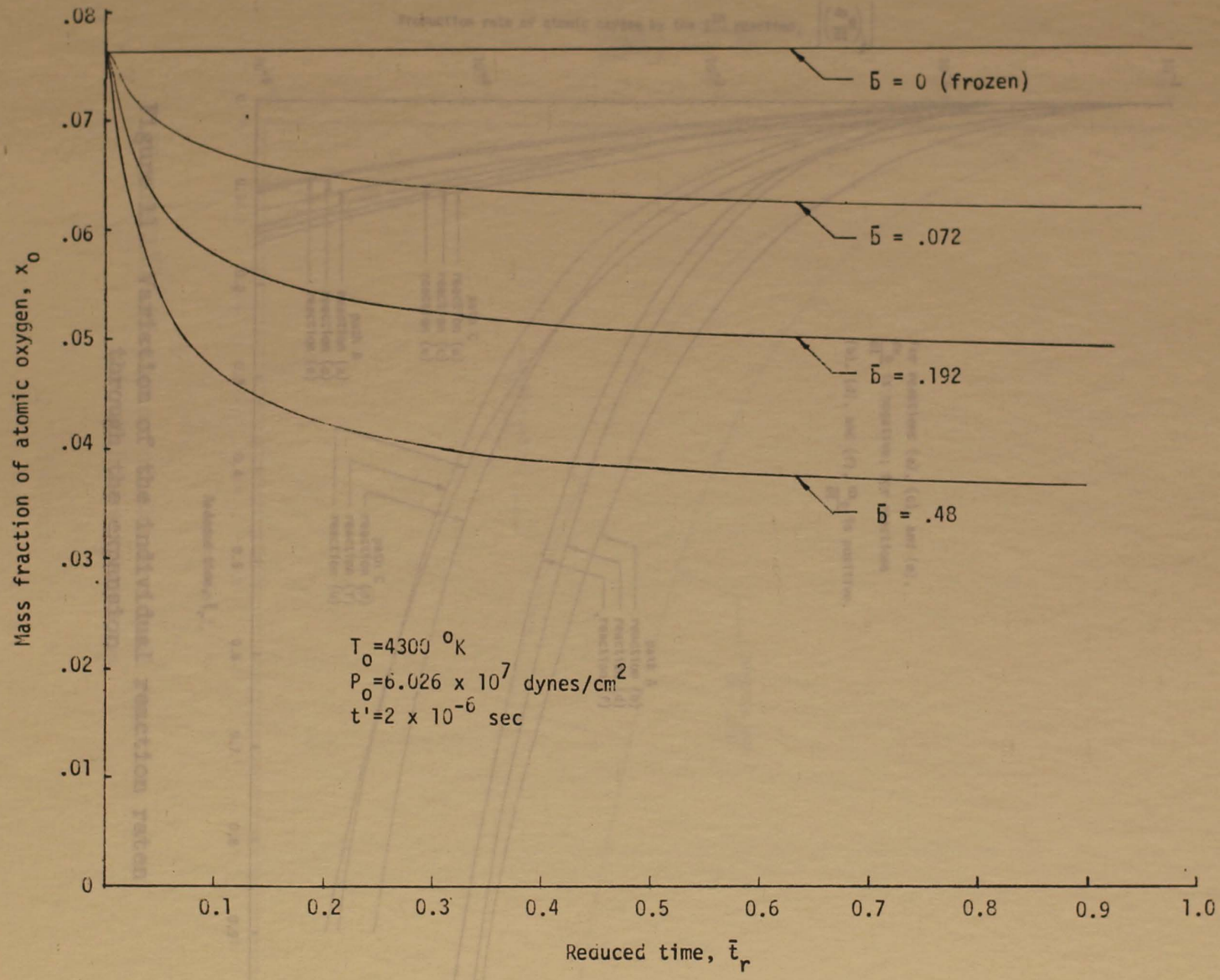

Figure 10. Composition variation through the expansion fan

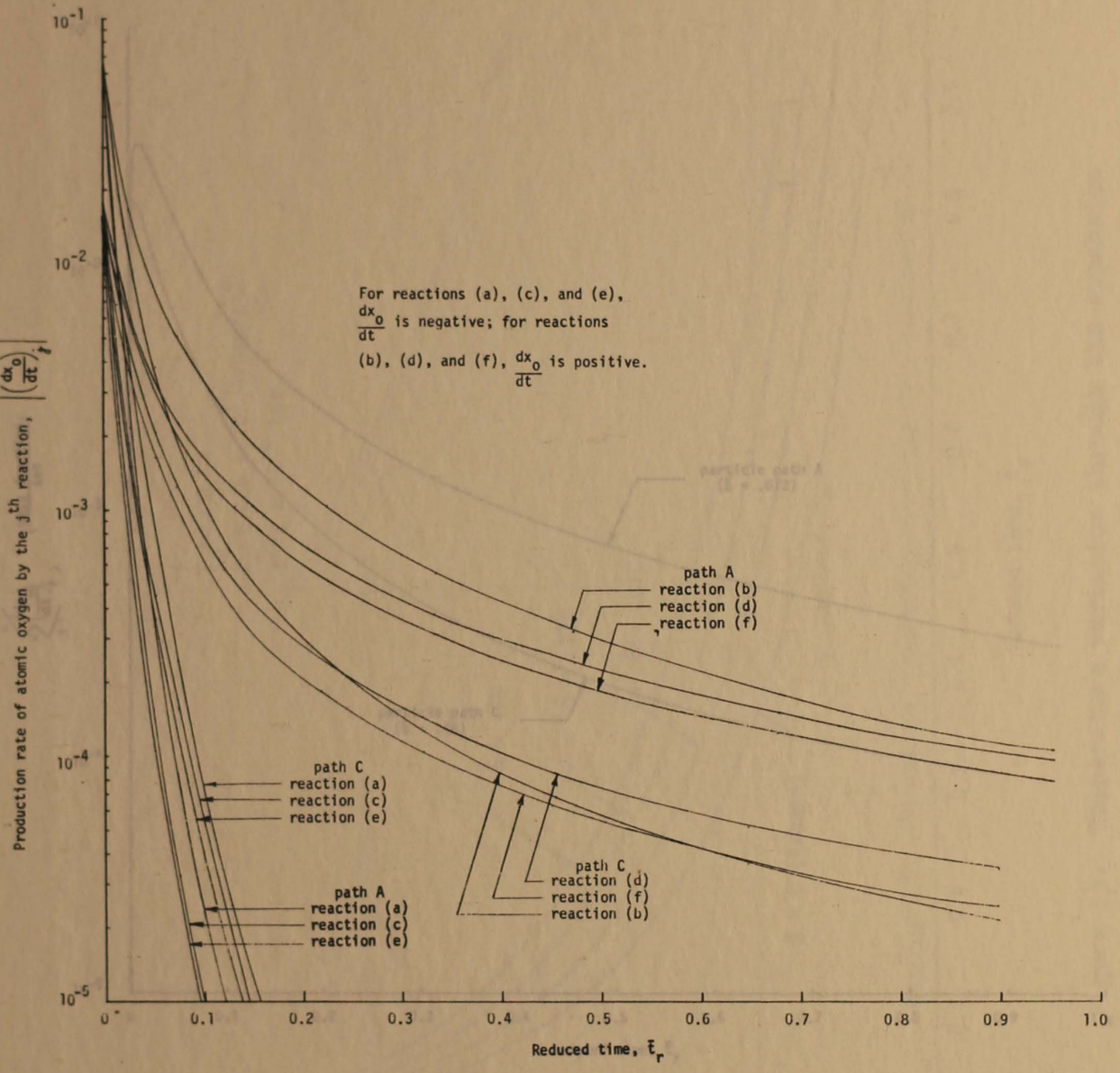

Figure 11. Variation of the individual reaction rates through the expansion

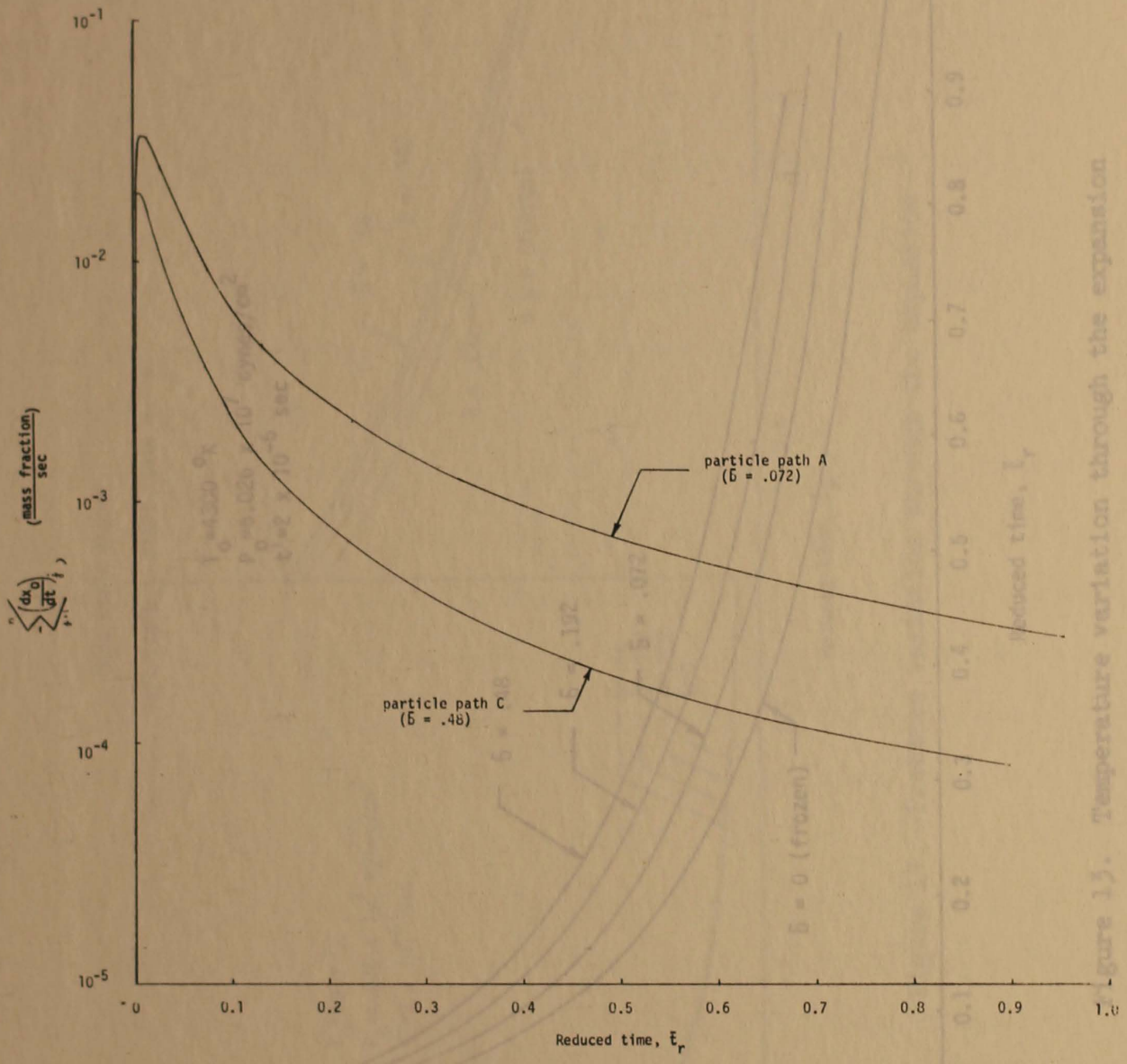

Figure 12. Variation of the combined reaction rates through the expansion

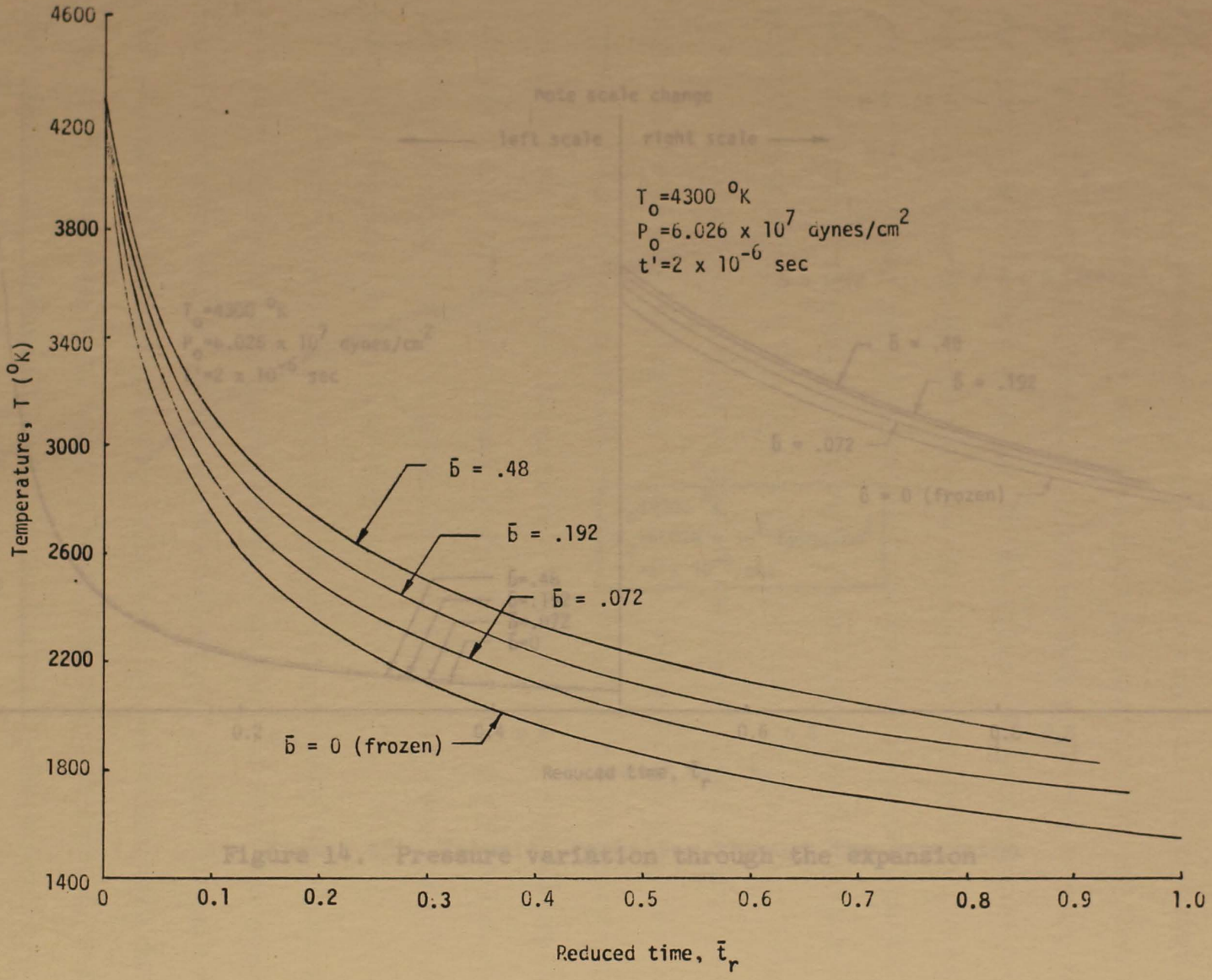

Figure 13. Temperature variation through the expansion

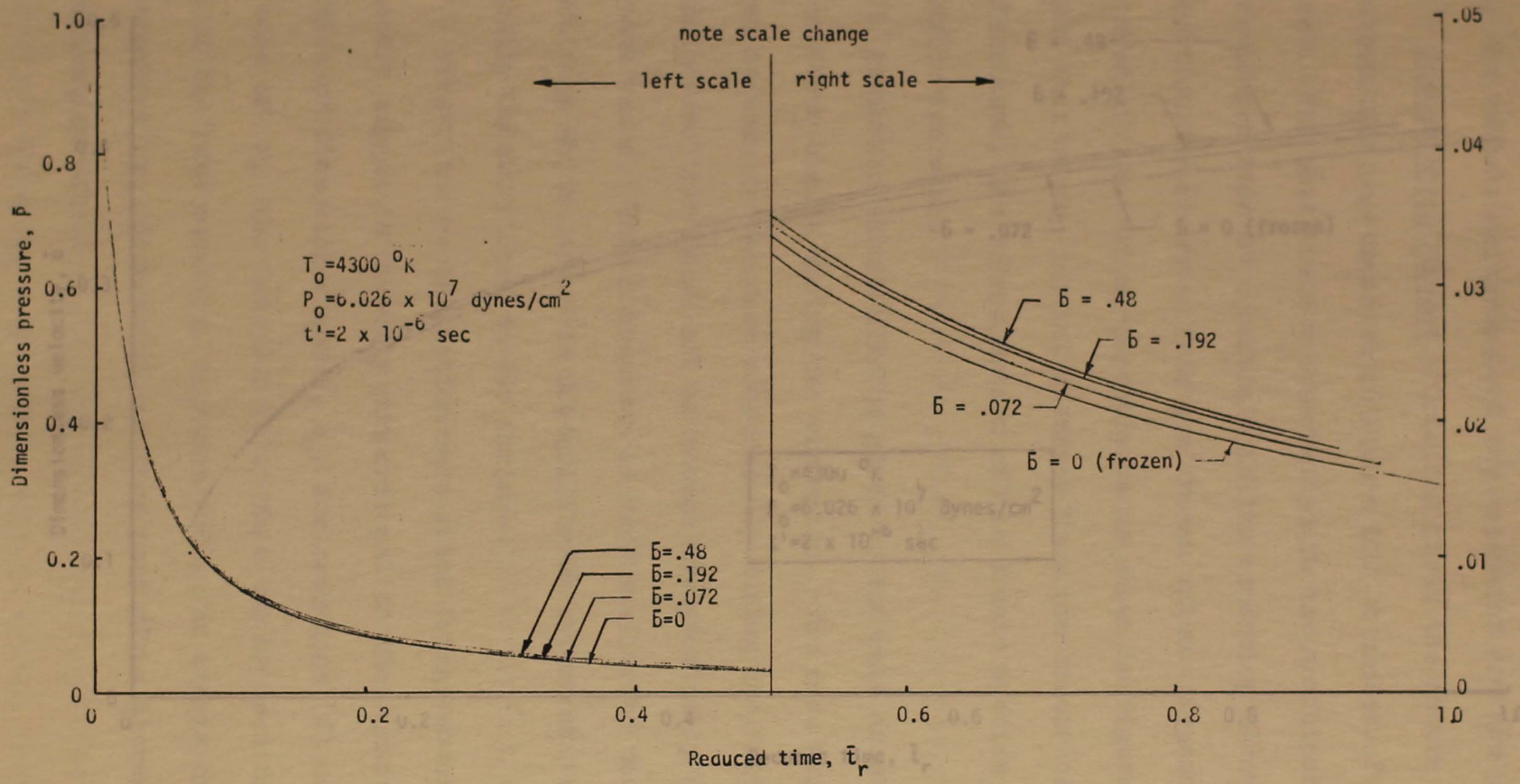

Figure 14. Pressure variation through the expansion

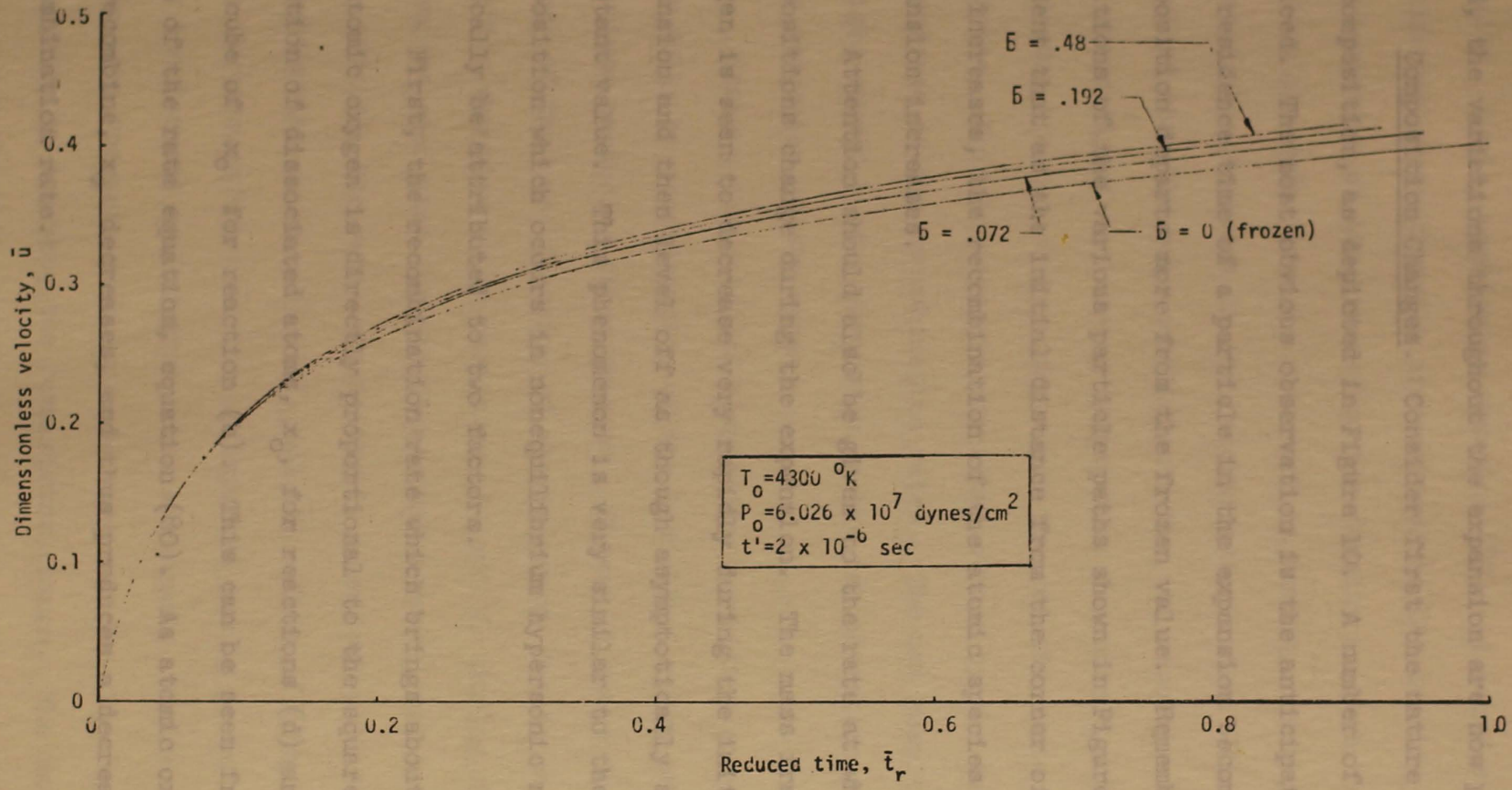

Figure 15. Velocity variation through the expansion

seconds for a similar expansion. With the significance of $\bar{t}_r$ in mind, the variations throughout the expansion are now presented.

Composition Changes. Consider first the nature of the variation in composition, as depicted in Figure 10. A number of things should be noticed. The most obvious observation is the anticipated one that as the residence time of a particle in the expansion becomes larger, the composition departs more from the frozen value. Remembering the positions of the various particle paths shown in Figure 9, it becomes evident that as the initial distance from the corner of the expansion fan increases, the recombination of the atomic species during the expansion increases.

Attention should also be given to the rate at which the compositions change during the expansion. The mass fraction of atomic oxygen is seen to decrease very rapidly during the initial part of the expansion and then level off as though asymptotically approaching a constant value. This phenomenon is very similar to the freezing of composition which occurs in nonequilibrium hypersonic nozzles. It can basically be attributed to two factors.

First, the recombination rate which brings about the decrease in atomic oxygen is directly proportional to the square of the mass fraction of dissociated atoms, x_o, for reactions (d) and (f) and to the cube of x_o for reaction (b). This can be seen from consideration of the rate equation, equation (80). As atomic oxygen, O, begins to recombine, x_o decreases, and thus produces a decrease in the recombination rate.

The second factor which controls the recombination rate is the density. Again considering equation (80), it becomes apparent that recombination is directly proportional to the density squared. At the beginning of the expansion, the density is high but, as the expansion proceeds, a rapid reduction in density occurs, resulting in a considerable decrease in the recombination rates. It might also be recalled that the rate coefficients for the recombination processes are generally of an inverse temperature dependence and as the expansion proceeds, the temperature drops and the reaction rate coefficients increase. This increase is more than offset by the density squared dependence of the recombination rates. The net result of the property changes caused by the expansion on the recombination rates is a sizeable reduction of the rates.

Perhaps the rates of composition variation can be understood more fully by consideration of the individual rates of the various reactions producing these changes. Figure 11 shows the time rate of change of the mass fraction of atomic oxygen due to each separate reaction experienced by particles A and C during the expansion. It can be seen that for the dissociation reactions, reactions (a), (c), and (e), the rates are initially identical with the corresponding recombination rates, (b), (d), and (f). This of course is consistent with the assumption that the undisturbed gas is in equilibrium and thus the forward and reverse rates are equal. As the expansion proceeds, the forward rates decrease very rapidly allowing the recombination rates to dominate the composition change. The nature of the various recombination rates should also be noted. The rates are more

rapid along path A than they are along path C. This is due to the fact that the mass fraction of O remains greater along path A. Since the recombination rate is proportional to the mass fraction, x_o, to at least the second power, a high value of x_o will give a fast recombination rate. (It should be remembered that while the recombination rates are somewhat higher for path A than for paths B and C the residence time of the particle is much less along path A and therefore, the total recombination occurring during the expansion remains less for particle A than for B or C). Particular attention should be given to the behavior of reaction (b), i.e., the recombination produced by the collision of three atoms of O. As can be seen by considering the values of the rate coefficients, atomic oxygen, O, is more effective collision partner as the third body in an oxygen recombination collision than is O_2 or N_2. This is apparent during the initial phase of the expansion. Since along path A, the value of x_o does not decrease drastically, reaction (b) remains the leading reaction in producing recombination. However, along particle path C, a sizeable reduction takes place in the mass fraction of atomic oxygen and a corresponding increase occurs in the mass fraction of molecular oxygen, O_2. Since the rate of reaction (b) is proportional to the third power of x_o, this rate decreases more rapidly than that of reactions (d) and (f), since they are dependent on the square of x_o. In fact, the increase in x_{o_2} causes the rate of reaction (d) to decrease even less rapidly and thus it produces a greater percent of the recombination as the expansion proceeds.

Combining the contributions from all of the six reactions considered, the overall time rate of change of x_o along paths A and C is obtained and displayed in Figure 12. As previously discussed, the net rate is initially zero at the equilibrium condition and rapidly assumes a negative value as the expansion proceeds and the recombination reactions begin to dominate. A maximum value is quickly reached beyond which the total rate rapidly decreases due to the decrease in density and mass fraction of atomic oxygen.

Freezing Criteria. Particular attention should be paid to the individual reaction rates with regard to the establishment of freezing criteria. Frozen flow is said to exist along a specific particle path when the relaxation times of the processes become so large compared to the residence time of the particle that the rate controlled quantities exhibit no appreciable change during the remainder of the expansion.

In the nonequilibrium "ideal dissociating gas" model proposed by Freeman (1958) and used by Bray (1958), only one rate controlled quantity and one overall rate equation are considered. A freezing criterion, based on the fact that for frozen flow the composition change produced by the one rate equation approaches zero, can be readily established for such a model. For many realistic nonequilibrium problems, however, a simple model of this nature is not adequate.

A more complicated model, such as that used in the present investigation, precludes the establishment of a simple freezing criterion. For a gas mixture in which a number of rate processes

occur simultaneously, the rate of each process must approach zero for completely frozen flow to exist. As can be seen in the present illustration, the various reaction rates do not exhibit similar variations as the expansion proceeds. Consider first the rates of the recombination reactions (b), (d), and (f), along particle path A as depicted in Figure 11. Reaction (b), $2O+O \rightarrow O_2+O$, is seen to be the dominant reaction in producing recombination during the initial portion of the expansion. It might, therefore, seem appropriate to base a freezing criterion on this single reaction. However, as the flow expands to a lower density, reactions (d) and (f) produce an increasingly higher percentage of the recombination and thus tend to impede the freezing process. Consideration of flow along path C illustrates this phenomena even more vividly. Reaction (b) is initially the most important process for producing recombination. As the expansion proceeds and the atomic oxygen in the flow decreases, reaction (b) exhibits an increasingly smaller effect on the composition changes and reaction (d) becomes the dominant one in producing recombination. The freezing process then becomes more dependent upon reactions (d) and (f) than upon reaction (b).

The complications which arise in establishing a freezing criterion for flow in which a number of rate processes are considered become evident from the above discussion. Such problems become even greater for systems in which the various rate processes are controlled by different mechanisms. In the above example, all of the recombination is produced by three-body collisions and thus the rates are proportional to the density squared. For more complicated reacting

systems, such as that considered by Hall, et al., (1962), in which exchange reactions like $N + O_2 \rightleftharpoons NO + O$ and $O + N_2 \rightleftharpoons NO + N$ may be present during the recombination process, the species changes may be due to both two-body and three-body collisions. Thus, some rates will be proportional to the density and others to the square of the density. The complications which result with respect to the establishment of the freezing criterion is apparent. Each reaction rate must be carefully analyzed with respect to its variation during the expansion and its effect upon the other rate processes. No simple freezing criterion is available for such cases.

It is, therefore, evident that extreme care must be exercised in establishing a criterion for freezing when more than one rate process is present in the flow.

The preceding discussion indicates the importance of the ability of an investigation of this type to handle a number of simultaneous reactions, each of which may have different rate coefficients. While the type of rate consideration proposed by Freeman (1958) is very useful in many cases in predicting the general behavior of reacting gas flow systems, it is not adequate for the detailed investigation of systems in which the rates considered may be quite different. Thus, the present type of formulation is often necessary.

The effects of the chemical nonequilibrium on the thermodynamic properties of the gas during the expansion will now be evaluated.

Thermodynamic Properties. Attention will now be given to the variation of the thermodynamic properties of the reacting gas mixture

as it undergoes the expansion. The translational temperature T has been found by many investigators working with reacting systems to be affected by chemical nonequilibrium far more than the other thermodynamic variables. Therefore, the temperature variation along the various particle paths will be considered first. Figure 13 shows the temperature profiles through the unsteady expansion fan. A direct correlation between the temperatures and the amount of recombination can be seen by comparing Figures 10 and 13. As the mass fraction of O decreases, i.e., as recombination of the atomic oxygen occurs, the energy of dissociation is returned to the flow and an increase in the translational temperature of the gas results. Along particle path A, a small amount of recombination occurs and the corresponding temperature increase above the frozen value is relatively small. For paths B and C, as more and more recombination takes place, a considerable amount of the energy which was tied up in dissociation is returned to the flow and manifests itself in the form of increased temperatures. It should also be noted that the portion of the expansion in which the temperature departs from the frozen values is identical with that in which the recombination occurs. Beyond about $\bar{t}_r = 0.3$ very little recombination occurs. Similarly, beyond this point the temperature profiles become nearly parallel, indicating that very little chemical energy is being released to raise the temperature. It is apparent from Figure 13 that temperature is influenced greatly by the chemical state of the gas mixture and is a good indicator of the degree of nonequilibrium of the flow.

It is also desirable to ascertain the effect of nonequilibrium on the pressure of the gas during the expansion. In Figure 14 the pressure variation is displayed along the various particle paths. The pressure is seen to depart only slightly from the frozen values. However, as the expansion proceeds and the gas expands to very low pressures, the pressure change due to nonequilibrium can become an appreciable percent of the static pressure.

Density variation is not shown graphically because it is affected only slightly by the chemical state of the gas.

Velocity Variation. The flow velocity is of considerable interest in many applications of the unsteady expansion, particularly in those dealing with the design of facilities for producing high velocity, high enthalpy flow. The effect of the chemical state of the gas on the velocity is therefore quite important. Figure 15 provides an insight into this effect for the present example. It can be seen that as the recombination increases, the velocity of the gas increases. This is to be expected since some of the energy released by the recombination of the oxygen atoms in forming molecules is converted into flow energy. The velocity increase for the present nonequilibrium case is seen to be as much as four percent higher than the velocity for a similar frozen expansion. The percent will be slightly higher for the case in which the flow is allowed to relax completely to equilibrium. To obtain the maximum velocity from an unsteady expansion, it is necessary for the process to take place in a state of chemical equilibrium.

The basic effects of nonequilibrium chemistry on the flow in the expansion fan have been pointed out. Attention will now be given to flow in the near-steady region.

Near-Steady Region

The expansion fan region is assumed to be terminated by a trailing characteristic line. Two boundary conditions are employed in the calculation of the near-steady region. First, the output from the expansion fan calculation is used as input along the trailing characteristic of the expansion fan. Secondly, the particle velocity at the face of the piston is assumed to be that of the piston. Using these conditions, the near-steady region was calculated for the present example. The results are presented below.

Compositions. The variation of the mass fraction of atomic oxygen as the particles proceed through the near-steady region is shown in Figure 16. The values are plotted versus the dimensionless time, $\bar{t} - \bar{t}_e$, where $\bar{t}_e$ is the value of the dimensionless time $\bar{t}$ at which the particle entered the near-steady region. Thus a direct comparison can be made between the different particles at a given $(\bar{t}-\bar{t}_e)$, since this coordinate is a direct measure of the time spent by the particles in the steady region. The particle path labeled $\bar{b} = 0$ is that of the particle at the piston face. Such a particle goes through the expansion fan completely frozen since no relaxation time is available and therefore enters the steady region with its initial composition unchanged. Consequently, it has a higher concentration of atomic oxygen, and, as was discussed previously, the recomination rates are

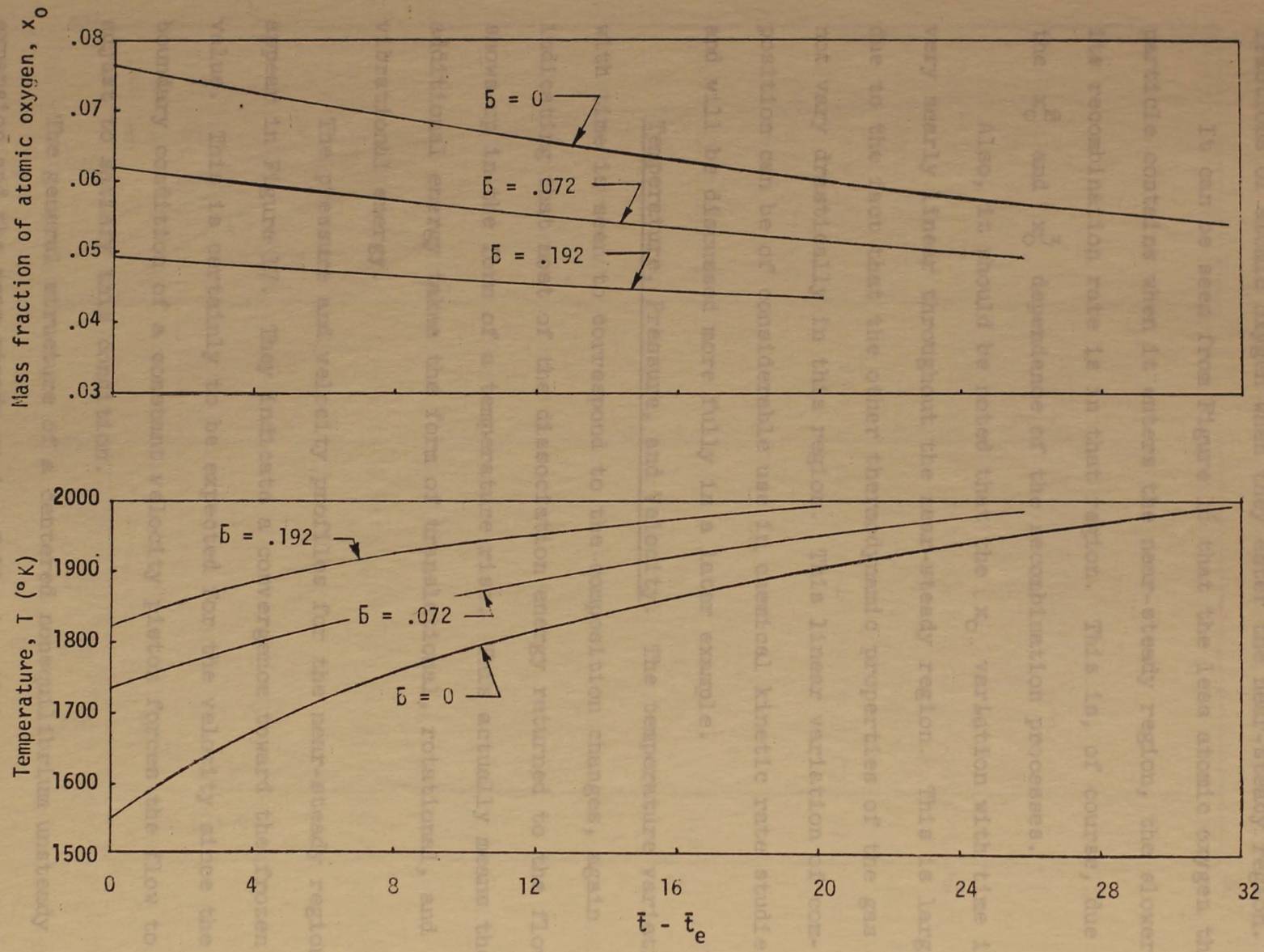

Figure 16. Composition and temperature variation in the near-steady region

higher than they are for particles B and C, which have smaller mass fractions of atomic oxygen when they enter the near-steady region.

It can be seen from Figure 16 that the less atomic oxygen the particle contains when it enters the near-steady region, the slower its recombination rate is in that region. This is, of course, due to the x_o^2 and x_o^3 dependence of the recombination processes.

Also, it should be noted that the x_o variation with time is very nearly linear throughout the near-steady region. This is largely due to the fact that the other thermodynamic properties of the gas do not vary drastically in this region. This linear variation of composition can be of considerable use in chemical kinetic rate studies, and will be discussed more fully in a later example.

Temperature, Pressure, and Velocity. The temperature variation with time is seen to correspond to the composition changes, again indicating that most of the dissociation energy returned to the flow shows up in the form of a temperature rise. This actually means the additional energy takes the form of translational, rotational, and vibrational energy.

The pressure and velocity profiles for the near-steady region appear in Figure 17. They indicate a convergence toward the frozen value. This is certainly to be expected for the velocity since the boundary condition of a constant velocity piston forces the flow to adjust to satisfy this condition.

The general structure of a centered nonequilibrium unsteady expansion and the near-steady region following it have been examined

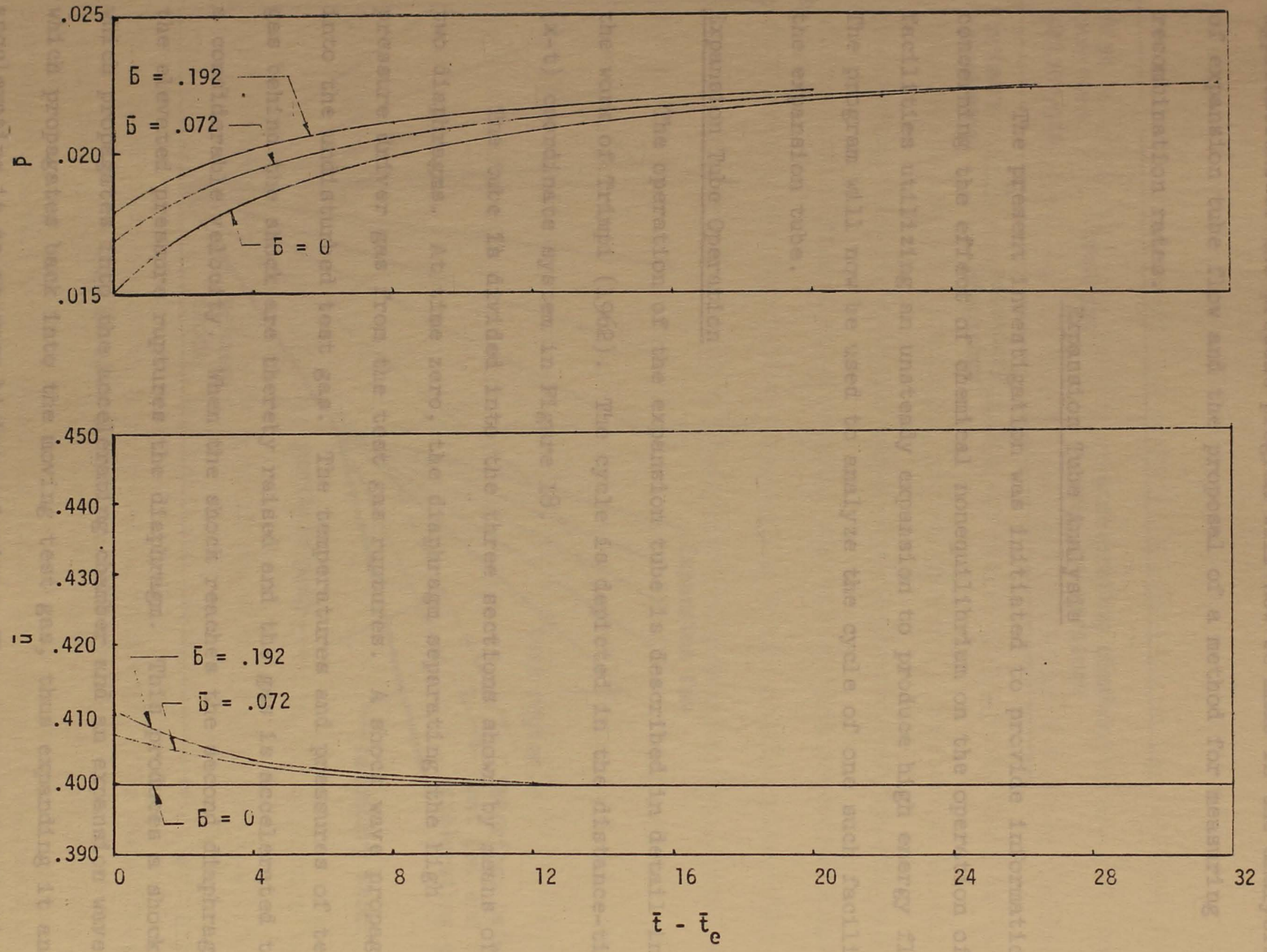

Figure 17. Pressure and velocity variation in the near-steady region

and the effects of nonequilibrium chemistry discussed. More specific applications of the present program will now be made in the analysis of expansion tube flow and the proposal of a method for measuring recombination rates.

Expansion Tube Analysis

The present investigation was initiated to provide information concerning the effect of chemical nonequilibrium on the operation of facilities utilizing an unsteady expansion to produce high energy flow. The program will now be used to analyze the cycle of one such facility, the expansion tube.

Expansion Tube Operation

The operation of the expansion tube is described in detail in the work of Trimpi (1962). The cycle is depicted in the distance-time (x-t) coordinate system in Figure 18.

The tube is divided into the three sections shown by means of two diaphragms. At time zero, the diaphragm separating the high pressure driver gas from the test gas ruptures. A shock wave propagates into the undisturbed test gas. The temperatures and pressures of test gas behind the shock are thereby raised and the gas is accelerated to a considerable velocity. When the shock reaches the second diaphragm, the elevated pressure ruptures the diaphragm. This produces a shock which propagates into the accelerating chamber and an expansion wave which propagates back into the moving test gas, thus expanding it and accelerating it to an even higher velocity. The gas used for testing

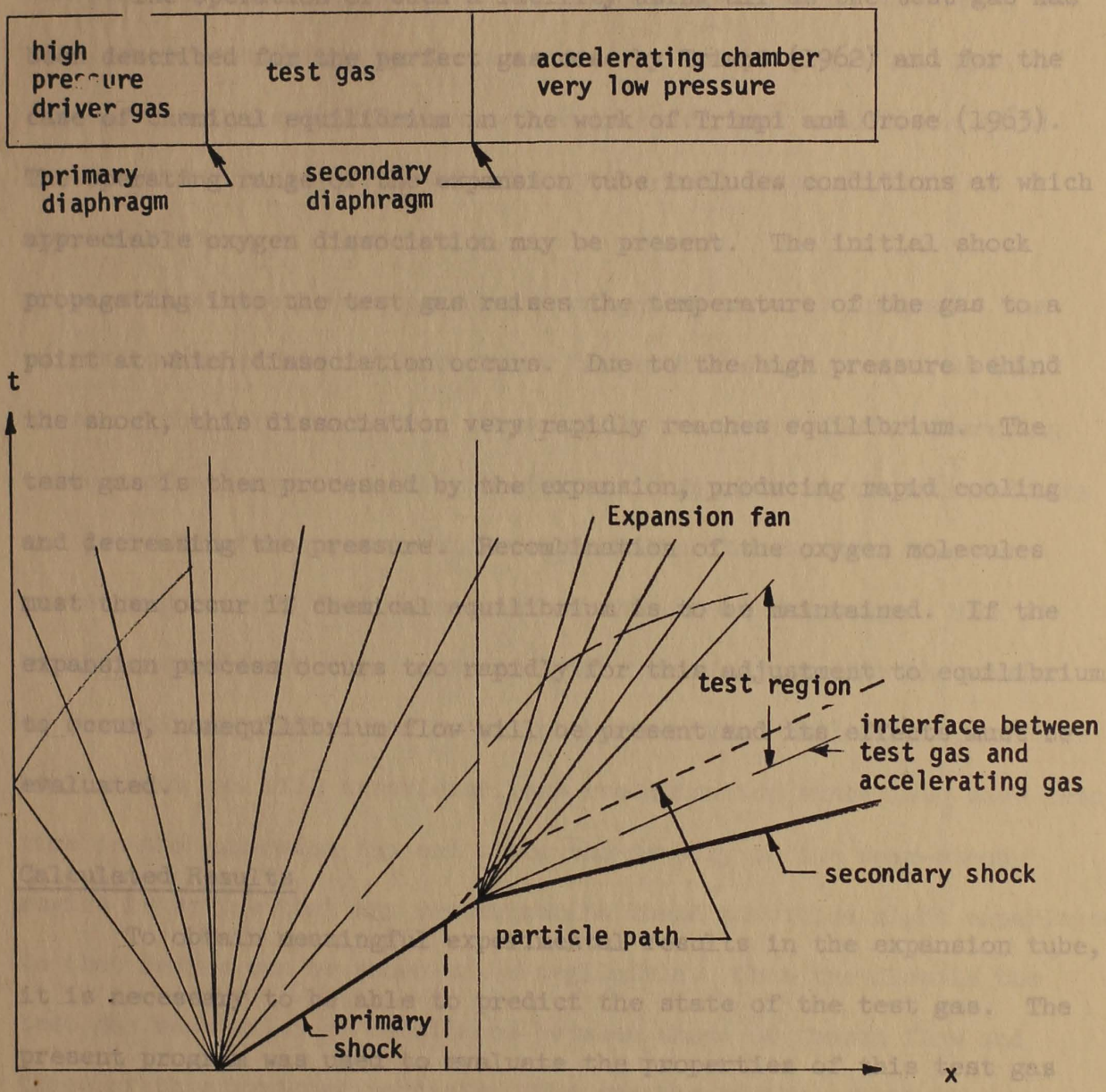

Figure 18. Expansion tube cycle

purposes is then the constant property (at least in the perfect gas and equilibrium cases) gas bounded by the tail of the expansion and the contact surface between the test gas and accelerating gas.

The operation of such a facility using air as the test gas has been described for the perfect gas case by Trimpi (1962) and for the case of chemical equilibrium in the work of Trimpi and Grose (1963). The operating range of the expansion tube includes conditions at which appreciable oxygen dissociation may be present. The initial shock propagating into the test gas raises the temperature of the gas to a point at which dissociation occurs. Due to the high pressure behind the shock, this dissociation very rapidly reaches equilibrium. The test gas is then processed by the expansion, producing rapid cooling and decreasing the pressure. Recombination of the oxygen molecules must then occur if chemical equilibrium is to be maintained. If the expansion process occurs too rapidly for this adjustment to equilibrium to occur, nonequilibrium flow will be present and its effects must be evaluated.

Calculated Results

To obtain meaningful experimental results in the expansion tube, it is necessary to be able to predict the state of the test gas. The present program was used to evaluate the properties of this test gas for a particular expansion tube operating condition. The conditions behind the initial shock, i.e., the conditions in the test gas after it has been processed by the shock but before it undergoes the unsteady expansion, were taken to be those considered in the general example

discussed previously. An additional condition that the velocity of the test gas at that point is 3.3×10^5 cm per sec was specified. The same species, O, O_2, and N_2 were considered as well as the reactions and reaction rates of the previous example. For such conditions, and with proper conditions in the accelerating chamber, the test gas, if expanded in an equilibrium state, could reach test conditions which duplicate a velocity of 35,000 feet per second at an altitude of 200,000 feet.

Calculations were performed using the computer program. The expansion was carried to much lower temperatures and pressures than those of the first example. A reasonable length of the accelerating chamber of an expansion tube is 150 feet. Results of the calculations are presented for a gas particle which makes its way into the test gas at a point 150 feet downstream of the second diaphragm. The particle considered then represents the limiting case for the amount of recombination which can occur in the test gas. All other particles in the test gas will experience less recombination since they have less time in the expansion fan and since the density in the near-steady region is so low that any recombination these particles might experience in that region can be shown to be negligible. Thus the flow in the test gas must exist at conditions between those of frozen flow and those of this limiting particle. The results of the calculation are shown in Figures 19, 20, and 21. The method of Trimpi and Gross (1963) is used to calculate the equilibrium curves. A particle is chosen which will, if expanded in a state of chemical equilibrium, obtain a velocity of 35,000 feet per second and properties equivalent to those

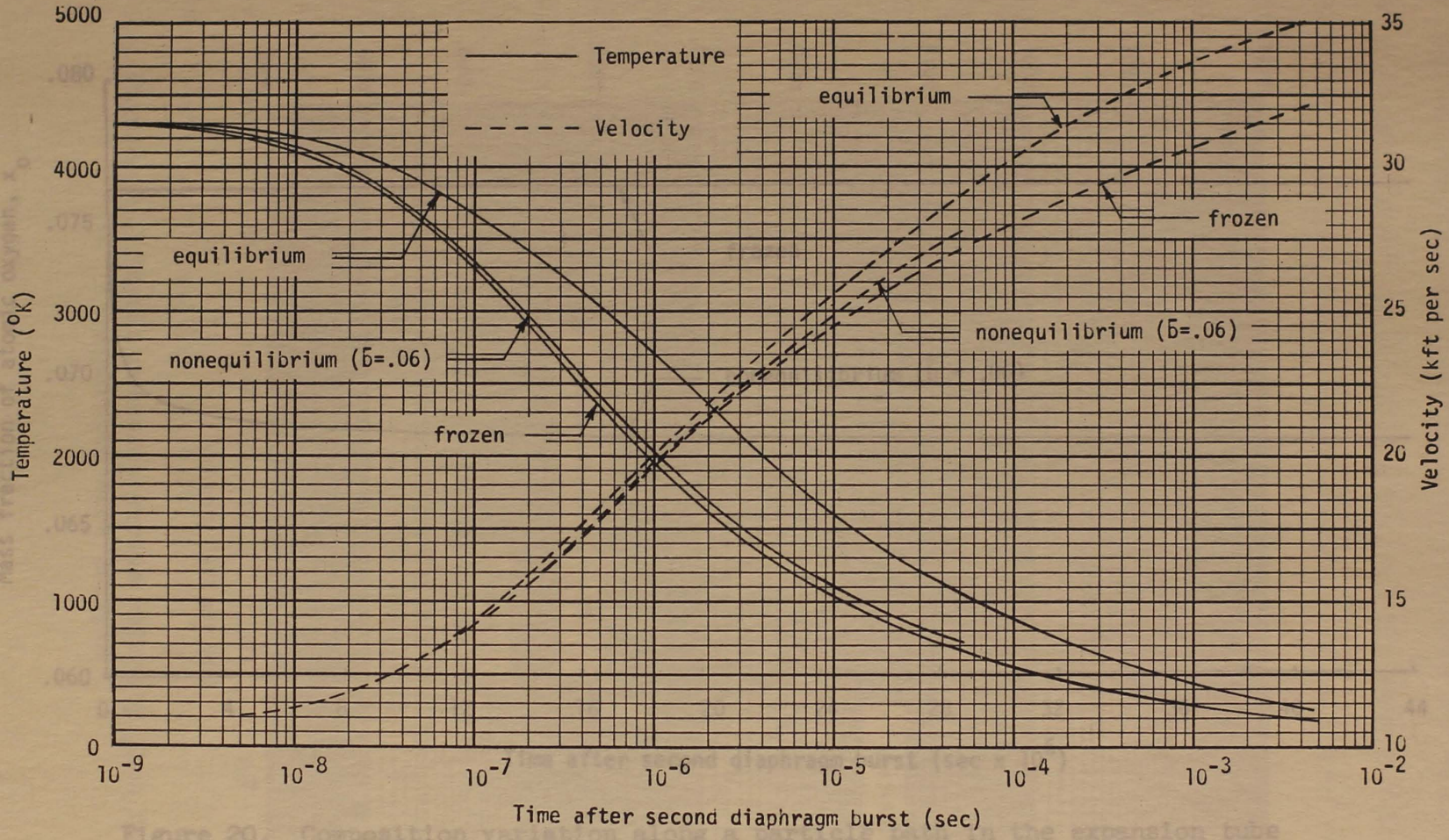

Figure 19. Temperature and velocity variation in the expansion tube

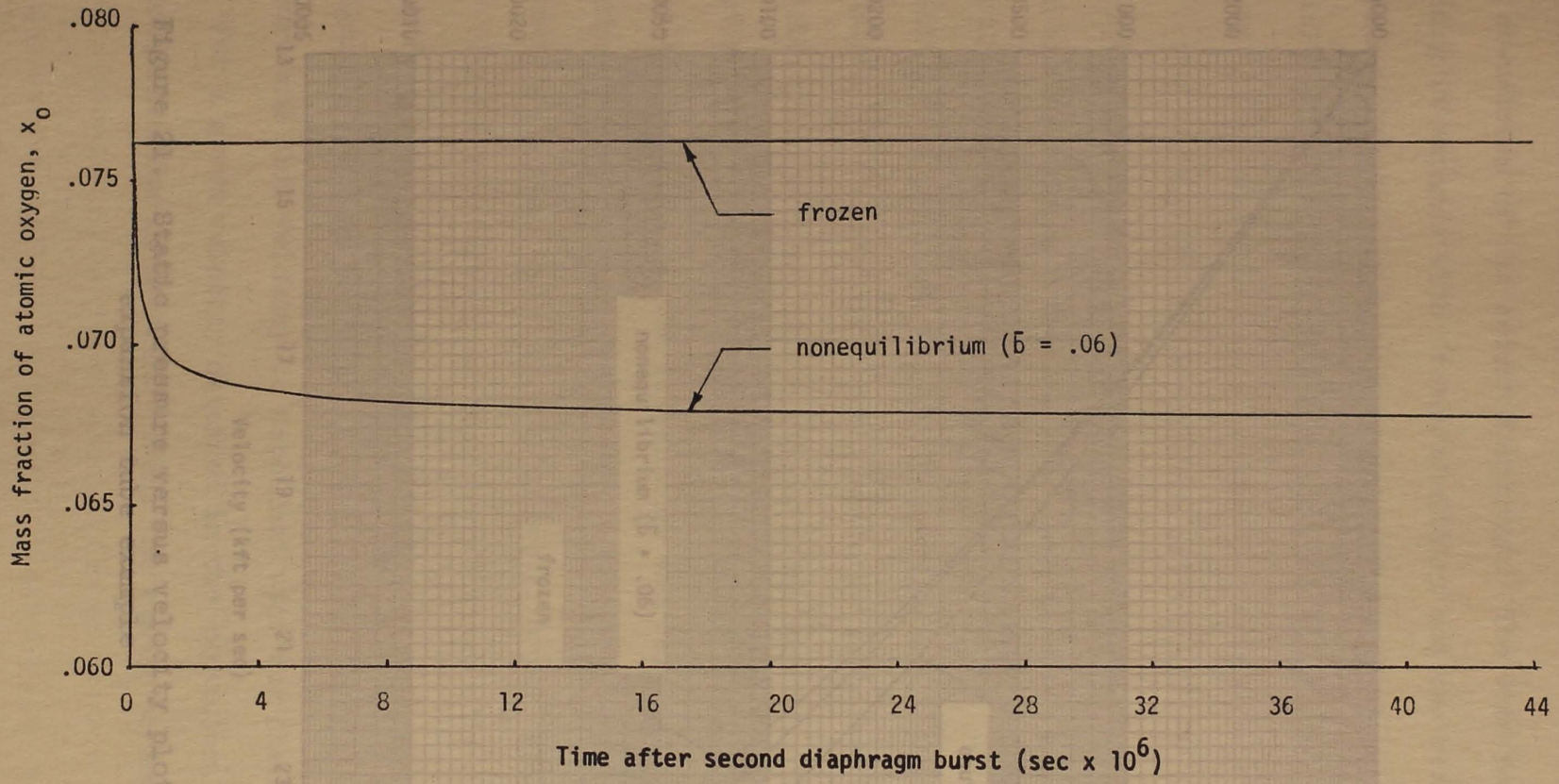

Figure 20. Composition variation along a particle path in the expansion tube

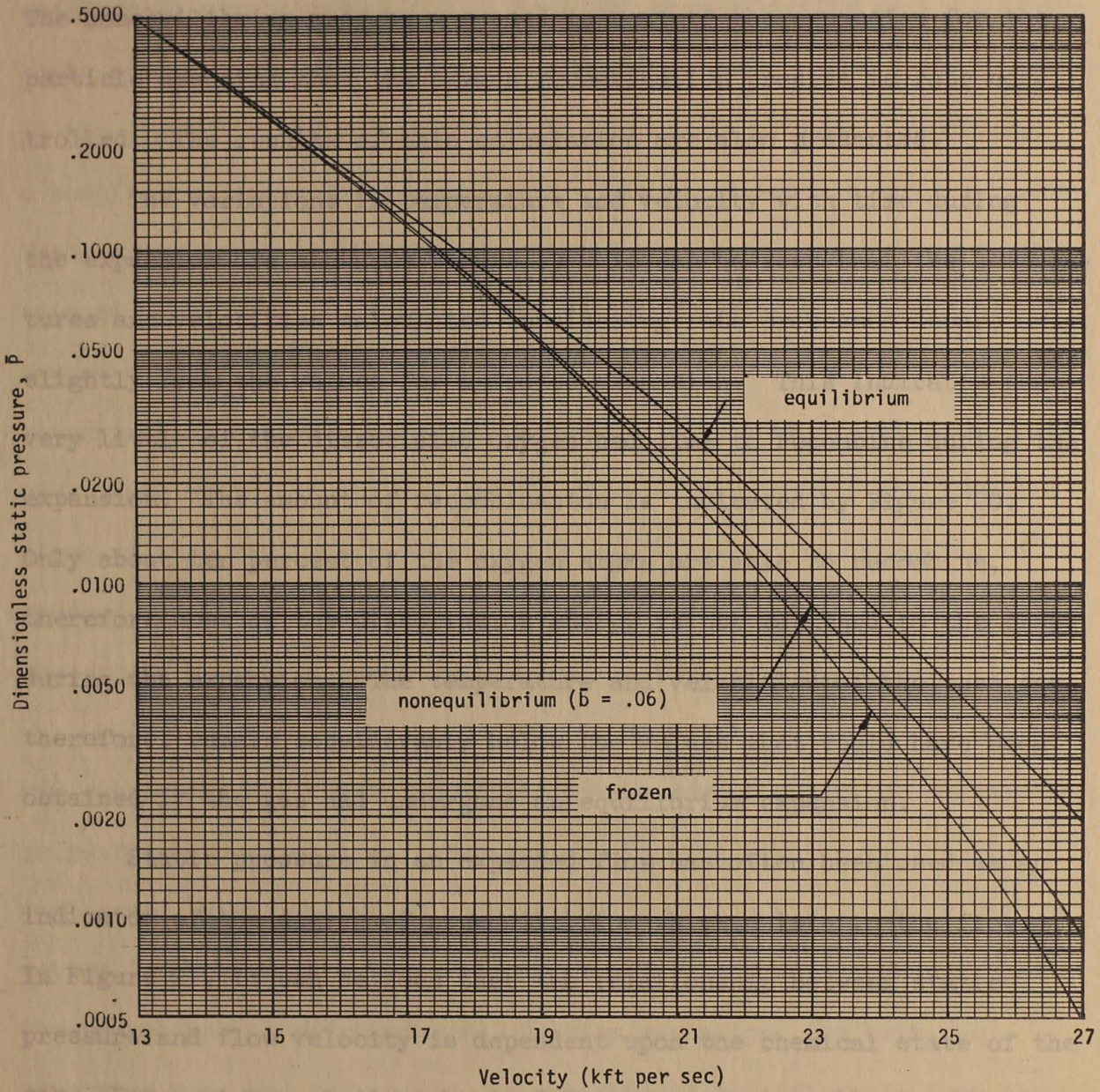

Figure 21. Static pressure versus velocity plot for the expansion tube example

at 200,000 feet altitude at the time it leaves the expansion fan 150 feet downstream of the second diaphragm. The same particle was analyzed assuming it expands with frozen chemistry and the results are presented. The nonequilibrium program was used to compute the expansion for the particle assuming that the oxygen recombination process is rate controlled. The results of this calculation are also presented.

The variations in temperature and velocity with time during the expansion are shown in Figure 19. It can be seen that the temperatures and velocities calculated considering rate processes depart only slightly from the values for a frozen expansion. This indicates that very little of the dissociated oxygen had time to recombine during the expansion. The amount of recombination is indicated by Figure 20. Only about ten percent of the oxygen atoms are able to recombine, therefore most of the dissociation energy is not returned to the flow during the expansion. The temperature and velocities of the test gas, therefore, remain considerably below the values that could have been obtained if the gas had undergone an equilibrium expansion.

Static pressure in an expanded flow has often been used as an indicator of the degree of nonequilibrium which exists in the flow. In Figure 21, it can be seen that the relationship between static pressure and flow velocity is dependent upon the chemical state of the gas. For a given velocity obtained in the expansion, the existence of nonequilibrium in the flow lowers the static pressure considerably.

Expansion Tube, Hypersonic Nozzle Comparison

A comparison can be made at this point between the unsteady flow in the expansion tube and the quasi-one dimensional flow in a hypersonic wind-tunnel nozzle. Bray (1959) analyzed nonequilibrium flow in hypersonic nozzles using the Lighthill-Freeman gas model. The work of Hall et al. (1962) obtained a solution to the nozzle problem considering a complicated gas mixture containing a number of species and reactions. Their investigations both indicated that as the quasi-one-dimensional expansion proceeds to high velocities, the associated density drop causes a rapid decrease in the recombination rate. Therefore, the recombination of the atomic species, while appreciable during the initial phase of the expansion, quickly diminishes, leaving the compositions at essentially a constant value and allowing the expansion to proceed in a frozen manner. The same phenomena is seen to exist in the expansion tube flow and is shown graphically in Figure 20.

In addition to the similarity in composition change for the two expansions, a direct comparison can be seen for the thermodynamic properties and velocities. Temperature is, for both cases, highly influenced by the amount of nonequilibrium in the flow. It is, of course, increased above the frozen value by an amount dependent upon the recombination which occurs. Density variation, for both the expansion tube and the nozzle, is not altered significantly from the equilibrium case by nonequilibrium in the flow. Static pressure, in both instances, is lowered as nonequilibrium increases. The flow velocity of the test gas in the expansion tube and the hypersonic-

wind-tunnel nozzle are lowered when the recombination rates are not adequate to return the dissociation energy to the flow.

The general effects of nonequilibrium on the flow quantities in an expansion tube are seen to be very similar to the same effects on flow through a hypersonic nozzle.

Expansion Tube Comments

Freezing of the test gas was shown to be present in the expansion tube as well as in the wind-tunnel nozzle. The question might arise, therefore, as to the advantage of using the expansion tube. As was shown by Trimpi (1962), the expansion tube cycle can produce a high enthalpy test gas without subjecting the test gas to the reservoir conditions required for tunnel flow. Therefore, the expansion tube test gas is never raised to conditions where excessive dissociation and ionization occurs. Although some nonequilibrium may be present in the flow, it is very much less than would be experienced by a wind tunnel operating with the same test conditions. In fact, the reservoir pressures and temperatures which would be required to produce the test conditions in a wind tunnel for the example presented are beyond the range of present design capability.

The present example was used to show the value of the present program in analyzing expansion tube flow. The results shown are not indicative of expansion tube flow in general. Operating conditions were purposely chosen which would produce considerable dissociation. Expansion tube operation can cover a wide range, much of which does not involve appreciable dissociation. For much of the operating range

of the expansion tube, densities are higher and the degree of dissociation much lower. For such conditions, the nonequilibrium effects will be much less. An extension of the present work will be undertaken to evaluate a wide range of operating conditions. The present program should prove very useful in such an evaluation.

Application to Rate Studies

A great many gas dynamic problems of current interest require an accurate knowledge of reaction rates for their solution. The present state of computer technology permits the inclusion of the rate chemistry of component gases in the analysis of flow problems which can be solved by numerical techniques. Many of these problems are dominated by recombination reactions, i.e., by the recombination of two atoms to form a molecule.

Consider as an example the rocket nozzle. The exhaust gas, whether it be hydrogen heated by a nuclear reactor or the products of chemical combustion, is initially at a temperature at which dissociation of some of the molecules occurs. As the gas is expanded through the nozzle, the temperature and pressure decrease and, to maintain chemical equilibrium, the atoms must recombine. However, the recombination process is rate controlled. The exit velocity of the gas and thus the specific impulse of the rocket, as well as the heat transfer to the nozzle, is thus dependent upon the rate at which this recombination occurs. An accurate knowledge of recombination rates is therefore a prerequisite for the solution of such problems.

Studies of the effects of various catalysts on the recombination rates are needed to prescribe what additives should be included in the fuel to promote rapid recombination and thus allow the maximum exit velocities to be obtained.

Similarily, accurate recombinations rate are needed to analyze flow in hypersonic wind tunnels in which the test gas is expanded from reservoir conditions at which some of the gas is dissociated. The analysis of the expansion of air around reentry vehicles after the air has become dissociated in the stagnation region must also account for recombination and the rates at which it occurs.

The above examples were cited simply to indicate the need for accurate data describing the rates of numerous recombination reactions. Despite this great need, very little experimental work has been done in the direct measurement of recombination rates. Most investigators have undertaken the job of determining the forward rate, i.e., the rate of dissociation of the molecules into atoms. Assuming that the physical mechanisms governing the reaction rates are the same for equilibrium as they are for departures from equilibrium, the equilibrium constant based on concentrations, K_c, is used with k_f, the dissociation rate coefficient, to obtain k_r, the recombination rate coefficient, through the expression, $K_c = \frac{k_f}{k_r}$, which is completely valid at equilibrium. However, the uncertainty which exists in the knowledge of the mechanisms of the various rates could lead to considerable error in the rate predicted by such a mechanism for flow in which the departures from

equilibrium are great. It therefore appears that before recombination rates can be adopted which are accurate for any degree of nonequilibrium in the flow, these recombination rates must be directly measured. The following discussion outlines an experiment for such a measurement and, using the program developed earlier, examines the feasibility of such an experiment.

Outline of the Proposed Experiment

Consider the physical set up shown in Figure 22. The proposed experiment utilizes a shock tube with a second diaphragm and an accelerating chamber added. Observation windows are included in the accelerating chamber. At time zero, the first diaphragm breaks, thus allowing a shock to propagate into the test gas. The shock reflects from the second diaphragm, producing a region of high temperature, high pressure flow adjacent to the second diaphragm. The second diaphragm is then ruptured by controlled means, allowing a shock to propagate into the accelerating gas and causing the test gas to be processed by an expansion wave. As can be seen in the x-t diagram of Figure 22, the net result is that the nearly constant property region between the tail of the expansion fan and the gas interface is given a downstream velocity and passes each of the observation windows. The particles A, B, C, and D should be noted. Particle A is the particle adjacent to the second diaphragm when it breaks. It goes through the expansion with zero residence time and is in the near-constant property region for its entire travel down the tube. It is always next to the gas interface. Particles B, C, and D are respectively further from the

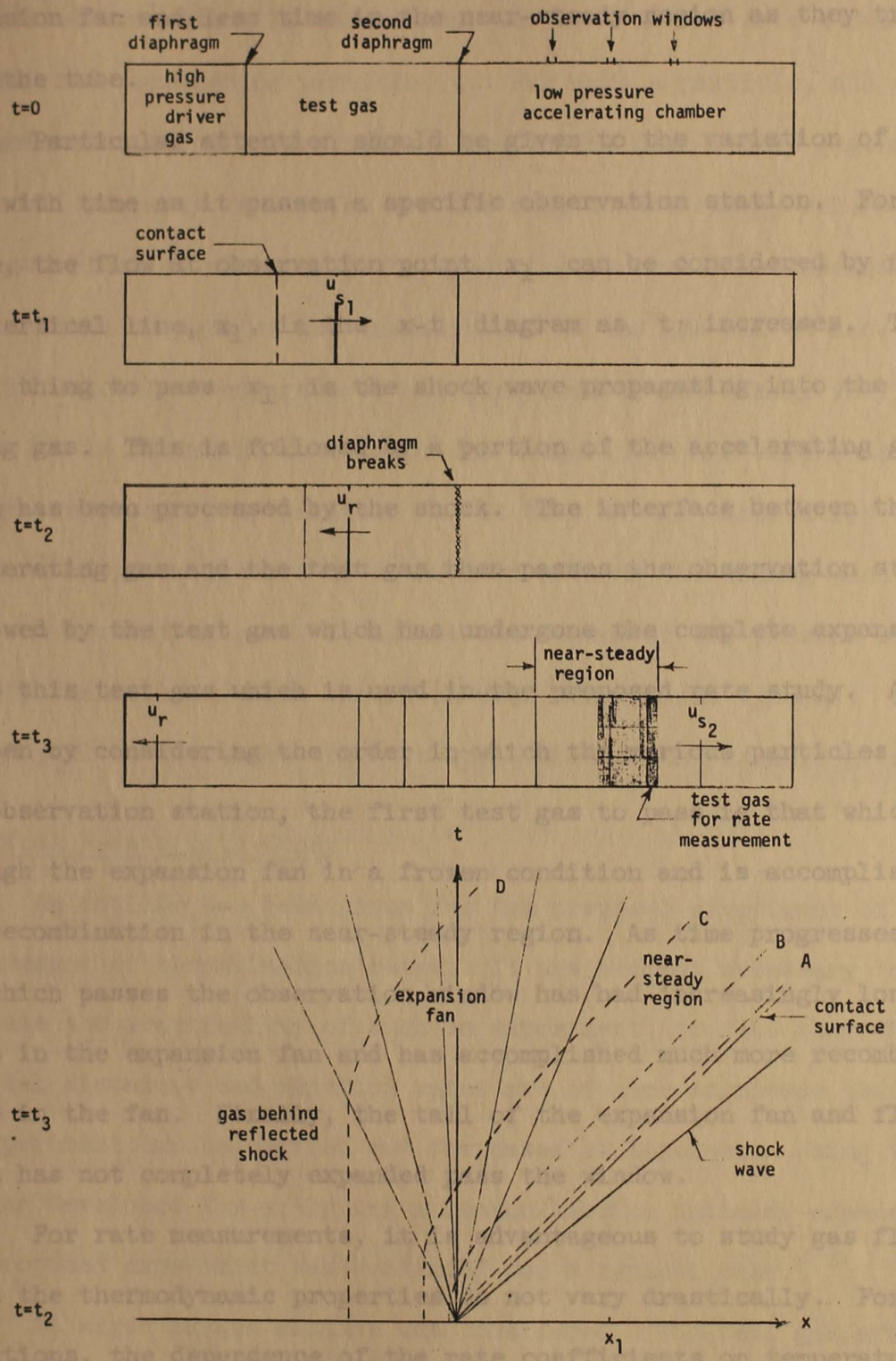

x-t diagram of the expansion after the second diaphragm burst

Figure 22. Rate experiment diagram

diaphragm when it breaks, thus spend successively more time in the expansion fan and less time in the near-steady region as they travel down the tube.

Particular attention should be given to the variation of the flow with time as it passes a specific observation station. For example, the flow at observation point x_1 can be considered by following the vertical line, x_1, in the x-t diagram as t increases. The first thing to pass x_1 is the shock wave propagating into the accelerating gas. This is followed by a portion of the accelerating gas which has been processed by the shock. The interface between the accelerating gas and the test gas then passes the observation station followed by the test gas which has undergone the complete expansion. It is this test gas which is used in the proposed rate study. As can be seen by considering the order in which the various particles pass the observation station, the first test gas to pass is that which went through the expansion fan in a frozen condition and is accomplishing its recombination in the near-steady region. As time progresses, the gas which passes the observation window has had increasingly longer times in the expansion fan and has accomplished much more recombination while in the fan. Finally, the tail of the expansion fan and flow which has not completely expanded pass the window.

For rate measurements, it is advantageous to study gas flow in which the thermodynamic properties do not vary drastically. For such conditions, the dependence of the rate coefficients on temperature can be ascertained more accurately and the coefficients can be evaluated

for a specific range of conditions. The temperature and pressure can be held more constant in the present instance if the rate studies are carried out considering particle A. For such a particle, all of the recombination which occurs takes place in the near-steady region. Thus, all property variations are due only to the energy released by the recombination and not to the expansion process. Measurements of considerable changes in the compositions of the gas can be made of flow in which the temperatures and pressures do not change very much.

It is desirable to measure the temperature and composition of the gas represented by particle A at each of the observation windows. A number of investigators have proposed methods for making such measurements in a reacting gas. It is not the object of the present work to specify the methods which should be used for various systems. One method will be discussed which is applicable to the example presented.

Numerical Feasibility Study

An outline has been given for the proposed experiment of direct measurement of recombination rates. It now becomes necessary to validate the practicality of such an experiment, to show that the times, physical distances and reaction rates are of such magnitude that such an experiment can be carried out for cases of interest. Using the program developed for analyzing a nonequilibrium unsteady expansion, the proposed experiment was evaluated for a typical case.

An argon oxygen mixture was considered. The test gas, after having its temperature and pressure raised by the reflected shock, was

assumed to be in a state of thermodynamic and chemical equilibrium with the following properties.

$$\rho_o = 10^{-3} \frac{gm}{cm^3}$$

$$T_o = 4000^oK$$

$x_o = 0.05306$ = mass fraction of O

$x_{O_2} = 0.04694$ = mass fraction of O_2

$x_A = 0.90$ = mass fraction of A.

The velocity of the gas was considered to be zero behind the reflected shock. The following reactions were considered:

(a) $O_2 + O \rightarrow 3O$

(b) $3O \rightarrow O_2 + O$

(c) $2O_2 \rightarrow 2O + O_2$

(d) $O_2 + 2O \rightarrow 2O_2$

(e) $O_2 + A \rightarrow 2O + A$

(f) $2O + A \rightarrow O_2 + A$.

Recombination rate coefficients believed to represent the best available values were used in the calculations and are listed in Appendix F.

Due to the relatively short vibrational relaxation times of O_2 and the small contribution the vibrational energy of O_2 makes to the total energy of the system, the vibrational energy of O_2 was considered to remain in equilibrium throughout the process.

In the calculation of this case, the expansion was assumed to be represented by the original physical model proposed for this work, i.e., the constant velocity piston withdrawal from a gas mixture at equilibrium. Thus, for the present analysis, the interface between the test gas and the accelerating gas was represented by the piston path. Such a representation produces some small degree of error, since, for the actual case, the interface velocity would vary slightly due to the recombination occuring in the flow, whereas the piston velocity used to represent it remains constant. However, for the present feasibility study, it is felt that the piston model adequately represents the process. A piston velocity of 1.09×10^5 centimeters per second was prescribed.

Calculations were carried out for this case for both the expansion fan and the near-steady regions. The results may be seen in Figures 23 and 24. The variations are depicted as a function of the dimensionless time, $\bar{t} - \bar{t}_o$, where $\bar{t}_o$ is the time at which the particle first entered the expansion fan.

Consider first the composition variation with time along the four prescribed particle paths. Along paths C and D, a large portion of the time is spent in the expansion fan and the composition is subject to variable rates of change. The flow bounded by path A,

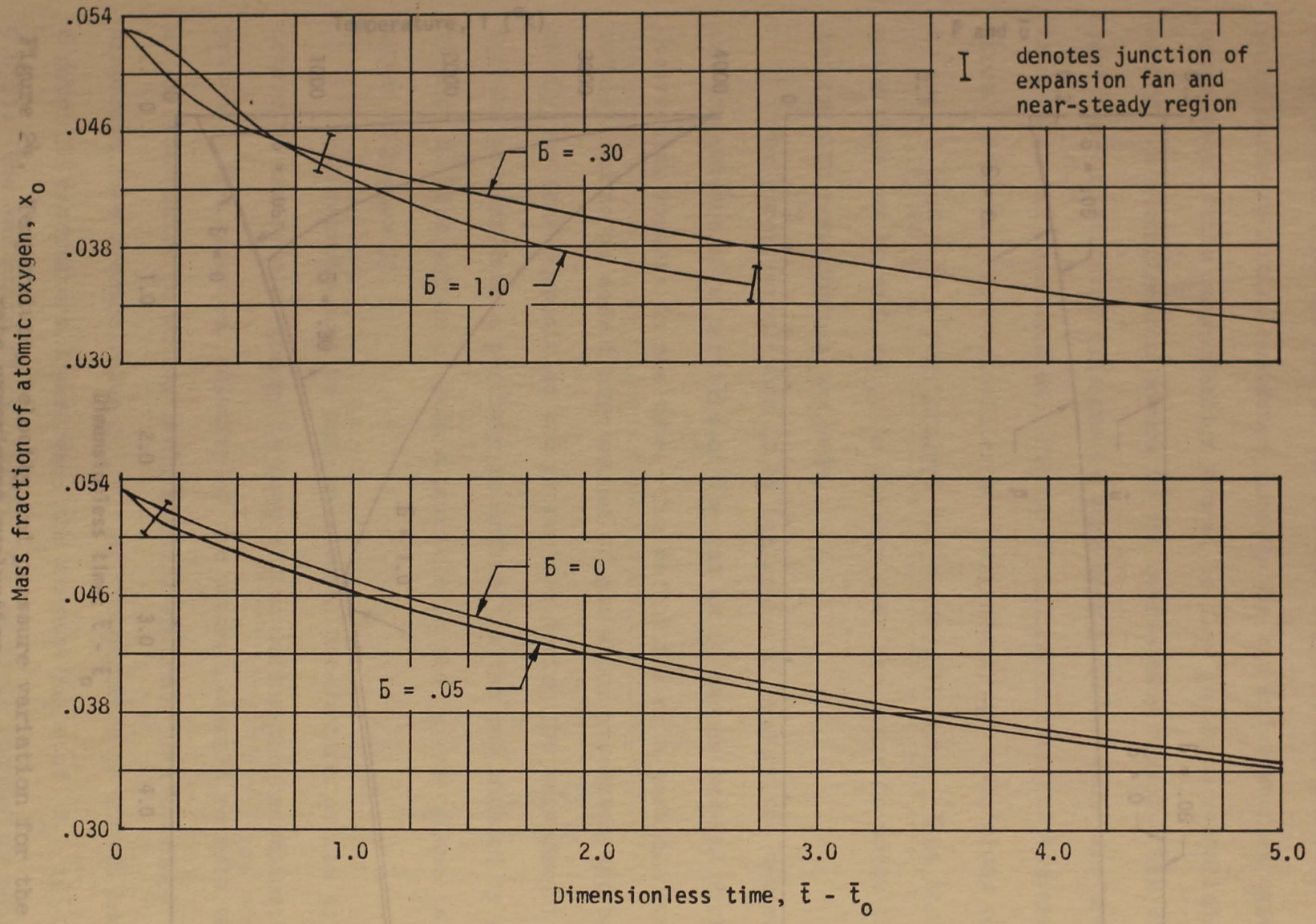

Figure 23. Composition variation for the rate experiment evaluation

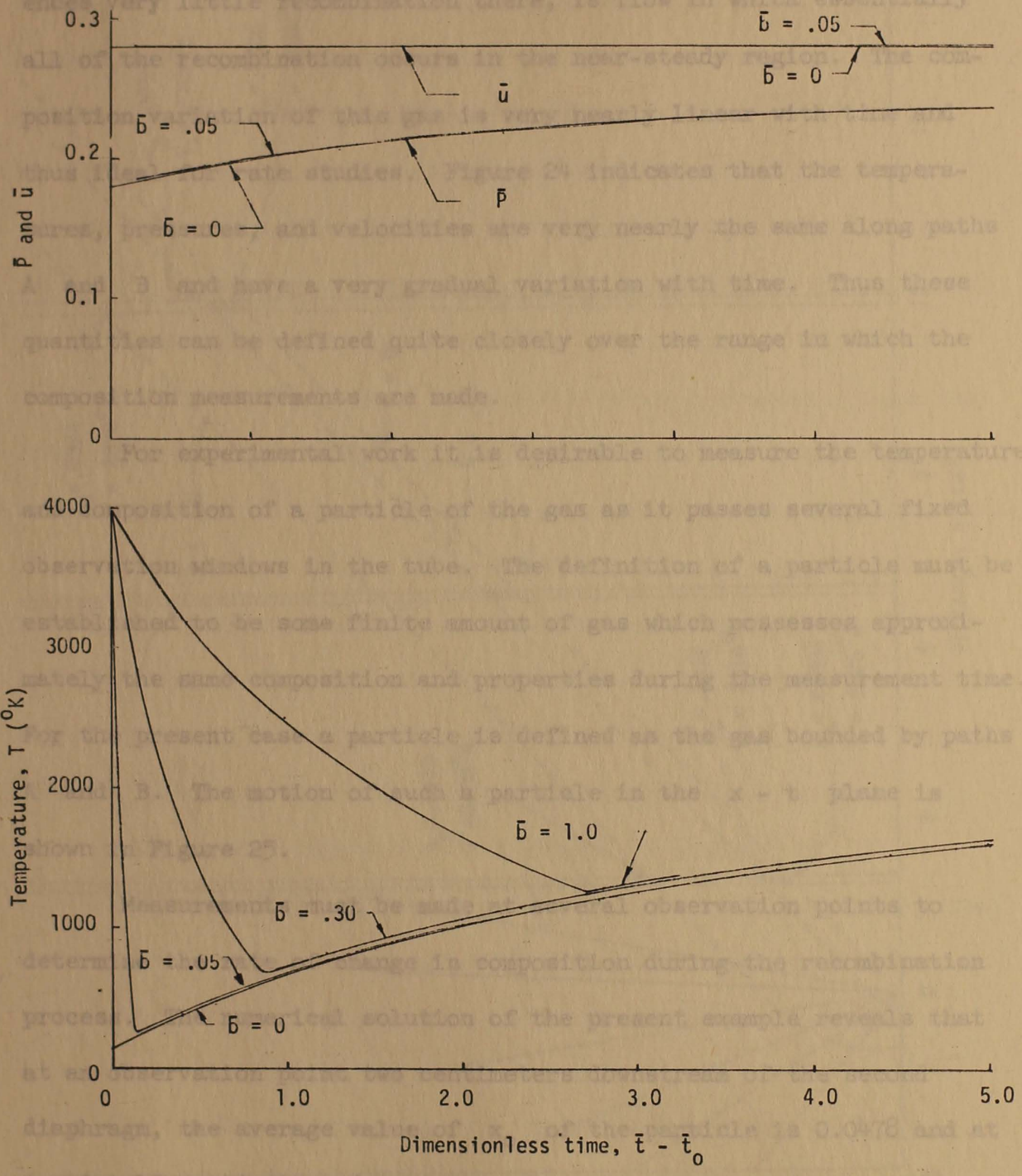

Figure 24. Temperature, velocity, and pressure variation for the rate experiment evaluation

which emerges from the fan at its initial composition, and path B, which has very little residence time in the fan and therefore experiences very little recombination there, is flow in which essentially all of the recombination occurs in the near-steady region. The composition variation of this gas is very nearly linear with time and thus ideal for rate studies. Figure 24 indicates that the temperatures, pressures, and velocities are very nearly the same along paths A and B and have a very gradual variation with time. Thus these quantities can be defined quite closely over the range in which the composition measurements are made.

For experimental work it is desirable to measure the temperature and composition of a particle of the gas as it passes several fixed observation windows in the tube. The definition of a particle must be established to be some finite amount of gas which possesses approximately the same composition and properties during the measurement time. For the present case a particle is defined as the gas bounded by paths A and B. The motion of such a particle in the $x - t$ plane is shown in Figure 25.

Measurements must be made at several observation points to determine the rate of change in composition during the recombination process. The numerical solution of the present example reveals that at an observation point two centimeters downstream of the second diaphragm, the average value of x_o of the particle is 0.0478 and at a point 12 centimeters downstream, the average value of x_o is 0.0353. The variation of x_o within the particle bounded by paths A and B is less than 2.5 percent. Due to its high velocity, the

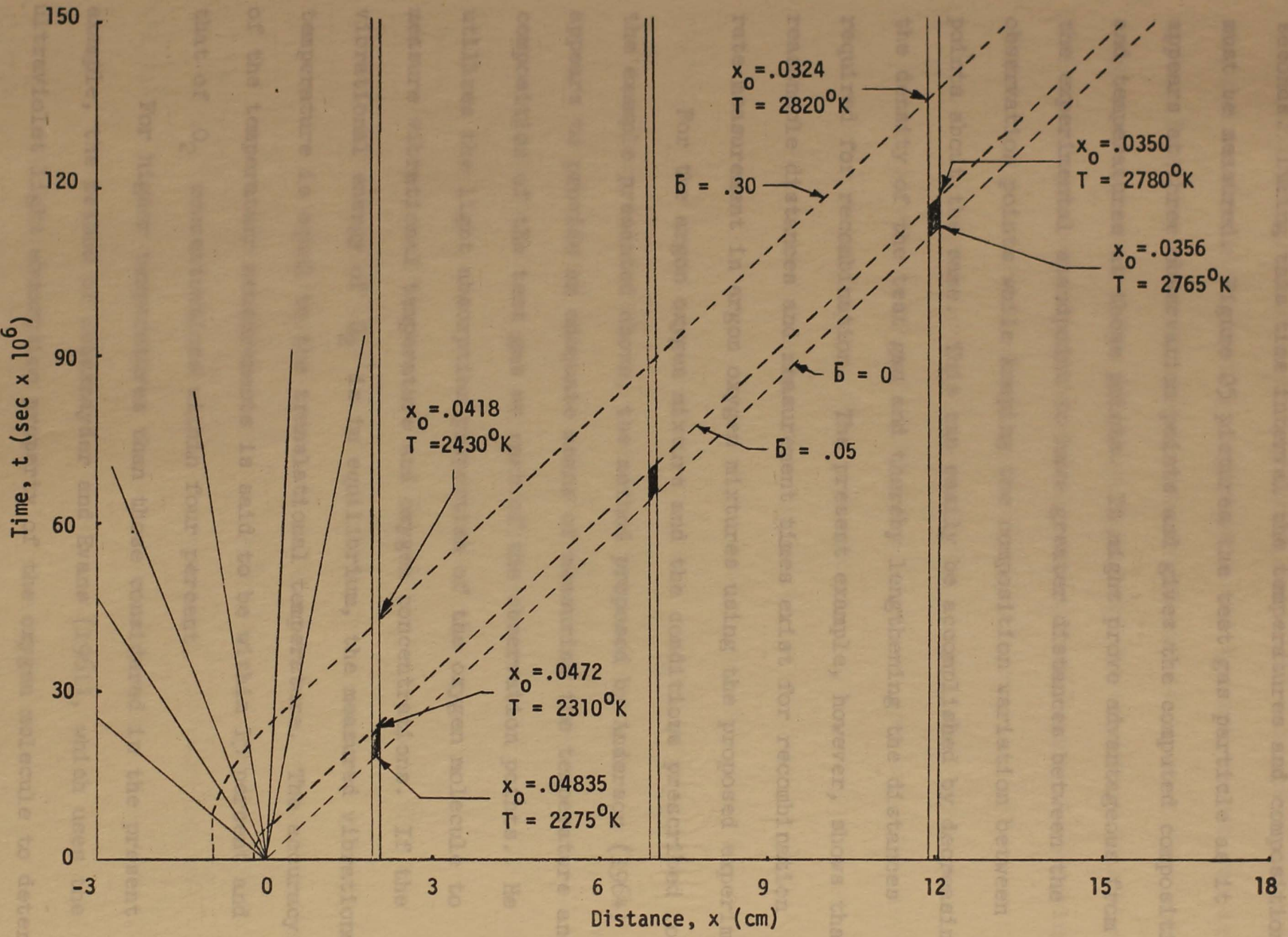

Figure 25. The x-t diagram for the rate experiment evaluation

particle passes an observation point in approximately 6×10^{-6} seconds. During this time interval the temperatures and compositions must be measured. Figure 25 pictures the test gas particle as it appears at three observation points and gives the computed compositions and temperatures at these points. It might prove advantageous from the experimental standpoint to have greater distances between the observation points while keeping the composition variation between points about the same. This can easily be accomplished by decreasing the density of the test gas and thereby lengthening the distances required for recombination. The present example, however, shows that reasonable distances and measurement times exist for recombination rate measurement in argon oxygen mixtures using the proposed experiment.

For the argon oxygen mixture and the conditions prescribed for the example presented above, the method proposed by Anderson (1964) appears to provide an adequate means of measuring the temperature and composition of the test gas at each of the observation points. He utilizes the light absorption properties of the oxygen molecule to measure vibrational temperature and oxygen concentrations. If the vibrational energy of O_2 is in equilibrium, the measured vibrational temperature is equal to the translational temperature. The accuracy of the temperature measurements is said to be within 15 percent and that of O_2 concentrations within four percent.

For higher temperatures than those considered in the present example, the method of Schexnayder and Evans (1961), which uses the ultraviolet light absorption property of the oxygen molecule to determine O_2 concentrations, might prove useful.

It is not the purpose of the present investigation to prescribe a specific measurement technique but to establish a means of processing the gas to obtain a suitable condition in which measurements can be made. From the numerical case presented above, it is seen that this can be accomplished. The proposed experiment is therefore feasible and should prove quite useful in the direct measurement of recombination rates.

SUMMARY AND CONCLUSIONS

The Analysis

A method of approach has been established for analyzing the flow in an unsteady one-dimensional expansion containing vibrational excitation and chemical nonequilibrium. The basic conservation equations, generalized equations of state, and rate equations were established. From this system of equations, the characteristic curves and their associated compatibility relations were derived. The derivation showed conclusively that for a system in which finite rate processes are considered, no matter how fast, the frozen speed of sound (the speed of sound calculated assuming the rate controlled quantities are frozen at their local value) is analogous to the unambigious sound speed of the perfect gas case in specifying the characteristic directions. If the equilibrium flow model is postulated, the equilibrium sound speed was shown to be the correct one for this purpose.

The characteristics of the nonequilibrium unsteady expansion were established for a general gas mixture and generalized rate equations, thus establishing an approach which could be used for any gas model. The equations defining the characteristic curves and their compatibility relations were established in both the Eulerian and Lagrangian coordinate systems. It is believed that this work provides the first derivation of the characteristic equations of an unsteady expansion which possesses the generality needed for handling any reacting system of gases.

A thermodynamic model was developed to describe the reacting gas mixtures of interest in the present investigation. Assumptions were made which were quite adequate for the present investigation, but could be refined for more extended studies. Improvements in the thermodynamic model could include the consideration of ionization and more exact treatment of vibrational and electronic energies.

A numerical procedure was developed for applying the characteristic equations in finite difference form to obtain a solution over the flow field. This procedure proved satisfactory for the cases investigated. Calculations were performed for applications of current interest using the IBM 7094 electronic digital computer.

General Application

A calculated example was presented which used an approximate model for air and included a number of simultaneous chemical reactions. The results were evaluated to provide a clear physical picture of a reacting mixture of gases being processed by an unsteady, one-dimensional expansion. The variations in thermodynamic properties and compositions were analyzed along particle paths through the expansion.

It was seen that the rate of recombination of atom species was rapid during the initial part of the expansion, but decreased quickly as the density decreased. This rapid decrease in recombination rates as the gas expanded to low densities resulted in an apparent freezing of the compositions, i.e., as the densities became very small the gas compositions asymtotically approached a constant value.

Individual reaction rates were considered in an effort to understand the chemical nonequilibrium processes more fully. It was seen that the recombination reactions were dominant during most of the expansion for the nonequilibrium cases calculated.

The reaction resulting from the collision of three atoms of O was found to produce the greater portion of the recombination during the early part of the expansion when the atomic oxygen content was high. As appreciable recombination occurred, decreasing the amount of atomic oxygen, the other reactions played a large role in producing the recombination of oxygen atoms.

The establishment of a criterion for freezing was considered. It became evident that for a process in which a number of simultaneous rate processes are considered, no simple test for freezing can be established. The variations in the different rate equations were not similar throughout the expansion. One rate process may be dominant during one portion of the expansion only to become relatively unimportant compared to another process at a later point in the expansion. Thus, each rate process must be considered in establishing a criterion for the existence of frozen flow.

Temperature was found to be the thermodynamic variable most influenced by the rate chemistry. Considerable increases in temperature above the frozen value were observed when a large amount of recombination of the dissociated atoms occurred. A great deal of the dissociation energy was returned to the flow by the recombination process, resulting in the increased excitation of the translational, rotational, and vibrational energy modes.

Static pressure proved to be fairly sensitive in the nonequilibrium processes. An increase in static pressure was noted as recombination occurred. In like manner, the flow velocity increased as the recombination process returned energy to the flow.

Calculated results were presented for both the expansion fan and the near-steady region. Rapid property variations were, of course, characteristic of the expansion fan. Throughout the near-steady region between the expansion fan and the piston face, the variations in properties and compositions were very nearly linear with time, thus suggesting the value of this region for use in rate studies.

An extension to the present work of increasing the understanding of the structure of a nonequilibrium unsteady expansion could be made in several directions. First, a more exact gas model for air could be formulated which would be applicable over a wider range of conditions. Such a model would include more exact representation of vibrational and electronic energies, the additional apecies N and NO, and the reactions associated with the production of these species. Cases could also be treated utilizing the present program and an air model which would consider vibrational energy as a rate controlled quantity. A further need in the analysis of unsteady expansions is for an equilibrium solution of the expansion which is consistent with the gas model used in the nonequilibrium case. Equilibrium solutions are presently available which are dependent upon charts of thermodynamic properties.

One further extension is recommended with respect to the physical model of the expansion. The boundary condition defined by

the constant velocity piston withdrawal, while being convenient for computing purposes and an adequate representation of the physical situation for most applications, does not quite duplicate the actual process needed for some cases. Because of the high values of piston velocity considered in applications of the nature discussed earlier, the physical mechanism used to provide the expansion is not the withdrawal of a piston. It is instead the bursting of a diaphragm between a high and low pressure region. The boundary of the near-steady region is therefore no longer a constant velocity piston face, but the interface between the gases which were initially in the separate chambers. Because of pressure changes in the near-steady region due to recombination in the flow, the shock propagating into the low pressure gas will possess a velocity which varies slightly with time. Thus, the interface velocity varies slightly with time, producing a boundary condition which differs slightly from the constant velocity piston condition used in the present work. This extension to the present work should provide a more exact representation of many applications of the nonequilibrium unsteady expansion and serve as a check on the error involved in using the piston model.

Expansion Tube Application

The computer program was used to analyze the flow in an expansion tube for one set of operating conditons. It was concluded from the results obtained that for the particular case calculated the composition of the gas did not vary drastically and the flow properties were nearly those of a chemically frozen expansion. Similarities were

seen between nonequilibrium flow in an expansion tube and that in a hypersonic nozzle. The method of analysis was concluded to be satisfactory for evaluating expansion tube flow.

Much work remains to be done in the analysis of expansion tube flow. Calculations should be made over the entire range of operating conditions of the expansion tube to define the equilibrium, nonequilibrium, and frozen regimes of operation of the facility. Future studies may also include the analysis of the expansion with the test gas made up of a mixture representing planetary atmospheres. The present program appears adequate to handle these future problems.

Rate Studies

An experiment was outlined which uses an unsteady expansion to process a gas for direct measurement of recombination rates. A case using an argon oxygen mixture was calculated and, from the results, it was concluded that the proposed experiment is quite feasible. The variations in compositions and thermodynamic properties with distance were shown to be quite reasonable for making recombination rate measurements. The work presented a suitable method for creating a gas flow in which the rate measurements could be made.

Implementation of the experiment provides opportunities for a great deal of further work. Instrumentation must be selected which can handle the composition and temperature measurements in the desired ranges of study for various gases of interest. The experiment itself should be performed for a number of gases. Effects of catalysts on reaction rates will be a valuable area of study using this method.

It is apparent that a great deal of work in the measurement of recombination rates remains to be done and can be done utilizing the proposed experiment.

LIST OF REFERENCES

Anderson, O. L. 1964. An experimental method for measuring the flow properties of air under equilibrium and nonequilibrium flow conditions, pp. 299-313. In W. C. Nelson (ed.), The High Temperature Aspects of Hypersonic Flow. The Macmillan Company, New York.

Appleton, J. P. 1960a. The structure of a centered rarefaction wave in an ideal dissociating gas. University of Southampton Aeronautics and Astronautics Report No. 136, Southampton.

Appleton, J. P. 1960b. The structure of a Prandtl-Meyer expansion fan in an ideal dissociating gas. University of Southampton Aeronautics and Astronautics Report No. 146, Southampton.

Appleton J. P. 1963. Calculations of the structure of unsteady rarefaction waves in oxygen argon mixtures, allowing for vibrational relaxation. Royal Aircraft Establishment TN-AERO-2873, London.

Arave, R. J. 1963. Centered rarefaction wave in a chemically reacting gas. Master's thesis, University of Seattle, Seattle, Washington.

Atallah, S. 1961. The kinetics of air in a hypersonic shock wave. Air Force Cambridge Research Laboratories, AFCRL-761. Cambridge, Mass.

Bray, K. N. C. 1959. Atomic recombination in a hypersonic wind tunnel nozzle. J. Fluid Mech. 6: 1-32.

Broer, L. J. F. 1958. Characteristics of the equations of motion of a reacting gas. J. Fluid Mech. 4: 276-282.

Byron, S. R. 1959. Measurement of the rate of dissociation of oxygen. J. Chem. Phys. 30(6): 1380-1392.

Camac, M. and A. Vaughn. 1961. O_2 dissociation rates in O_2 - A_r mixtures. J. Chem. Phys. 34(2): 460-470.

Chu, B. T. 1957. Wave propagation and the method of characteristics in reacting gas mixtures with application to hypersonic flow. WADC TN-57-213, Wright Patterson Air Force Base, Ohio.

Clarke, J. F. and M. McChesney. 1964. The Dynamics of Real Gases. Butterworth Inc., Washington.

Courant, R. and K. O. Friedrichs. 1948. Supersonic Flow and Shock Waves. Interscience Publishers, New York.

Der, J. J. 1963. Theoretical studies of supersonic two-dimensional and axisymmetric nonequilibrium flow, including calculations of flow through a nozzle. NASA TR R-164, Washington, D. C.

Eckerman, J. 1958. The measurement of the rate of dissociation of oxygen at high temperatures. Ph. D. dissertation, The Catholic University of America, Washington, D. C.

Fowler, R. H. and E. A. Guggenheim. 1939. Statistical Thermodynamics. The Macmillan Company, New York.

Freeman, N. C. 1958. Nonequilibrium flow of an ideal dissociating gas. J. Fluid Mech. 4:407-425.

Glasstone, S. 1944. Theoretical Chemistry. D. Van Nostrand Company Inc., Princeton, New Jersey.

Hall, J. G., A. Q. Eschenroeder, and P. V. Marrone. 1962. Inviscid hypersonic air-flows with coupled nonequilibrium processes. IAS Paper No. 62-67, Institute of the Aerospace Sciences, New York.

Hansen, C. F. 1959. Approximations for the thermodynamic and transport properties of high-temperature air. NASA TR R-50, Washington, D. C.

Jacobs, T. A., R. A. Hartunian, R. A. Giedt, and R. Wilkins. 1963. Direct measurements of recombination rates in a shock tube. Physics of Fluids 6(7): 972-974.

Lamb, H. 1932. Hydrodynamics. Dover Publications, New York.

Landau, L. D. and E. Teller. 1936. Physik Z. Sowjetunion 10:34-44.

Lee, J. F., F. W. Sears, and D. L. Turcotte. 1963. Statistical Thermodynamics. Addison Wesley Publishing Company, Reading, Mass.

Liepmann, H. W. and A. Roshko. 1957. Elements of Gasdynamics. John Wiley and Sons, New York.

Lighthill, M. J. 1957. Dynamics of a dissociating gas - part I, equilibrium flow. J. Fluid Mech. 2:1-32.

Matthews, D. L. 1959. Interferometric measurement in the shock tube of the dissociation rate of oxygen. Phys. of Fluids 2(2): 170-178.

McCracken, D. D. 1961. A Guide to Fortran Programming. John Wiley and Sons, New York.

Moore, C. E. 1949. Atomic Energy Levels. NBS Circular No. 467, National Bureau of Standards, Washington, D. C.

Moore, W. J. 1962. Physical Chemistry. Prentice-Hall, Englewood Cliffs, New Jersey.

Napolitano, L. G. 1960. Non-equilibrium centered rarefaction for a reacting mixture. AEDC TN-60-129. Arnold Engineering Development Center, Arnold Air Force Station, Tennessee.

Patterson, G. N. 1956. Molecular Flow of Gases. John Wiley and Sons, New York.

Penner, S. S. 1957. Chemistry Problems in Jet Propulsion. Pergamon Press, New York.

Resler, E. L. 1956. Sound speed in a reacting medium. J. Chem. Phys. 25(6): 1287-1288.

Resler, E. L. 1957. Characteristics and sound speed in nonisentropic gas flows with nonequilibrium thermodynamic states. J. Aero. Sciences 24(11): 785-790.

Roberts, R. C. 1947. The method of characteristics in compressible flow, part II (unsteady flow). Air Material Command Technical Report No. F-TR-1173D-ND, Wright Patterson Air Force Base, Ohio.

Schexnayder, C. J. and J. S. Evans. 1961. Measurements of the dissociation rate of molecular oxygen. NASA TR R-108, Washington, D. C.

Staff, Dow Chemical Company. 1960. JANAF Thermochemical Tables. The Dow Chemical Company, Midland, Michigan.

Trimpi, R. L. 1962. A preliminary theoretical study of the expansion tube, a new device for producing high-enthalpy, short-duration hypersonic gas flows. NASA TR R-133, Washington, D. C.

Trimpi, R. L. and W. L. Grose, 1963. Charts for the analysis of isentropic one-dimensional unsteady expansions in equilibrium real air with particular reference to shock-initiated flows. NASA TR R-167, Washington, D. C.

Vincenti, W. G. 1961. Lectures on Physical Gas Dynamics. Stanford University, Stanford, California.

Wegener, P. P. and J. D. Cole. 1962. Experiments on the propagation of weak disturbances in stationary super-sonic nozzle flow of chemically reacting gas mixtures, pp. 348-359. In Eighth Symposium (International) on Combustion. Williams and Wilkins Co., Baltimore.

Wierum, F. A. 1962. Prandtl-Meyer expansion of an ionizing monatomic gas. Ph. D. dissertation, Rice University, Houston.

Wood, W. W. and J. G. Kirkwood, 1957. Characteristic equation for reactive flow. J. Chem. Phys. 27(2): 596.

Wood, W. W. and F. R. Parker. 1958. Structure of a centered rarefaction wave in a relaxing gas. Phys. of Fluids 1(3): 230-241.

Wray, K. L. 1962. Chemical kinetics of high temperature air, pp. 181-204. In F. R. Riddell (ed.), Hypersonic Flow Research. Academic Press, New York.

APPENDICES

Appendix A. Derivation of Characteristic Equations in the Eulerian Coordinate System

The set of equations, (1), (2), (3), and (6), describes the one-dimensional unsteady flow of a reacting gas mixture. It was shown that the frozen speed of sound in a reacting gas can be expressed by equation (15). The following manipulations are performed in order to get the governing equations into a form convenient for obtaining the characteristic directions for this set of equations. To simplify the ensuing manipulations only one of the rate controlled variables, q_k, is considered and is denoted simply as q. It will be apparent later that this does not limit the generality of the development of the characteristic equations.

First, the thermal equation of state, equation (4), is used to eliminate ρ as a dependent variable. This equation may be written in the form:

$$\frac{Dh}{Dt} = \left(\frac{\partial h}{\partial P}\right)_{\rho,q} \frac{DP}{Dt} + \left(\frac{\partial h}{\partial \rho}\right)_{P,q} \frac{D\rho}{Dt} + \left(\frac{\partial h}{\partial q}\right)_{P,\rho} \frac{Dq}{Dt} \tag{A1}$$

or, rearranging,

$$\frac{D\rho}{Dt} = \left[\frac{Dh}{Dt} - \left(\frac{\partial h}{\partial P}\right)_{\rho,q} \frac{DP}{Dt} - \left(\frac{\partial h}{\partial q}\right)_{P,\rho} \frac{Dq}{Dt}\right] \Bigg/ \left(\frac{\partial h}{\partial \rho}\right)_{P,q} . \tag{A2}$$

From the energy equation,

$$\frac{Dh}{Dt} - \frac{1}{\rho}\frac{DP}{Dt} = 0, \tag{3}$$

an expression for $\frac{Dh}{Dt}$ can be obtained which will permit equation (A2) to be written as

$$\frac{D\rho}{Dt} = \frac{\left[\frac{1}{\rho} - \left(\frac{\partial h}{\partial P}\right)_{\rho,q}\right]\frac{DP}{Dt} - \left(\frac{\partial h}{\partial q}\right)_{P,\rho}\frac{Dq}{Dt}}{\left(\frac{\partial h}{\partial \rho}\right)_{P,q}}. \tag{A3}$$

Since

$$a_f^2 = \frac{\left(\frac{\partial h}{\partial \rho}\right)_{P,q}}{\frac{1}{\rho} - \left(\frac{\partial h}{\partial P}\right)_{\rho,q}} \tag{15}$$

equation (A3) can be written

$$\frac{D\rho}{Dt} = \frac{1}{a_f^2}\frac{DP}{Dt} - \frac{\left(\frac{\partial h}{\partial q}\right)_{P,\rho}\frac{Dq}{Dt}}{\left(\frac{\partial h}{\partial \rho}\right)_{P,q}}. \tag{A4}$$

Note that $\frac{Dq}{Dt} = \omega(P,\rho,q)$ and can thus be expressed without x or t dependence. Define the parameter k_1 as

$$k_1 = \frac{\left(\frac{\partial h}{\partial q}\right)_{P,\rho}}{\left(\frac{\partial h}{\partial \rho}\right)_{P,q}}.$$

Substitute the expression for $\frac{D\rho}{Dt}$, equation (A4), into the continuity equation, equation (1). The resulting equation is

$$\frac{1}{a_f^2}\frac{DP}{Dt} + \rho\left(\frac{\partial u}{\partial x}\right) - k_1\left(\frac{\partial q}{\partial t}\right) - uk_1\left(\frac{\partial q}{\partial x}\right) = 0$$

or

$$\frac{1}{a_f^2}\left(\frac{\partial P}{\partial t}\right) + \frac{u}{a_f^2}\left(\frac{\partial P}{\partial x}\right) + \rho\left(\frac{\partial u}{\partial x}\right) - k_1\left(\frac{\partial q}{\partial t}\right) - uk_1\left(\frac{\partial q}{\partial x}\right) = 0 . \qquad (A5)$$

The momentum, energy, and rate equations are used in their previously given form, i.e.,

$$\left(\frac{\partial u}{\partial t}\right) + u\left(\frac{\partial u}{\partial x}\right) + \frac{1}{\rho}\left(\frac{\partial P}{\partial x}\right) = 0, \qquad (2)$$

$$\left(\frac{\partial h}{\partial t}\right) + u\left(\frac{\partial h}{\partial x}\right) - \frac{1}{\rho}\left(\frac{\partial P}{\partial t}\right) - \frac{u}{\rho}\left(\frac{\partial P}{\partial x}\right) = 0, \qquad (3)$$

and

$$\left(\frac{\partial q}{\partial t}\right) + u\left(\frac{\partial q}{\partial x}\right) = \omega . \qquad (6)$$

It should be remembered that q represents the rate controlled variables and is actually more than one variable in most cases. Thus one equation with the form of equation (6) must be included for each rate dependent quantity considered. It will be evident from the

ensuing manipulations that the characteristic directions are not dependent upon the number of q components considered. Therefore to simplify the presentation only one q will be carried along in the process of obtaining the characteristic directions.

Since u, h, P, and q are functions of the independent variables x and t, the following equations may be written.

$$dP = \left(\frac{\partial P}{\partial t}\right)_x dt + \left(\frac{\partial P}{\partial x}\right)_t dx \tag{A6}$$

$$du = \left(\frac{\partial u}{\partial t}\right)_x dt + \left(\frac{\partial u}{\partial x}\right)_t dx \tag{A7}$$

$$dh = \left(\frac{\partial h}{\partial t}\right)_x dt + \left(\frac{\partial h}{\partial x}\right)_t dx \tag{A8}$$

$$dq = \left(\frac{\partial q}{\partial t}\right)_x dt + \left(\frac{\partial q}{\partial x}\right)_t dx \tag{A9}$$

The objective now becomes that of using equations (6), (A9), (A8), (A6), (A7), (3), (A5), and (2) to establish characteristic curves, i.e., lines along which partial derivatives with respect to the independent variables do not necessarily exist. Such a solution can only exist if the matrix of coefficients for the set of governing

equations is equal to zero. The characteristic directions are obtained by setting the matrix of coefficients equal to zero and evaluating for this condition.

$$\begin{vmatrix} 1 & u & 0 & 0 & 0 & 0 & 0 & 0 \\ dt & dx & 0 & 0 & 0 & 0 & 0 & 0 \\ 0 & 0 & dt & dx & 0 & 0 & 0 & 0 \\ 0 & 0 & 0 & 0 & dt & dx & 0 & 0 \\ 0 & 0 & 0 & 0 & 0 & 0 & dt & dx \\ 0 & 0 & 1 & u & -\frac{1}{\rho} & -\frac{u}{\rho} & 0 & 0 \\ -k_1 & -k_1 u & 0 & 0 & \frac{1}{a_f^2} & \frac{u}{a_f^2} & 0 & \rho \\ 0 & 0 & 0 & 0 & 0 & \frac{1}{\rho} & 1 & u \end{vmatrix} = 0 \qquad (A10)$$

This equation reduces to

$$(dx - udt)^2 \left[\frac{dx}{dt} - (u + a_f)\right] \left[\frac{dx}{dt} - (u - a_f)\right] = 0. \qquad (A10)$$

It should be noted at this point that for each additional value of q considered, the factor (dx-udt) will be raised to one higher power. Thus an increase in the number of rate processes considered will not introduce any additional characteristic directions. Setting each factor of equation (A10) equal to zero, the characteristic directions are seen to be

$$\frac{dx}{dt} = u, \qquad (A11)$$

$$\frac{dx}{dt} = u + a_f, \tag{A12}$$

and

$$\frac{dx}{dt} = u - a_f. \tag{A13}$$

The compatibility relations can now be developed along these characteristic lines. Along the line described by

$$\frac{dx}{dt} = u$$

equation (3),

$$\left(\frac{\partial h}{\partial t}\right) + u\left(\frac{\partial h}{\partial x}\right) - \frac{1}{\rho}\left[\left(\frac{\partial P}{\partial t}\right) + u\left(\frac{\partial P}{\partial x}\right)\right] = 0,$$

becomes

$$\left[\left(\frac{\partial h}{\partial t}\right) + \left(\frac{\partial h}{\partial x}\right)\frac{dx}{dt}\right] - \frac{1}{\rho}\left[\left(\frac{\partial P}{\partial t}\right) + \left(\frac{\partial P}{\partial x}\right)\frac{dx}{dt}\right] = 0.$$

But

$$\frac{dh}{dt} = \left(\frac{\partial h}{\partial t}\right) + \left(\frac{\partial h}{\partial x}\right)\frac{dx}{dt}$$

and

$$\frac{dP}{dt} = \left(\frac{\partial P}{\partial t}\right) + \left(\frac{\partial P}{\partial x}\right)\frac{dx}{dt}$$

so that along the characteristic curve $\frac{dx}{dt} = u$, the ordinary differential equation,

$$\frac{dh}{dt} - \frac{1}{\rho}\frac{dP}{dt} = 0, \tag{21}$$

applies. Also along this curve equation (6) becomes

$$\left(\frac{\partial q}{\partial t}\right) + \left(\frac{\partial q}{\partial x}\right)\frac{dx}{dt} = \omega,$$

which may be written as

$$\frac{dq}{dt} = \omega. \tag{22}$$

Along the direction $\frac{dx}{dt} = u + a_f$, if equation (A5) is (16)

multiplied by $\frac{a_f}{\rho}$ and added to equation (2), the resulting expression is

$$\left(\frac{\partial u}{\partial t}\right) + (u + a_f)\left(\frac{\partial u}{\partial x}\right) + \frac{1}{\rho a_f}\left[\left(\frac{\partial P}{\partial t}\right) + (u + a_f)\left(\frac{\partial P}{\partial x}\right)\right] - \frac{a_f}{\rho}\frac{\left(\frac{\partial h}{\partial q}\right)\omega}{\left(\frac{\partial h}{\partial \rho}\right)} = 0,$$

which reduces to

$$\frac{du}{dt} + \frac{1}{\rho a_f}\left(\frac{dP}{dt}\right) - \frac{a_f}{\rho}\frac{\left(\frac{\partial h}{\partial q}\right)\omega}{\left(\frac{\partial h}{\partial \rho}\right)} = 0. \tag{17}$$

Along the direction $\frac{dx}{dt} = u - a_f$, (18)

if equation (A5) is multiplied by $\frac{a_f}{\rho}$ and subtracted from equation (2), the resulting expression is

$$\left(\frac{\partial u}{\partial t}\right) + (u - a_f)\left(\frac{\partial u}{\partial x}\right) - \frac{1}{a_f \rho}\left[\left(\frac{\partial P}{\partial t}\right) + (u - a_f)\left(\frac{\partial P}{\partial x}\right)\right] + \frac{a_f}{\rho}\frac{\left(\frac{\partial h}{\partial q}\right)\omega}{\left(\frac{\partial h}{\partial \rho}\right)} = 0$$

or

$$\frac{du}{dt} - \frac{1}{a_f \rho}\left(\frac{dP}{dt}\right) + \frac{a_f}{\rho}\frac{\left(\frac{\partial h}{\partial q}\right)_\omega}{\left(\frac{\partial h}{\partial \rho}\right)} = 0. \qquad (19)$$

Appendix B. The Lagrangian Transformation

A transformation is developed below for converting the governing equations of the problem from the Eulerian to the Lagrangian coordinate system.

Derivation of the Transformation

In the Lagrangian system, the two independent variables are b and t. The coordinate b specifies the particle being considered and t is the time coordinate. The value of b is defined as the position x of that particular particle when $t = t_o$.

Consider the unsteady flow in a tube of cross section unity and apply the conservation of mass principle. This is illustrated in Figure 26.

It should be remembered that the particle specified by b represents a fixed amount of mass. Initially the total mass of the fluid element is given by the integral

$$\int_o^b \rho_o \, db.$$

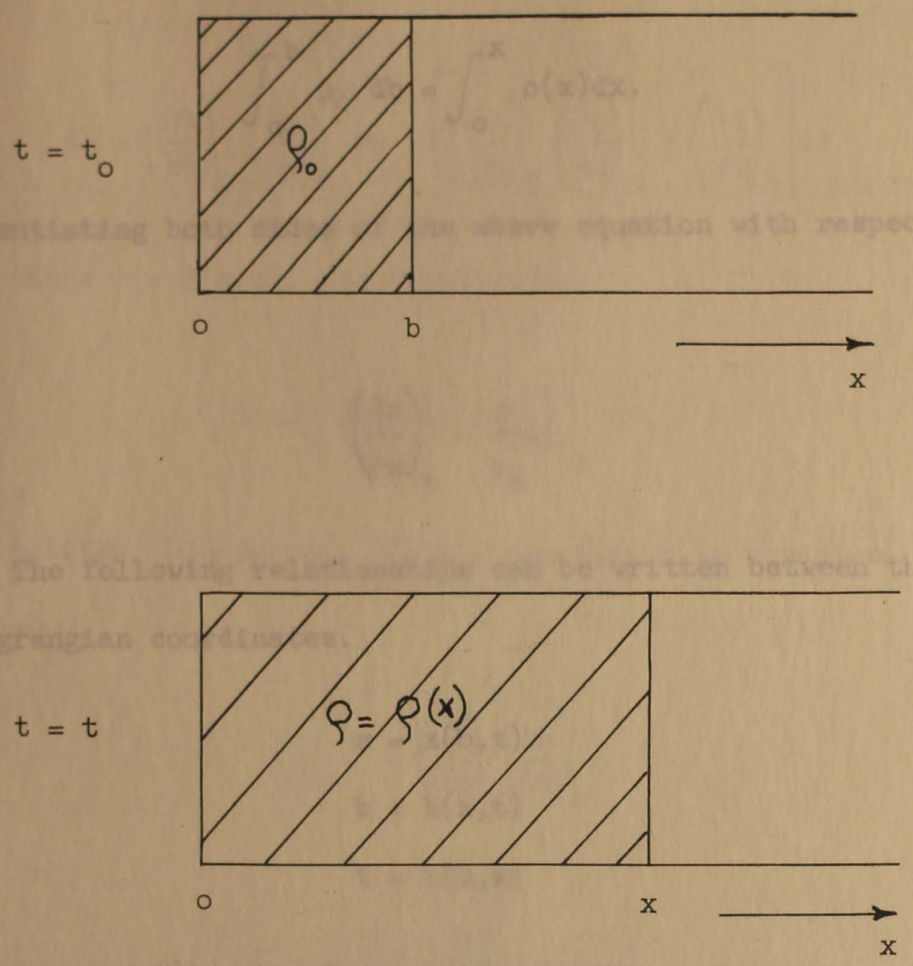

Figure 26. Conservation of mass illustration

At some later time, t, the total mass of the same fluid element can be expressed as

$$\int_o^x \rho(x)dx.$$

Conservation of mass dictates the equating of the two expressions, thus

$$\int_o^b \rho_o \, db = \int_o^x \rho(x) dx. \tag{B1}$$

Differentiating both sides of the above equation with respect to x yields

$$\left(\frac{\partial b}{\partial x}\right)_t = \frac{\rho}{\rho_o}. \tag{B2}$$

The following relationships can be written between the Eulerian and Lagrangian coordinates.

$$x = x(b,t)$$

$$b = b(x,t)$$

$$t = t(b,x)$$

Any property, λ, of the system, can be written as a function of any two of the variables, x, b, and t. The following relations may therefore be written.

$$d\lambda = \left(\frac{\partial \lambda}{\partial b}\right)_t db + \left(\frac{\partial \lambda}{\partial t}\right)_b dt \tag{B3}$$

$$db = \left(\frac{\partial b}{\partial x}\right)_t dx + \left(\frac{\partial b}{\partial t}\right)_x dt \tag{B4}$$

The substitution of equation (B4) into equation (B3) gives

$$d\lambda = \left(\frac{\partial\lambda}{\partial b}\right)_t \left(\frac{\partial b}{\partial x}\right)_t dx + \left[\left(\frac{\partial\lambda}{\partial b}\right)_t \left(\frac{\partial b}{\partial t}\right)_x + \left(\frac{\partial\lambda}{\partial t}\right)_b\right] dt \tag{B5}$$

Since $\lambda = \lambda(x,t)$, the expression,

$$d\lambda = \left(\frac{\partial\lambda}{\partial x}\right)_t dx + \left(\frac{\partial\lambda}{\partial t}\right)_x dt, \tag{B6}$$

may be written. Comparison of this expression to equation (B5) shows that

$$\left(\frac{\partial}{\partial x}\right)_t = \left(\frac{\partial}{\partial b}\right)_t \left(\frac{\partial b}{\partial x}\right)_t \tag{B7}$$

and

$$\left(\frac{\partial}{\partial t}\right)_x = \left(\frac{\partial}{\partial b}\right)_t \left(\frac{\partial b}{\partial t}\right)_x + \left(\frac{\partial}{\partial t}\right)_b . \tag{B8}$$

Also, the expression

$$dx = \left(\frac{\partial x}{\partial b}\right)_t db + \left(\frac{\partial x}{\partial t}\right)_b dt \tag{B9}$$

holds, and since $\left(\frac{\partial x}{\partial t}\right)_b = u$ and from equation (B2), $\left(\frac{\partial b}{\partial x}\right)_t = \frac{\rho}{\rho_o}$,

equation (B9) may be rearranged to give

$$db = \frac{\rho}{\rho_o} dx - \frac{\rho}{\rho_o} u dt. \tag{B10}$$

Remembering that

$$db = \left(\frac{\partial b}{\partial t}\right)_x dt + \left(\frac{\partial b}{\partial x}\right)_t dx \tag{B11}$$

and comparing equations (B10) and (B11), it becomes evident that

$$\left(\frac{\partial b}{\partial t}\right)_x = - \frac{\rho}{\rho_o} u. \tag{B12}$$

Substituting (B2) and (B12) into (B7) and (B8) gives

$$\left(\frac{\partial}{\partial x}\right)_t = \frac{\rho}{\rho_o}\left(\frac{\partial}{\partial b}\right)_t \tag{B13}$$

and

$$\left(\frac{\partial}{\partial t}\right)_x = - \frac{\rho}{\rho_o} u\left(\frac{\partial}{\partial b}\right)_t + \left(\frac{\partial}{\partial t}\right)_b. \tag{B14}$$

The substantial derivative may therefore be written as

$$\frac{D}{Dt} = \left(\frac{\partial}{\partial t}\right)_x + u\left(\frac{\partial}{\partial x}\right)_t = -u \frac{\rho}{\rho_o}\left(\frac{\partial}{\partial b}\right)_t + \left(\frac{\partial}{\partial t}\right)_b + \frac{u\rho}{\rho_o}\left(\frac{\partial}{\partial b}\right)_t$$

which reduces to

$$\frac{D}{Dt} = \left(\frac{\partial}{\partial t}\right)_b. \tag{B15}$$

Equations (B13), (B14), and (B15) are then the transformation equations for going from the Eulerian to the Lagrangian coordinate system.

Transformation of the Governing Equations

The transformations developed above, when applied to the governing equations in the Eulerian system, produce the following results.

The continuity equation,

$$\frac{D\rho}{Dt} + \rho\left(\frac{\partial u}{\partial x}\right)_t = 0, \tag{1}$$

becomes

$$\left(\frac{\partial \rho}{\partial t}\right)_b + \frac{\rho^2}{\rho_o}\left(\frac{\partial u}{\partial b}\right)_t = 0 \tag{24}$$

in Lagrangian coordinates.

The momentum equation,

$$\frac{Du}{Dt} + \frac{1}{\rho}\left(\frac{\partial P}{\partial x}\right)_t = 0, \tag{2}$$

becomes

$$\left(\frac{\partial u}{\partial t}\right)_b + \frac{1}{\rho_o}\left(\frac{\partial P}{\partial b}\right)_t = 0. \tag{25}$$

The energy equation,

$$\frac{Dh}{Dt} - \frac{1}{\rho}\frac{DP}{Dt} = 0, \tag{3}$$

becomes

$$\left(\frac{\partial h}{\partial t}\right)_b - \frac{1}{\rho}\left(\frac{\partial P}{\partial t}\right)_b = 0 \tag{26}$$

and the rate equation,

$$\frac{Dq}{Dt} = \omega, \tag{6}$$

becomes

$$\left(\frac{\partial q}{\partial t}\right)_b = \omega \tag{27}$$

in the Lagrangian coordinate system.

Appendix C. Solution as Time Approaches Zero

In order to prescribe the necessary boundary conditions for the problem, a solution must be obtained for the expansion as $t \to 0$. From physical reasoning it appears that such a solution should be that of a frozen expansion. The mathematical work to follow shows this to be the case.

It is convenient at this point to transform the governing equations from the b-t plane to the y-t coordinate system. The coordinate y is defined as $y = \frac{b}{t}$; therefore the following may be written.

$$y=y(b,t) \qquad b=b(y,t) \qquad t=t(b,y)$$

Thus any dependent variable can be expressed as a function of any two of the three independent variables, b, y, and t.

Let Ψ represent a typical dependent variable.

$$d\Psi = \left(\frac{\partial \Psi}{\partial y}\right)_t dy + \left(\frac{\partial \Psi}{\partial t}\right)_y dt \tag{C1}$$

$$dy = \left(\frac{\partial y}{\partial b}\right)_t db + \left(\frac{\partial y}{\partial t}\right)_b dt \tag{C2}$$

Substitute equation (C2) into (C1) to obtain

$$d\psi = \left(\frac{\partial \psi}{\partial y}\right)_t \left(\frac{\partial y}{\partial b}\right)_t db + \left[\left(\frac{\partial \psi}{\partial y}\right)_t \left(\frac{\partial y}{\partial t}\right)_b + \left(\frac{\partial \psi}{\partial t}\right)_y\right] dt. \tag{C3}$$

Since $\psi = \psi(b,t)$, the relation,

$$d\psi = \left(\frac{\partial \psi}{\partial b}\right)_t db + \left(\frac{\partial \psi}{\partial t}\right)_b dt, \tag{C4}$$

can be written. Comparing equations (C3) and (C4) yields the expressions,

$$\left(\frac{\partial \psi}{\partial b}\right)_t = \left(\frac{\partial \psi}{\partial y}\right)_t \left(\frac{\partial y}{\partial b}\right)_t \tag{C5}$$

and

$$\left(\frac{\partial \psi}{\partial t}\right)_b = \left(\frac{\partial \psi}{\partial y}\right)_t \left(\frac{\partial y}{\partial t}\right)_b + \left(\frac{\partial \psi}{\partial t}\right)_y, \tag{C6}$$

where

$$y = \frac{b}{t}, \quad \left(\frac{\partial y}{\partial b}\right)_t = \frac{1}{t}, \quad \text{and} \quad \left(\frac{\partial y}{\partial t}\right)_b = -\frac{y}{t}.$$

The transformation equations between the y-t and b-t coordinate systems may then be written as

$$\left(\frac{\partial}{\partial b}\right)_t = \frac{1}{t}\left(\frac{\partial}{\partial y}\right)_t \tag{C7}$$

and

$$\left(\frac{\partial}{\partial t}\right)_b = -\frac{y}{t}\left(\frac{\partial}{\partial y}\right)_t + \left(\frac{\partial}{\partial t}\right)_y . \tag{C8}$$

Equations (C7) and (C8) are used to transform the governing equations from the b-t system to the y-t system. The governing equations in the b-t system were previously shown to be:

energy

$$\left(\frac{\partial h}{\partial t}\right)_b = \frac{1}{\rho}\left(\frac{\partial P}{\partial t}\right)_b ,$$

rate

$$\left(\frac{\partial q}{\partial t}\right)_b = \omega ,$$

momentum

$$\rho_o \left(\frac{\partial u}{\partial t}\right)_b + \left(\frac{\partial P}{\partial b}\right)_t = 0 ,$$

combined mass, momentum, and state

$$\frac{\rho^2}{\rho_o}\left(\frac{\partial u}{\partial b}\right)_t + k_3\left(\frac{\partial h}{\partial t}\right)_b + k_2\left(\frac{\partial P}{\partial t}\right)_b + k_1\left(\frac{\partial q}{\partial t}\right)_b = 0 ,$$

where

$$k_1 = -\frac{\left(\frac{\partial h}{\partial q}\right)}{\left(\frac{\partial h}{\partial \rho}\right)},\quad k_2 = -\frac{\left(\frac{\partial h}{\partial P}\right)}{\left(\frac{\partial h}{\partial \rho}\right)},\quad \text{and } k_3 = \frac{1}{\left(\frac{\partial h}{\partial \rho}\right)}.$$

In the y-t system these equations may be written as:

mass

$$\frac{\rho^2}{\rho_o}\frac{1}{t}\left(\frac{\partial u}{\partial y}\right)_t + k_3\left[\left(\frac{\partial h}{\partial t}\right)_y - \frac{y}{t}\left(\frac{\partial h}{\partial y}\right)_t\right] + k_2\left[\left(\frac{\partial P}{\partial t}\right)_y - \frac{y}{t}\left(\frac{\partial P}{\partial y}\right)_t\right] + k_1\left[\left(\frac{\partial q}{\partial t}\right)_y - \frac{y}{t}\left(\frac{\partial q}{\partial y}\right)_t\right] = 0, \qquad (C9)$$

momentum

$$\rho_o\left[\left(\frac{\partial u}{\partial t}\right)_y - \frac{y}{t}\left(\frac{\partial u}{\partial y}\right)_t\right] + \frac{1}{t}\left(\frac{\partial P}{\partial y}\right)_t = 0, \qquad (C10)$$

energy

$$\left(\frac{\partial h}{\partial t}\right)_y - \frac{y}{t}\left(\frac{\partial h}{\partial y}\right)_t - \frac{1}{\rho}\left(\frac{\partial P}{\partial t}\right)_y + \frac{1}{\rho}\left(\frac{y}{t}\right)\left(\frac{\partial P}{\partial y}\right)_t = 0, \qquad (C11)$$

rate

$$\left(\frac{\partial q}{\partial t}\right)_y - \frac{y}{t}\left(\frac{\partial q}{\partial y}\right)_t = 0. \qquad (C12)$$

Multiply the above equations by t and let $t \to 0$. The resulting equations are as follows:

mass

$$\frac{\rho^2}{\rho_o}\left(\frac{\partial u}{\partial y}\right)_t - k_3\, y\left(\frac{\partial h}{\partial y}\right)_t - k_2\, y\left(\frac{\partial P}{\partial y}\right)_t - k_1\, y\left(\frac{\partial q}{\partial y}\right)_t = 0 \qquad (C13)$$

momentum

$$-\rho_o\, y\left(\frac{\partial u}{\partial y}\right)_t + \left(\frac{\partial P}{\partial y}\right)_t = 0 \qquad (C14)$$

energy

$$-y\left(\frac{\partial h}{\partial y}\right)_t + \frac{1}{\rho}\, y\left(\frac{\partial P}{\partial y}\right)_t = 0 \qquad (C15)$$

rate

$$\left(\frac{\partial q}{\partial y}\right)_t = 0 \qquad (C16)$$

Substitute the rate and energy equations into the mass equation to obtain the expression,

$$\frac{\rho^2}{\rho_o}\left(\frac{\partial u}{\partial y}\right)_t - \left[\left(\frac{k_3}{o} + k_2\right) y\right]\left(\frac{\partial P}{\partial y}\right)_t = 0. \qquad (C17)$$

Comparing the above equation to the momentum equation it can be seen that $y = \frac{\rho a_f}{\rho_o}$.

The governing equations are then reduced to the following as $t \to 0$.

$$\frac{du}{dy} - \frac{1}{\rho_o y}\frac{dP}{dy} = 0 \qquad (C18)$$

$$\frac{dq}{dy} = 0 \qquad (C19)$$

For the thermodynamic models used in the present investigation, the condition, $\frac{dq}{dy} = 0$, also establishes that γ is constant. The relationships $\frac{P}{P_o} = \left(\frac{\rho}{\rho_o}\right)^{\gamma_o}$ and $a_f = \sqrt{\gamma_o \frac{P}{\rho}}$ can then be written. Using these expressions and the relationship, $y = \frac{\rho a_f}{\rho_o}$, it can be readily shown that

$$\frac{\rho}{\rho_o} = \left(\frac{y}{a_{f_o}}\right)^{\frac{2}{\gamma_o+1}}, \quad \frac{P}{P_o} = \left(\frac{y}{a_{f_o}}\right)^{\frac{2\gamma_o}{\gamma_o+1}} \tag{C20}$$

and

$$\frac{T}{T_o} = \left(\frac{y}{a_{f_o}}\right)^{\frac{2(\gamma_o-1)}{\gamma_o+1}}. \tag{C21}$$

Since

$$P = P_o \left(\frac{1}{a_{f_o}}\right)^{\frac{2\gamma_o}{\gamma_o+1}} \left(y\right)^{\frac{2\gamma_o}{\gamma_o+1}},$$

$$\frac{dP}{dy} = P_o \left(\frac{1}{a_{f_o}}\right)^{\frac{2\gamma_o}{\gamma_o+1}} \left(\frac{2\gamma}{\gamma_o+1}\right)\left(y\right)^{\frac{\gamma_o-1}{\gamma_o+1}},$$

and can be substituted into equation (C18). Integration of the resulting equation yields

$$u = \frac{P_o}{\rho_o\, a_{f_o}} \left(\frac{2\gamma_o}{\gamma_o-1}\right)\left(\frac{y}{a_{f_o}}\right)^{\frac{\gamma_o-1}{\gamma_o+1}} + \text{constant}.$$

The condition that $u = u_o$ when $\frac{y}{a_{f_o}} = 1$ allows the evaluation of

the constant and the expression for velocity becomes

$$u = \frac{P_o}{\rho_o a_{f_o}} \left(\frac{2\gamma_o}{\gamma_o - 1} \right) \left[\left(\frac{y}{a_{f_o}} \right)^{\frac{\gamma_o - 1}{\gamma_o + 1}} - 1 \right] + u_o . \qquad \text{(C22)}$$

Equations (C20), (C21), and (C22) then permit the calculation of the unsteady expansion for the case of frozen flow.

Appendix D. Development of the Thermodynamic Model

The complexity of the gas model dictates that a detailed development of the model be presented. In the work to follow, the various energy modes comprising the internal energy of the gas mixture are discussed and the assumptions and approximations inherent in the gas model are evaluated. The formulation of equilibrium constants is also presented.

Development of the Internal Energy Model

The assumption was made that the reacting gas is made up of a mixture of perfect gases. Therefore the internal energy of the mixture is equal to the sum of the internal energies of the component species. The internal energy of each species is made up of the translational, rotational, vibrational, and electronic energies of that species plus any energy of dissociation or ionization required for the species to exist at that state. The immediate objective is the evaluation of each of the above contributors to the internal energy and from this evaluation, to establish a useable expression

for the internal energy of the reacting gas mixture. From statistical mechanics, the expression for internal energy per unit mass can be written in terms of the partition function Z as follows:

$$E_i = \frac{x_i}{\mu_i} RT^2 \left[\frac{\partial \left(\ln Z_i \right)}{\partial T} \right]. \tag{D1}$$

Due to the form of this equation, it may also be written in the same manner for each energy mode.

A number of references present the derivation of equation (D1) and the partition functions which are subsequently developed. Typical references are cited as the work progresses. A detailed development of equation (D1) may be found in the works of Penner (1957) and Lee et al., (1963).

Translational Energy. The partition function for translational motion may be written as,

$$Z_{TRAN} = v \left(\frac{2\pi mkT}{\mathcal{h}^2} \right)^{3/2}, \tag{D2}$$

where v represents specific volume, m is the mass of the molecule considered, and k and $\mathcal{h}$ are the Boltzmann and Planck constants respectively. The derivation of this expression may be found in many test books, among them the works of Fowler and Guggenheim (1939) and Clarke and McChesney (1964). Substituting equation (D2) into equation (D1), the translational internal energy of the i^{th} specie is seen to be

$$E_{TRAN_i} = \frac{x_i}{\mu_i} RT^2 \left\{ \frac{\partial}{\partial T} \left[\ln v \left(\frac{2\pi mkT}{\mathcal{h}^2} \right)^{3/2} \right] \right\}, \tag{D3}$$

which reduces to

$$E_{TRAN_i} = \frac{x_i}{\mu_i}\left(\frac{3}{2} RT\right). \tag{D4}$$

The translational internal energy of the mixture may therefore be written in the form

$$E_{TRAN} = \sum_{i=1}^{n} \frac{x_i}{\mu_i}\left(\frac{3}{2} RT\right). \tag{D5}$$

Rotational Energy. The rotational energy modes of the diatomic molecules are assumed to be in equilibrium with the translational energy. Atomic species possess no rotational energy. Using the dumbell model to represent diatomic molecules, the rotational partition function for such molecules has been shown to be

$$Z_{ROT} = \frac{8\pi^2 IkT}{\sigma h^2}$$

by such authors as Glasstone (1944). The molecular moment of inertia is denoted by I and σ is the molecular symmetry number. The rotational energy for the i^{th} species may therefore be written

$$E_{ROT_i} = \frac{x_i}{\mu_i} f_i RT, \tag{D7}$$

where f_i is one for a diatomic species and zero for a monatomic species.

The total rotational energy for the gas mixture is then given by the expression

$$E_{ROT} = \sum_{i=1}^{n} \frac{x_i}{\mu_i} f_i \, RT. \tag{D8}$$

Vibrational Energy. In the present work, two different approaches are provided for handling the vibrational energy of the gas. The first approach allows the vibrational energy to be rate controlled. Thus the case of vibrational nonequilibrium may be handled. Using this approach, the term e_{v_i} is included in the expression for internal energy and vibrational rate equations are used to obtain values of e_{v_i} as the calculation proceeds through the flow field. In the second approach, the vibrational energy is assumed to remain in equilibrium with the translational and rotational energy modes. For atomic species, no vibrational energy exists. The vibrational partition function for a diatomic molecule represented by the harmonic oscillator model can be expressed in the form

$$Z_{VIB_i} = \frac{\exp(-\theta_{v_i}/2T)}{1 - \exp(-\theta_{v_i}/T)}, \tag{D9}$$

where θ_{v_i} is referred to as the characteristic vibrational temperature of the molecule and is defined as

$$\theta_{v_i} = \frac{h\nu}{k}. \tag{D10}$$

The quantity ν is the vibrational frequency of the molecule considered.

The development of the vibrational partition function given above can be found in such references as Moore (1963) and Glasstone (1944).

Again substituting the partition function into equation (D1), the contribution to the internal energy due to the vibrational energy of the i^{th} specie is obtained and may be written as

$$E_{VIB_i} = f_i \frac{x_i}{\mu_i} R\theta_{v_i}\left[\frac{1}{2} + \frac{1}{\exp(\theta_{v_i}/T) - 1}\right]. \qquad (D11)$$

In the evaluation of certain derivatives needed in the compatibility equations, this expression becomes extremely cumbersome when a number of species are considered. It is useful at this point to develop a simple linear approximation for the vibrational energy. Lighthill (1957), in his ideal dissociating gas model, used the approximation that the vibrational energy of a diatomic molecule is always excited to one half of its maximum value, i.e., $e_v = \frac{1}{2} RT$. In the present work, the linear approximation,

$$E_{VIB_i} = f_i \frac{x_i}{\mu_i}\left(\beta_i RT + \beta_i'\right) \qquad (D12)$$

is used. The constants are evaluated using equation (D11) for the specific temperature range required in the problem. This approximation is a considerable improvement over Lighthill's model and should produce very little error in the results. A comparison between the approximate and exact expressions for the vibrational energies of N_2 and O_2 is presented in Figure 27.

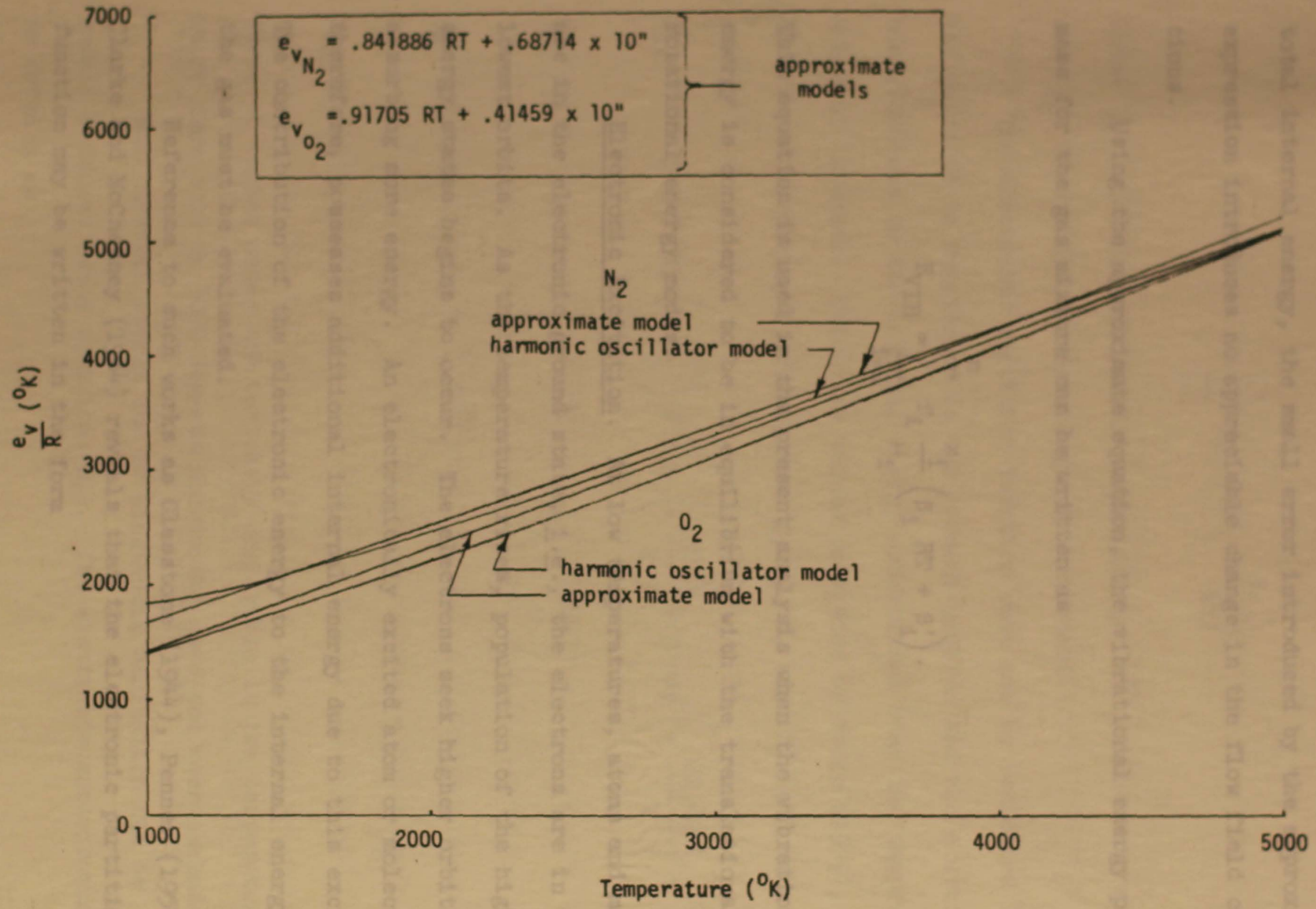

Figure 27. Comparison of approximate and harmonic oscillator vibrational energy models for N_2 and O_2

Since the vibrational energy comprises only a fraction of the total internal energy, the small error introduced by the approximate expression introduces no appreciable change in the flow field calculations.

Using the approximate equation, the vibrational energy per unit mass for the gas mixture can be written as

$$E_{VIB} = \sum_{i=1}^{n} f_i \frac{x_i}{\mu_i} \left(\beta_i \, RT + \beta_i' \right). \qquad (D13)$$

This equation is used in the present analysis when the vibrational energy is considered to be in equilibrium with the translational and rotational energy modes.

Electronic Excitation. At low temperatures, atoms and molecules are in the electronic ground state, i.e., the electrons are in their lowest orbits. As the temperature rises, population of the higher energy states begins to occur. The electrons seek higher orbits, thus absorbing more energy. An electronically excited atom or molecule, therefore, possesses additional internal energy due to this excitation. The contribution of the electronic energy to the internal energy of the gas must be evaluated.

Reference to such works as Glasstone (1944), Penner (1957), or Clarke and McChesney (1964) reveals that the electronic partition function may be written in the form

$$Z = \sum_{l=1}^{L} g_{i_l} \exp\left(-\frac{\epsilon_{i_l}}{kT}\right), \tag{D14}$$

where g_{i_l} is the statistical weight of the i^{th} electronic state and ϵ_{i_l} is the electronic energy of that state.

The electronic partition function must now be evaluated for the gases to be considered in the present problem and the electronic contributions to the internal energy ascertained over the temperature range of interest. Using the values presented by Moore (1949), the electronic partition functions for O, O_2, N, and N_2 can be written as

$$\begin{aligned}
Z_{EL}(O) &= 5 + 3\exp\left(-\frac{228}{T}\right) + \exp\left(-\frac{326}{T}\right) + 5\exp\left(-\frac{22{,}800}{T}\right) + \ldots \\
Z_{EL}(O_2) &= 3 + 2\exp\left(-\frac{11390}{T}\right) + \exp\left(-\frac{18990}{T}\right) + \ldots \\
Z_{EL}(N) &= 4 + 10\exp\left(-\frac{27{,}700}{T}\right) + \ldots \\
Z_{EL}(N_2) &= 1 + \ldots
\end{aligned} \tag{D15}$$

Terms of higher order are obviously negligible in the temperature range from 1000 to 5000 degrees Kelvin and have not been included.

The internal energy due to electronic excitation can be radily obtained using equation (D1). The electronic contribution may be written as

$$E_{EL_i} = \frac{x_i}{\mu_i} \frac{\sum_{l=1}^{L} R g_{i_l} \epsilon_{i_l} \exp\left(-\frac{\epsilon_{i_l}}{T}\right)}{Z_{EL_i}}, \qquad (D16)$$

and can be evaluated using the electronic partition functions listed in equation (D15). Calculations show that these energies make up very small portions of the total internal energies. The effect of neglecting electronic excitation (the triplet ground state of O is not neglected but is treated as a single ground state, i.e., $Z_{EL}(O) = 9$) is illustrated in Figures 28 and 29 for the gases of interest. For temperatures between 1000 and 5000°K the error introduced into the internal energy by neglecting electronic excitation above the ground state never exceeds six percent. Only for O, which comprises a relatively small proportion of an air model, is the error that large, and then only at low temperatures. For N_2, which makes up a large portion of an air model, the error is less than 1.6 percent. The neglecting of electronic excitation is then a convenient assumption which will not be a source of appreciable error in the calculations.

Combined Expression for Internal Energy. Incorporating the contributions from the various energy modes and adding the energies of formation for the various species, an expression for the total internal energy of the mixture may be written as

$$E = \sum_{i=1}^{n} \left\{ \frac{x_i}{\mu_i} \left[\frac{3}{2} RT + f_i RT + f_i e_{v_i} + N_o \Delta_i \right] \right\}. \qquad (63)$$

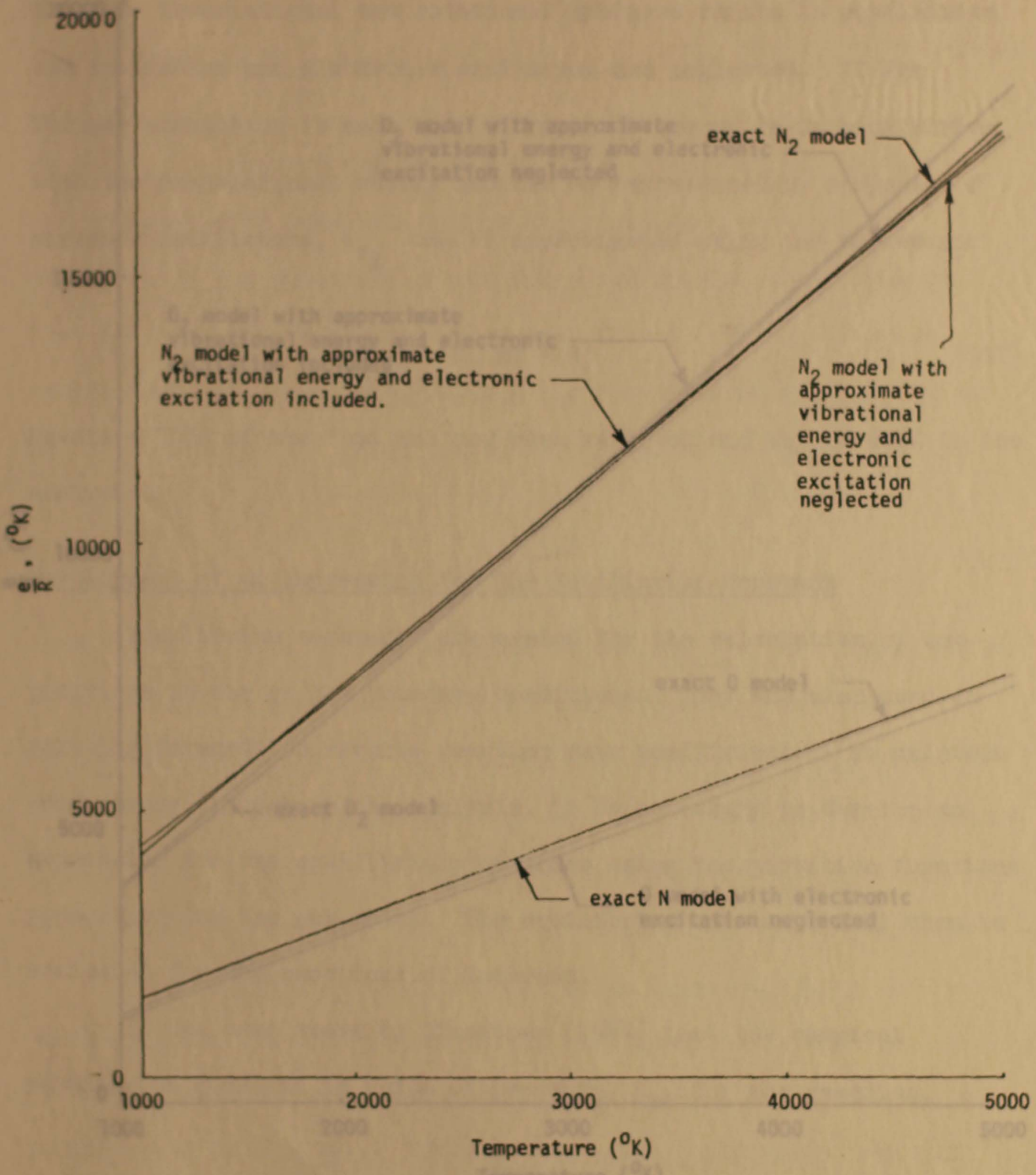

Figure 28. Comparison of internal energy models of N and N_2

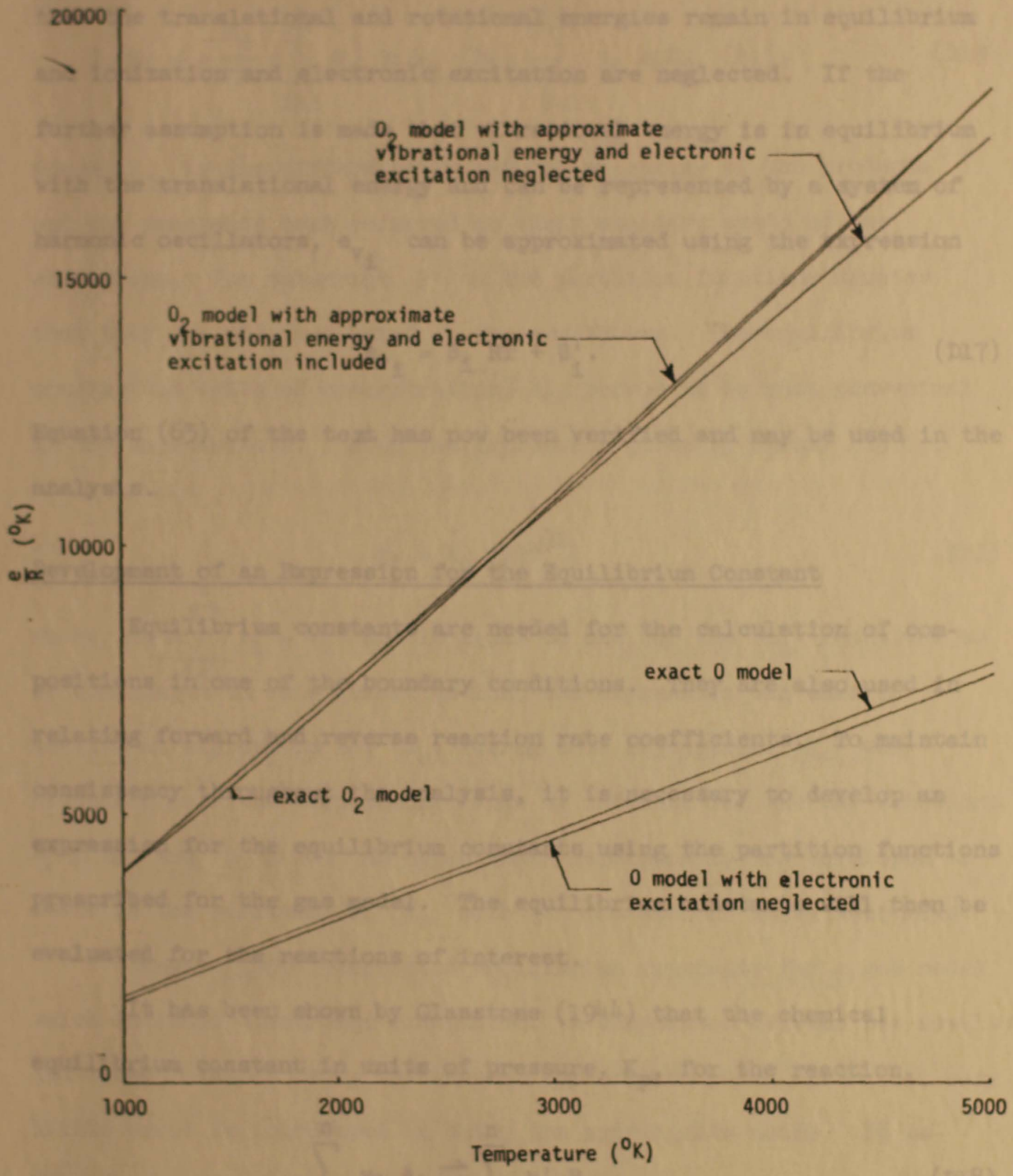

Figure 29. Comparison of internal energy models of O and O_2

The basic assumptions involved in arriving at this expression are that the translational and rotational energies remain in equilibrium and ionization and electronic excitation are neglected. If the further assumption is made that vibrational energy is in equilibrium with the translational energy and can be represented by a system of harmonic oscillators, e_{v_i} can be approximated using the expression

$$e_{v_i} = \beta_i \, RT + \beta_i' . \tag{D17}$$

Equation (63) of the text has now been verified and may be used in the analysis.

Development of an Expression for the Equilibrium Constant

Equilibrium constants are needed for the calculation of compositions in one of the boundary conditions. They are also used in relating forward and reverse reaction rate coefficients. To maintain consistency throughout the analysis, it is necessary to develop an expression for the equilibrium constants using the partition functions prescribed for the gas model. The equilibrium constants will then be evaluated for the reactions of interest.

It has been shown by Glasstone (1944) that the chemical equilibrium constant in units of pressure, K_p, for the reaction,

$$\sum_{i=1}^{n} \nu_i \, A_i \rightleftharpoons \sum_{i=1}^{n} \nu_i' \, B_i , \tag{D18}$$

where the A_i are the reactants, the B_i the products, and ν_i and

ν_i' their respective stoichiometric coefficients, can be written as

$$\ln K_P = -\frac{E_o}{RT} + \sum_{i=1}^{n} \nu_i' \ln Z_{P_i}(B_i) - \sum_{i=1}^{n} \nu_i \ln Z_{P_i}(A_i), \qquad (D19)$$

where E_o is the difference in zero point energy of the products and the reactants both referred to their standard state at one atmosphere. The subscript P on the partition functions denotes that they are also evaluated at one atmosphere. The equilibrium constant in units of concentration, K_c, proves to be most convenient in the calculations. Using the expression given by Penner (1957);

$$K_P = K_c (RT)^{\Delta n}, \qquad (D20)$$

where $\Delta n = \sum_{i=1}^{n} \nu_i' - \nu_i$ and is equal to one for the K_p reactions to be considered in this investigation, the expression was used to develop an expression for K_c. Using this expression, K_c was evaluated over the temperature range of interest for the two reactions $N_2 \rightleftharpoons 2N$ and $O_2 \rightleftharpoons 2O$. An approximate relationship was developed to describe the variation of K_c with T for each of these reactions.

Hansen (1959) calculated equilibrium constants for a gas model which included electronic excitation. A comparison between his results and those obtained using the present approximate model shows that very little error is introduced by using the approximate model. It is felt that the error introduced by the approximate expressions for K_c is well within the accuracy of the reaction rate coefficients used and

should not be detrimental to the analysis. Therefore, the following approximate expressions are used in the numerical work.

$$K_c\ (O_2 \leftrightharpoons 2O) = 21.5 \exp\left(-\frac{59475.5}{T}\right) \qquad \text{(D21)}$$

$$K_c\ (N_2 \leftrightharpoons 2N) = 19.0 \exp\left(-\frac{113{,}455.4}{T}\right) \qquad \text{(D22)}$$

Appendix E. Physical Constants and Reaction Rates

The cgs systems of units was used in the numerical work. Certain physical constants were needed and the values used are listed below.

$R = 8.3147 \times 10^{7}$ $\quad \frac{\text{erg}}{\text{mole } ^{o}\text{K}}$ - universal gas constant

$k = 1.3804 \times 10^{-16}$ $\quad \frac{\text{erg}}{\text{molecule } ^{o}\text{K}}$ - Boltzmann constant

$N_o = 6.02338 \times 10^{23}$ $\quad \frac{\text{molecules}}{\text{mole}}$ - Avogadro's number

$\hbar = 6.62517 \times 10^{-27}$ erg - sec - Planck's constant

The characteristic vibrational temperature of O_2 was taken as 2270° and the heat of formation of O was that given by the JANAF Tables (1964), i.e., $\Delta_o = 4.105 \times 10^{-12}$ $\frac{\text{ergs}}{\text{molecule}}$.

Some uncertainty of the numerical accuracy must exist in a problem in which rate processes are considered because of the limited knowledge of the reaction rate coefficients. This is true for the present problem. A survey of reaction rate literature was conducted in order to secure the best state-of-the-art values for use in the present work. The presentations of Wray (1962), Atallah (1961), Byron (1959), Eckerman (1958), Camac and Vaughn (1961), Mathews (1959), and Schexnayder and Evans (1961) were evaluated. The rate coefficients suggested by Attallah (1961) were selected as the most appropriate for the range of consitions considered in this investigation. The constants used in equation (81) to describe the reaction rate coefficients are listed in Table 2.

The recombination rate coefficients were obtained using the forward rate coefficients and the equilibrium constant, K_c.

While the accuracy of these coefficients leaves much to be desired, it is felt that the values used are the best available at present.

Table 2. Reaction rate constants

Reaction	A_j	B_j	E_j
$O_2+O \rightarrow 3O$	1.29×10^{18}	-0.5	8.2×10^{-12}
$O_2+O_2 \rightarrow O_2+2O$	1.46×10^{21}	-1.5	8.2×10^{-12}
$O_2+N_2 \rightarrow N_2+2O$	2.36×10^{20}	-1.5	8.2×10^{-12}
$O_2+A \rightarrow A+2O$	1.6222×10^{20}	-1.5	8.2×10^{-12}
$3O \rightarrow O_2+O$	1.075×10^{15}	-0.5	0
$O_2+2O \rightarrow 2O_2$	1.216667×10^{18}	-1.5	0
$N_2+2O \rightarrow O_2+N_2$	2.36×10^{20}	-1.5	0
$A+2O \rightarrow O_2+A$	1.35185×10^{17}	-1.5	0

Appendix F. The Fortran Program

```
1111 CALL LOAD(LERR)
     IF(LERR-2)1,2,2
   2 STOP
   1 WRITE(6,3001)MG
     DO 3020 L=1,LL
     DO 3021 I=1,ILIM
     X(I,1,L)=XB(I)
     EV(I,1,L)=EVB(I)
3021 CONTINUE
3020 CONTINUE
     TO=TB
     TBAR(1,1)=0
     DO 778 MG=1,MGLIM
     IF(MG-1)779,779,780
 780 DO 781 K=1,KK
     PBAR(K,1)=PBAR(K,LLIM+1)
     RHOBA(K,1)=RHOBA(K,LLIM+1)
     HBAR(K,1)=HBAR(K,LLIM+1)
     VBAR(K,1)=VBAR(K,LLIM+1)
     T(K,1)=T(K,LLIM+1)
     YBAR(K,1)=YBAR(K,LLIM+1)
     TBAR(K+1,1)=TBAR(K+1,LLIM+1)
     DO 782 I=1,ILIM
     X(I,K,1)=X(I,K,LLIM+1)
     EV(I,K,1)=EV(I,K,LLIM+1)
 782 CONTINUE
 781 CONTINUE
     YBAR(1,1)=YBAR(1,LLIM+1)
     GO TO 783
 779 DO 2032 K=1,KK
     PBAR(K,1)=PBARB
     RHOBA(K,1)=RHOBAB
     HBAR(K,1)=HBARB
     VBAR(K,1)=VBARB
     T(K,1)=TB
     YBAR(K,1)=1.
     TBAR(K+1,1)=TBAR(K,1)+.05
     DO2033I=1,ILIM
     X(I,K,1)=XB(I)
     EV(I,K,1)=CAPR*B7(I)*T(K,1)+B8(I)
2033 CONTINUE
2032 CONTINUE
 783 DO2034L=1,LL
     TBAR(1,L)=0
     IF((MG+15)-MGLIM)578,578,577
 577 IF((MG+9)-MGLIM)579,579,580
 579 VAR=.01
     GO TO 578
```

```
580 IF((MG+6)-MGLIM)581,581,582
581 VAR=.005
    GO TO 578
582 IF((MG+4)-MGLIM)583,583,584
583 VAR=.0025
    GO TO 578
584 IF((MG+2)-MGLIM)585,585,586
585 VAR=.001
    GO TO 578
586 VAR=.0005
578 YBAR(1,L+1)=YBAR(1,L)-VAR
    PBAR(1,L)  =YBAR(1,L)**((2.*GAMO)/(GAMO+1.))
    RHOBA(1,L)=YBAR(1,L)**(2./(GAMO+1.))
    T(1,L)=TO*YBAR(1,L)**(2.*(GAMO-1.)/(GAMO+1.))
    VBAR(1,L)=A2*2.*GAMO/(GAMO-1.)*(YBAR(1,L)**((GAMO-1.)/
   1(GAMO+1.))-1.)
              HBAR(1,L)=0
    DO2035I=1,ILIM
    HBAR(1,L)=((CAPR*T(1,L)*(5./2.+SMALLF(I))+B8(I)
   1+ENO*SDEL(I))*X(I,1,L)/U(I))/HO+HBAR(1,L)
2035 CONTINUE
2034 CONTINUE
    DO777L=1,LLIM
    DO775K=1,KLIM
    MTEST=0
    NE=0
    PBARA=PBAR(K,L+1)
    PBARB=PBAR(K+1,L)
    PBARC=PBAR(K,L)
    RHOBAA=RHOBA(K,L+1)
    RHOBAB=RHOBA(K+1,L)
    RHOBAC=RHOBA(K,L)
    VBARA=VBAR(K,L+1)
    VBARB=VBAR(K+1,L)
    VBARC=VBAR(K,L)
    HBARA=HBAR(K,L+1)
    HBARB=HBAR(K+1,L)
    HBARC=HBAR(K,L)
    TA=T(K,L+1)
    TB=T(K+1,L)
    TC=T(K,L)
    DO798I=1,ILIM
    XA(I)=X(I,K,L+1)
    XB(I)=X(I,K+1,L)
    XC(I)=X(I,K,L)
    EVA(I)=EV(I,K,L+1)
    EVB(I)=EV(I,K+1,L)
    EVC(I)=EV(I,K,L)
 798 CONTINUE
    TBARA=TBAR(K,L+1)
    TBARB=TBAR(K+1,L)
    TBARC=TBAR(K,L)
    YBARA=YBAR(K,L+1)
    YBARB=YBAR(K+1,L)
    YBARC=YBAR(K,L)
```

```
303 ATOP=0
    BTOP=0
    CTOP=0
    PTOP=0
    APA=1.
    BPA=1.
    PPA=1.
    DPA=1.
    AS=0
    BS=0
    PS=0
    DS=0
    DELA=0
    DELB=0
    DELP=0
    DELD=0
    SAX=0
    SBX=0
    SPX=0
    SDX=0
    SIGA=0
    SIGB=0
    SIGP=0
    SIGD=0
    ABOT=0
    BBOT=0
    CBOT=0
    PBOT=0
    SIMP=0
    DO 65 I=1,ILIM
    DXDA(I)=0
    DXDB(I)=0
    DXDP(I)=0
    DXDD(I)=0
 65 CONTINUE
    IF(MTEST)600,600,601
600 RHOBAP=RHOBAA
    PBARP=PBARA
    VBARP=VBARA
    HBARP=HBARA
    TP=TA
    DO3I=1,ILIM
    XP(I)=XA(I)
    EVP(I)=EVA(I)
    FRAN(I)=5./2.+SMALLF(I)
    BOT(I)=3./2.+SMALLF(I)
  3 CONTINUE
601 DO 604 I=1,ILIM
    XOUA(I)=XA(I)/U(I)
    XOUB(I)=XB(I)/U(I)
    XOUC(I)=XC(I)/U(I)
    XOUP(I)=XP(I)/U(I)
    ATOP=FRAN(I)*XOUA(I)+ATOP
```

```
      ABOT=BOT(I)*XOUA(I)+ABOT
      BTOP=FRAN(I)*XOUB(I)+BTOP
      BBOT=BOT(I)*XOUB(I)+BBOT
      CTOP=FRAN(I)*XOUC(I)+CTOP
      CBOT=BOT(I)*XOUC(I)+CBOT
      PTOP=FRAN(I)*XOUP(I)+PTOP
      PBOT=BOT(I)*XOUP(I)+PBOT
  604 CONTINUE
      TPA=TP
  300 GAMA=ATOP/ABOT
      GAMB=BTOP/BBOT
      GAMC=CTOP/CBOT
      GAMP=PTOP/PBOT
      ABFA=SQRT(GAMA/GAMO*PBARA/RHOBAA)
      ABFB=SQRT(GAMB/GAMO*PBARB/RHOBAB)
      ABFC=SQRT(GAMC/GAMO*PBARC/RHOBAC)
      ABFP=SQRT(GAMP/GAMO*PBARP/RHOBAP)
      ALPHA1=.5*(ABFA*RHOBAA+ABFP*RHOBAP)
      ALPHA2=.5*(ABFB*RHOBAB+ABFP*RHOBAP)
      TBARP=(A1*ALPHA2*TBARB+A1*ALPHA1*TBARA+YBARB*TBARB-
     1YBARA*TBARA)/(A1*(ALPHA1+ALPHA2))
      YBARP=(A1*ALPHA1*(TBARP-TBARA)+YBARA*TBARA)/TBARP
      YMULT=YBARP*TBARP
      YPROD=YBARC*TBARC
      IF(YMULT-YPROD)100,101,102
  102 TOO=(YBARC*TBARB-YBARB*TBARC)/(TBARB-TBARC)
      YBARD=(TOO+SQRT(TOO**2+4.*((YBARB-YBARC)/(TBARB-TBARC))
     1*YBARP*TBARP))/2.
      TBARD=(YBARP*TBARP)/YBARD
      TBCD=(TBARD-TBARC)/(TBARB-TBARC)
      PBARD=(PBARB-PBARC)*TBCD+PBARC
      RHOBAD=(RHOBAB-RHOBAC)*TBCD+RHOBAC
      TD=(TB-TC)*TBCD+TC
      HBARD=(HBARB-HBARC)*TBCD+HBARC
      VBARD=(VBARB-VBARC)*TBCD+VBARC
      DO103I=1,ILIM
      XD(I)=(XB(I)-XC(I))*TBCD+XC(I)
      EVD(I)=B7(I)*CAPR*TD+B8(I)
      XOUD(I)=XD(I)/U(I)
  103 CONTINUE
      GO TO 69
  100 TBARD=1./(2.*YMULT)*(YBARC*TBARC**2+YBARA*TBARA**2)
      YBARD=YMULT/TBARD
      YDCA=(YBARD-YBARC)/(YBARA-YBARC)
      PBARD=(PBARA-PBARC)*YDCA+PBARC
      RHOBAD=(RHOBAA-RHOBAC)*YDCA+RHOBAC
      TD=(TA-TC)*YDCA+TC
      HBARD=(HBARA-HBARC)*YDCA+HBARC
      VBARD=(VBARA-VBARC)*YDCA+VBARC
      DO104I=1,ILIM
      XD(I)=(XA(I)-XC(I))*YDCA+XC(I)
      EVD(I)=B7(I)*CAPR*TD+B8(I)
      XOUD(I)=XD(I)/U(I)
  104 CONTINUE
      GO TO 69
```

```
101 TBARD=TBARC
    YBARD=YBARC
    PBARD=PBARC
    RHOBAD=RHOBAC
    TD=TC
    HBARD=HBARC
    VBARD=VBARC
    DO105I=1,ILIM
    XD(I)=XC(I)
    EVD(I)=EVC(I)
    XOUD(I)=XD(I)/U(I)
105 CONTINUE
 69 IF(MD-2)1000,109,109
1000 DO1001J=1,JLIM
    CKA(J)=A(J)*TA**B(J)*EXP(-E(J)/(CK*TA))
    CKB(J)=A(J)*TB**B(J)*EXP(-E(J)/(CK*TB))
    CKD(J)=A(J)*TD**B(J)*EXP(-E(J)/(CK* TD))
    CKP(J)=A(J)*TP**B(J)*EXP(-E(J)/(CK*TP))
1001 CONTINUE
    DO 320 J=1,JLIM
    DO 321I=1,ILIM
    AP(J)=((XOUA(I)*RHOBAA*RHOO)**SMALLV(I,J))*APA
    BP(J)=((XOUB(I)*RHOBAB*RHOO)**SMALLV(I,J))*BPA
    PP(J)=((XOUP(I)*RHOBAP*RHOO)**SMALLV(I,J))*PPA
    DP(J)=((XOUD(I)*RHOBAD*RHOO)**SMALLV(I,J))*DPA
    APA=AP(J)
    BPA=BP(J)
    PPA=PP(J)
    DPA=DP(J)
321 CONTINUE
    APA=1.
    BPA=1.
    PPA=1.
    DPA=1.
320 CONTINUE
    DO322I=1,ILIM
    DO323J=1,JLIM
    VV=CAPV(I,J)-SMALLV(I,J)
    AS=AP(J)*VV*CKA(J)+AS
    BS=BP(J)*VV*CKB(J)+BS
    PS=PP(J)*VV*CKP(J)+PS
    DS=DP(J)*VV*CKD(J)+DS
323 CONTINUE
    DXDA(I)=(TPRIME*U(I))/(RHOBAA*RHOO)*AS
    DXDB(I)=(TPRIME*U(I))/(RHOBAB*RHOO)*BS
    DXDP(I)=(TPRIME*U(I))/(RHOBAP*RHOO)*PS
    DXDD(I)=(TPRIME*U(I))/(RHOBAD*RHOO)*DS
    AS=0
    BS=0
    PS=0
    DS=0
322 CONTINUE
109 DO115I=1,ILIM
    SAX=XOUA(I)+SAX
```

```
      SBX=XOUB(I)+SBX
      SPX=XOUP(I)+SPX
      SDX=XOUD(I)+SDX
      DELA=XOUA(I)*FRAN(I)+DELA
      DELB=XOUB(I)*FRAN(I)+DELB
      DELD=XOUD(I)*FRAN(I)+DELD
      DELP=XOUP(I)*FRAN(I)+DELP
  115 CONTINUE
      UA=1./SAX
      UB=1./SBX
      UP=1./SPX
      UD=1./SDX
      PRA=(PBARA*PO)/(RHOBAA*RHOO)
      PRB=(PBARB*PO)/(RHOBAB*RHOO)
      PRP=(PBARP*PO)/(RHOBAP*RHOO)
      PRD=(PBARD*PO)/(RHOBAD*RHOO)
      DO116I=1,ILIM
      SIGA=((-UA**2/U(I)*PRA*DELA+UA/U(I)*PRA*FRAN(I)+
     1(                    ENO*SDEL(I))/U(I))*DXDA(I))+SIGA
      SIGP=((-UP**2/U(I)*PRP*DELP+UP/U(I)*PRP*FRAN(I)+
     1(          ENO*SDEL(I))/U(I))*DXDP(I))+SIGP
          SIGD=((-UD**2/U(I)*PRD*DELD+UD/U(I)*PRD*FRAN(I)+
     1(          ENO*SDEL(I))/U(I))*DXDD(I))+SIGD
      SIGB=((-UB**2/U(I)*PRB*DELB+UB/U(I)*PRB*FRAN(I) +
     1(          ENO*SDEL(I))/U(I))*DXDB(I))+SIGB
  116 CONTINUE
  117 ALAM=SIGA
      BLAM=SIGB
      PLAM=SIGP
      DLAM=SIGD
      GO TO 119
  119 BETA=-CAPR*TA/RHOBAA*DELA
      BETB=-CAPR*TB/RHOBAB*DELB
      BETP=-CAPR*TP/RHOBAP*DELP
      BETD=-CAPR*TD/RHOBAD*DELD
      ANU=A3*ABFA/RHOBAA*ALAM/BETA
      BNU=A3*ABFB/RHOBAB*BLAM/BETB
      PNU=A3*ABFP/RHOBAP*PLAM/BETP
      ANP=.5*(ANU+PNU)
      BNP=.5*(BNU+PNU)
      SAP=A2/2.*(1./(RHOBAA*ABFA)+1./(RHOBAP*ABFP))
      SBP=A2/2.*(1./(RHOBAB*ABFB)+1./(RHOBAP*ABFP))
      PBARP=(SBP*PBARB+SAP*PBARA+ANP*(TBARP-TBARA)+BNP*
     1(TBARP-TBARB)+VBARA-VBARB)/(SBP+SAP)
      VBARP=VBARA+ANP*(TBARP-TBARA)-SAP*(PBARP-PBARA)
      DO121I=1,ILIM
      XP(I)=XD(I)+.5*(DXDD(I)+DXDP(I))*(TBARP-TBARD)
      XOUP(I)=XP(I)/U(I)
  121 CONTINUE
  122 HBARP=HBARD+2.*A4/(RHOBAD+RHOBAP)*(PBARP-PBARD)
      SUP=0
      PTOP=0
      DO125I=1,ILIM
```

```
      SIMP=(XP(I)*(B8(I)/U(I)+ENO*SDEL(I)/U(I)))+SIMP
      SUP=(XP(I)/U(I))+SUP
      PTOP=FRAN(I)*XOUP(I)+PTOP
  125 CONTINUE
      UP=1./SUP
      TP=(HO*HBARP-SIMP)/(CAPR*PTOP)
      BBARP=YBARP*TBARP
      RHOBAP=PBARP*UP/(CAPR*TP)*PO/RHOO
      DO 1717 I=1,ILIM
      EVP(I)=CAPR*B7(I)*TP+B8(I)
 1717 CONTINUE
      NE=NE+1
      MTEST=1
      IF(NE-NLIM)304,301,301
  304 TAPP=ABS(TP-TPA)
      IF(TAPP-DUM)401,401,303
  401 MGL=MGLIM-3
      IF(MG-MGL)398,398,301
  398 IF(L-2)399,399,301
  301 WRITE(6,130)L,K,NE,RHOBAP,PBARP,TP,VBARP,YBARP,TBARP,
     1 (XP(I),I=1,4),(EVP(I),I=1,4) ,BBARP

  130 FORMAT(1HO,6X,I4,10X,I4,10X,I4,10X,E16.8,E16.8,E16.8/(6E16.8))
  399 RHOBA (K+1,L+1)=RHOBAP
      PBAR(K+1,L+1)=PBARP
      HBAR(K+1,L+1)=HBARP
      T(K+1,L+1)=TP
      VBAR(K+1,L+1)=VBARP
      YBAR(K+1,L+1)=YBARP
      TBAR(K+1,L+1)=TBARP
      DO799I=1,ILIM
      X(I,K+1,L+1)=XP(I)
      EV(I,K+1,L+1)=EVP(I)
  799 CONTINUE
  775 CONTINUE
  777 CONTINUE
  778 CONTINUE
      GO TO 1111
      STOP
      END
```